CENTRE FOR ECONOMIC POLICY RESEARCH

CEPR PRESS

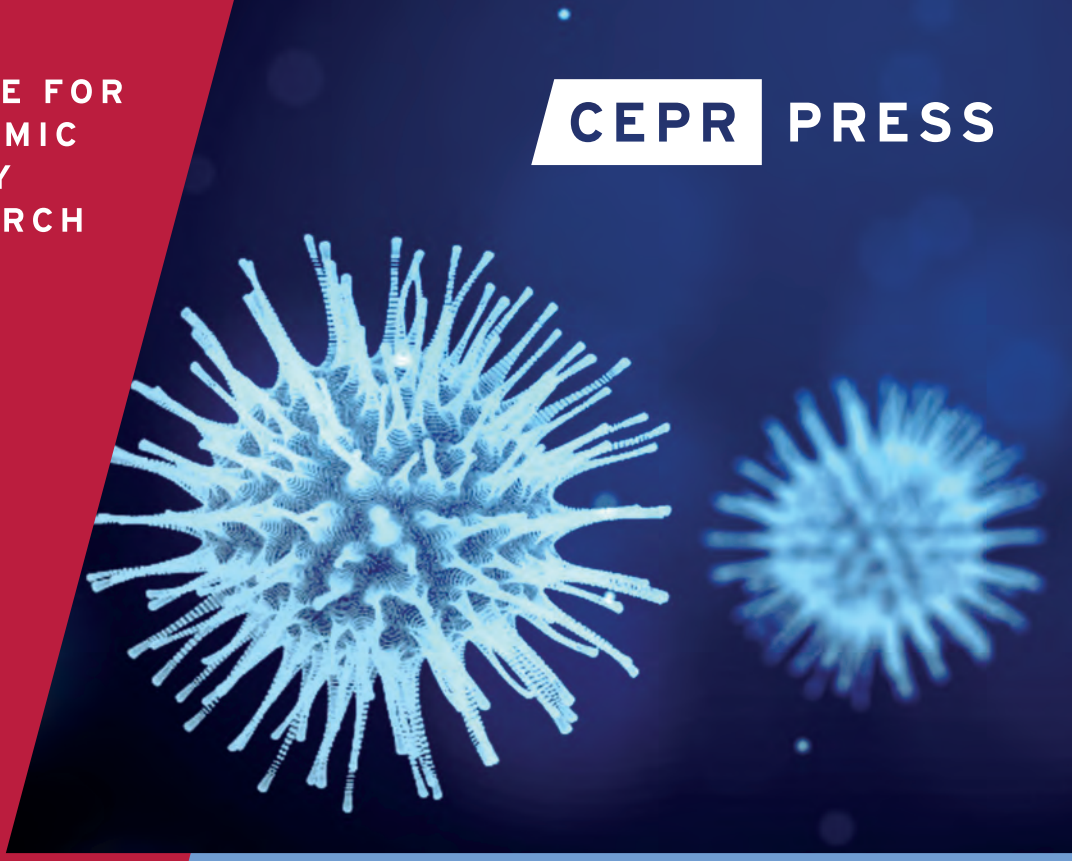

COVID ECONOMICS

VETTED AND REAL-TIME PAPERS

ISSUE 70
25 FEBRUARY 2021

Covid Economics
Vetted and Real-Time Papers

Covid Economics, Vetted and Real-Time Papers, from CEPR, brings together formal investigations on the economic issues emanating from the Covid outbreak, based on explicit theory and/or empirical evidence, to improve the knowledge base.

Founder: Beatrice Weder di Mauro, President of CEPR
Editor: Charles Wyplosz, Graduate Institute Geneva and CEPR

Contact: Submissions should be made at https://portal.cepr.org/call-papers-covid-economics. Other queries should be sent to covidecon@cepr.org.

The Centre for Economic Policy Research (CEPR)

The Centre for Economic Policy Research (CEPR) is a network of over 1,500 research economists based mostly in European universities. The Centre's goal is twofold: to promote world-class research, and to get the policy-relevant results into the hands of key decision-makers. CEPR's guiding principle is 'Research excellence with policy relevance'. A registered charity since it was founded in 1983, CEPR is independent of all public and private interest groups. It takes no institutional stand on economic policy matters and its core funding comes from its Institutional Members and sales of publications. Because it draws on such a large network of researchers, its output reflects a broad spectrum of individual viewpoints as well as perspectives drawn from civil society. CEPR research may include views on policy, but the Trustees of the Centre do not give prior review to its publications. The opinions expressed in this report are those of the authors and not those of CEPR.

Editorial Board

Ethics

Covid Economics will feature high quality analyses of economic aspects of the health crisis. However, the pandemic also raises a number of complex ethical issues. Economists tend to think about trade-offs, in this case lives vs. costs, patient selection at a time of scarcity, and more. In the spirit of academic freedom, neither the Editors of *Covid Economics* nor CEPR take a stand on these issues and therefore do not bear any responsibility for views expressed in the articles.

Submission to professional journals

The following journals have indicated that they will accept submissions of papers featured in *Covid Economics* because they are working papers. Most expect revised versions. This list will be updated regularly.

American Economic Journal, Applied Economics
American Economic Journal, Economic Policy
American Economic Journal, Macroeconomics
American Economic Journal, Microeconomics
American Economic Review
American Economic Review, Insights
American Journal of Health Economics
Canadian Journal of Economics
*Econometrica**
Economic Journal
Economics of Disasters and Climate Change
International Economic Review
Journal of Development Economics
*Journal of Econometrics**
Journal of Economic Growth
Journal of Economic Theory
*Journal of the European Economic Association**
Journal of Finance
Journal of Financial Economics
Journal of Health Economics
Journal of International Economics
*Journal of Labor Economics**
Journal of Monetary Economics
Journal of Public Economics
Journal of Public Finance and Public Choice
Journal of Political Economy
Journal of Population Economics
Quarterly Journal of Economics
*Review of Corporate Finance Studies**
Review of Economics and Statistics
*Review of Economic Studies**
Review of Financial Studies

(*) Must be a significantly revised and extended version of the paper featured in *Covid Economics*.

Covid Economics
Vetted and Real-Time Papers

Issue 70, 25 February 2021

Contents

Covid Economics Issue 70, 25 February 2021

A macroeconomic model of healthcare saturation, inequality and the output–pandemia tradeoff[1]

Enrique G. Mendoza,[2] Eugenio Rojas,[3] Linda L. Tesar[4] and Jing Zhang[5]

Date submitted: 16 February 2021; Date accepted: 18 February 2021

COVID-19 became a global health emergency when it threatened the catastrophic collapse of health systems as demand for health goods and services and their relative prices surged. Governments responded with lockdowns and increases in transfers. Empirical evidence shows that lockdowns and healthcare saturation contribute to explain the cross-country variation in GDP drops even after controlling for COVID-19 cases and mortality. We explain this output-pandemia tradeoff as resulting from a shock to subsistence health demand that is larger at higher capital utilization in a model with entrepreneurs and workers. The health system moves closer to saturation as the gap between supply and subsistence narrows, which worsens consumption and income inequality. An externality distorts utilization, because firms do not internalize that lower utilization relaxes healthcare saturation. The optimal policy response includes lockdowns and transfers to workers. Quantitatively, strict lockdowns and large transfer hikes can be optimal and yield sizable welfare gains because they prevent a sharp rise in inequality. Welfare and output costs vary in response to small parameter changes or deviations from optimal policies. Weak lockdowns coupled with weak transfers programs are the worst alternative and yet are in line with what several emerging and least developed countries have implemented.

1 The views expressed in this document are those of the authors and not those of the Federal Reserve Bank of Chicago or the Federal Reserve System. We thank participants at the Fifth Annual Conference on International Economics organized by the Federal Reserve Bank of Dallas, University of Houston, and Bank of Mexico for useful comments and suggestions.

2 University of Pennsylvania and NBER.
3 University of Florida.
4 University of Michigan and NBER
5 Federal Reserve Bank of Chicago.

Covid Economics 70, 25 February 2021: 1-48

1 Introduction

A distinguishing feature of the COVID-19 pandemia is that, unlike other viral illnesses that are either more lethal (e.g. Ebola, MERS) or just as contagious but less severe (e.g. Influenza, H1N1), it caused a large, sudden surge in use of human and material resources for prolonged hospitalizations and in demand for medical and cleaning supplies by the economy as a whole.[1] Thus, in addition to its infection and mortality rates, a key challenge posed by COVID-19 has been the threat of catastrophic collapse of health systems worldwide. The painful experiences of Bergamo, Guayaquil, Mexico City, New York City, Wuhan, and other cities, showed that collapsing health systems prevented hospitals from providing required care to COVID-19 patients and affected the provision of services to those affected by other conditions, both emergencies and elective treatments, thus increasing excess mortality well above the mortality rate of COVID-19 itself.

Governments responded to the threat of collapse of health systems by imposing severe lockdowns that required all non-essential businesses to close and households to obey strict stay-at-home orders, after attempts with weaker social-distancing restrictions failed to slow the spread of the disease. As we document in the next Section, lockdowns have been in place, with some shifting between relaxing and re-tightening, from March, 2020 until the present in several countries. These lockdowns resulted in the largest quarterly declines in GDP in history in many countries during the second quarter of 2020, with a median of -10.6 percent relative to the second quarter of 2019 in a sample with 48 countries (see Section 2 for details). Most countries also implemented policies to provide liquidity to households and firms by increasing transfers and suspending or deferring tax payments. On average, lockdowns have been stricter and transfers programs larger in advanced economies than in emerging and less developed countries. In many cases, these large fiscal interventions produced record-high public deficits and sharp increases in already-high public debt ratios.

The unprecedented economic costs of the lockdowns, on the one hand, and their effectiveness at preventing the collapse of health systems, on the other, pose a critical public policy trade-off: What is the socially-optimal severity of a lockdown that balances the need to contain a pandemia like COVID-19 against its large economic costs? Related to this are other central questions: How does the pandemia affect income and consumption inequality? What is the optimal size of transfers for workers to offset the adverse effects of the lockdown? How does heterogeneity in economic development and health-system strength affect the output-pandemia tradeoff?

This paper answers these questions by proposing a model that deviates from the widely-used approach of integrating the susceptible-infected-recovered (SIR) model of epidemiology into dynamic macroeconomic models. Instead, we propose a framework that focuses on the severe scarcity problem caused by the pandemia and captured by the saturation of health systems and the shortages of health goods. This approach is motivated by the observation that COVID-19 puts health systems at the risk of collapse despite its low mortality and large share of asymptomatic infections. The severe strain on health systems was evidenced by the suspension of regular hospital services to concentrate

[1] According to the CDC, the median length of hospitalizations for surviving patients in the U.S. as of October, 2020 was 10 to 13 days. Severe shortages of medical staff, ventilators, N95 masks, disinfectants, and various other health-related products were reported worldwide since the initial outbreak in January 2020.

on COVID treatment and by the sharp increases in occupancy of hospital beds, particular ICU beds, in demand for medical specialists and nurses, and in usage of critical equipment such as respiratory ventilators (see Section 2 for details). As a result, excess mortality rates rose significantly above those explained by COVID. For instance, while COVID's infection fatality rate is estimated at 0.65 percent (according to the CDC), excess weekly deaths as a percent of expected deaths between March and June, 2020, peaked at 154 percent in Spain, 108 in the United Kingdom, 90 in Italy, and 45 in the United States, and in Mexico City excess mortality reached 300 percent in the March-May period.[2]

The paper starts with an empirical examination of cross-country data that documents the effects of COVID-19 on resource scarcity and relative prices for health goods and services, excess mortality rates and severity of lockdowns. In addition, we conduct an empirical analysis showing that a non-trivial share of cross-country differences in observed output declines caused by the pandemia is explained by variables that proxy for the severity of lockdowns, resource shortages and pre-COVID-19 health system strength, even after controlling for COVID-19 cases and fatalities.

In the model, the pandemia arrives as a large, temporary shock to the subsistence demand for health goods and services in a Stone-Geary utility function. The shock is larger at higher capital utilization rates. The degree of saturation of the health sector is represented by the gap between the available supply of health goods and services and their subsistence level. The catastrophic (i.e., nonlinear) nature of a health-system collapse is captured by the Inada condition of Stone-Geary preferences. The tradeoff with economic activity works through the dependency of the subsistence demand for health on utilization. Lower utilization relaxes the capacity of the health system, moving it away from its saturation point, but it implies reduced demand for factors of production, reduced output and lower factor payments in the non-health sector. This also introduces a "utilization externality," because firms do not internalize the link between utilization and health-system-saturation when choosing utilization. The size of the hike on subsistence demand for health and the severity of the externality depend on the elasticity of the subsistence health demand to utilized capital. A planner who takes the externality into account has a social marginal cost of utilization higher than the private cost when a pandemia is active. This results in a socially-optimal reduction in utilization during a pandemia, which is decentralized as a competitive equilibrium by mandating an optimal lockdown (i.e., a binding constraint on utilization tighter than the technologically feasible limit).

In order to study the implications of the output-pandemia tradeoff for inequality and the design of liquidity-provision programs, the model includes two types of agents: entrepreneurs, who collect wages and all capital income from the health and non-health sectors, and workers, who collect only wage income. We show that, as the pandemia causes health-system saturation to worsen and the relative price of health goods to rise, inequality in terms of both relative income and relative excess consumption (or relative marginal utilities) of entrepreneurs vis-a-vis workers worsens. As a result, the optimal policy calls for increased transfers to workers.[3] Hence, the optimal policy response to a pandemia includes both a lockdown and higher transfers.

[2]See https://ourworldindata.org/excess-mortality-covid and https://www.washingtonpost.com/world/the_americas/mexico-citycoronavirus- excess-death-toll/2020/07/02/2baaab3e-bbbb-11ea-80b9-40ece9a701dc_story.html.

[3]Inequality makes transfers desirable even without a pandemia for a planner who is utilitarian or weights workers by more than their share of the population. Still, optimal transfers *rise* with a pandemia because inequality worsens.

Covid Economics 70, 25 February 2021: 1-48

In the model, aggregate allocations and prices are independent of individual allocations in both the decentralized and social planner's equilibria. In particular, the effects of the pandemia on utilization and the relative price of health goods are unaffected by agent heterogeneity, inequality and the planner's welfare weights. The effects of the pandemia on inequality and the optimal transfers, however, do depend on the severity of the utilization externality. The stronger the externality, the closer to saturation the pandemia brings the health system and the higher the increase in the price of health goods. This worsens income and excess consumption inequality, since the income of workers falls more and their consumption moves closer and faster to their subsistence levels, which makes larger transfers optimal. The size of the optimal transfers also depends on the planner's welfare weights and the fraction of workers relative to entrepreneurs (i.e., the pre-pandemia wealth distribution).

We explore the model's quantitative implications by examining numerical solutions based on a calibration to U.S. data. Key to this calibration are the determination of the subsistence demand for health in "normal times" (i.e. without a pandemia) and the parameterization of the function that drives the jump in this subsistence demand when the pandemia hits. We determine the former by estimating a standard linear-expenditure-system regression using U.S. data. For the latter, we use a linear function that simplifies the calibration into choosing the value of the elasticity of subsistence health demand with respect to utilized capital. Since little is known about this elasticity, we study results for the interval of values for which the competitive equilibrium with pandemia exists (0 to 0.107). Because of the Inada condition of the Stone-Geary utility, there is an upper bound of the elasticity at which workers' health consumption equals subsistence demand and hence there is no competitive equilibrium solution. For the weights of the planner's social welfare function, we focus on the case in which the planner's solution supports the competitive equilibrium in normal times.

Among the feasible elasticities, we study a particular scenario in which the planner's optimal lockdown yields an output drop equal to the drop in U.S. non-health GDP in the second quarter of 2020 (an elasticity of about 0.09). This scenario rationalizes the observed non-health output drop as resulting from an optimal lockdown that reduces utilization by 15 percentage points. The optimal increase in transfers equals 10.9 percentage points of GDP. This planner's equilibrium is compared with two competitive equilibria computed using the same elasticity: A "no lockdown" (NL) case in which policy is unchanged and an "observed lockdown" (OL) case in which the optimal lockdown is imposed in ad-hoc fashion. In the OL case, utilization and the other aggregate variables match the planner's but transfers are unchanged. This scenario shows the implications of implementing the optimal lockdown without the optimal transfers.

Assuming a pandemia that lasts four quarters, the optimal policies yield welfare gains of 0.82 and 0.33 percent v. the NL and OL cases, respectively (in terms of the standard welfare measure given by a compensating variation in consumption constant across time that equalizes lifetime utility under alternative regimes). Hence, a policy of implementing a lockdown as severe as the optimal one without increasing transfers yields a welfare gain of 0.49 percent relative to unchanged policies but it still means a loss of 0.33 percent relative to the optimal policy regime. This indicates that the adverse effects of the pandemia on inequality are large. Inequality is at its worst in the NL case, for which the ratio of excess consumption of entrepreneurs to workers rises to 16.5 during the pandemia, 4.75 times

Covid Economics 70, 25 February 2021: 1-48

higher than under the optimal policies (which by construction keep the ratio at its normal-times level of 3.5). In the OL case the ratio still rises to 9.5, 2.75 times larger than the optimal ratio. The same pattern affects income inequality: it worsens more in the NL than the OL case, because the relative price of health goods rises 158 percent in the former v. 101 in the latter. Thus, the entrepreneur's capital income from the health sector rises much more in the NL than the OL case. Increasing the elasticity of subsistence health demand to utilized capital above 0.09 yields much larger welfare gains and transfers, with the former growing infinitely large as the pandemia moves workers closer to their subsistence demand and at a much faster pace than for entrepreneurs. The relevance of inequality is also reflected in a comparison of these results with those for a representative-agent version of the model. This economy yields sharply smaller welfare gains for the same elasticities of subsistence health demand to utilized capital.

The results for the full interval of feasible elasticities of subsistence health demand to utilized capital show that pandemias start to have sizable effects on macro aggregates and inequality at elasticities above 0.05. The output-pandemia tradeoff produces concave, inverse relationships between the planner's optimal utilization (or non-health output) and that elasticity. Relative prices and excess consumption ratios in the NL and OL solutions, as well as the welfare gains under the optimal policies, are increasing and convex functions of the elasticity. Hence, small errors in measuring the elasticity result in non-trivial differences in the size of optimal lockdown and transfer policies and their effects on aggregate variables and inequality.

The planner neutralizes the strong adverse impact of the pandemia on consumption and income inequality as a result of the direct effect of higher transfers and the indirect effect of the lockdown. The latter reduces inequality because it mitigates the relative price hike and the rise in the excess consumption ratio. Preventing inequality from worsening contributes over 90 percent of the welfare gains of the optimal policies for all elasticities of subsistence health demand to utilized capital that produce non-negligible pandemias. The aggregate effect of the lockdown removing the utilization externality accounts for the remaining 10 percent. Inequality and distributional effects also makes the model more plausible. A planner in a representative-agent version of the model only gains by removing the utilization externality and as a result it needs larger elasticities of subsistence health demand to utilized capital (of at least 0.13) in order to yield non-trivial welfare gains. These elasticities, however, imply output drops much larger than those that have been observed.

We also conduct an analysis of the implications of deviating from the optimal policies for a large set of lockdown and transfer policy pairs. These deviations result in sizable welfare costs relative to the optimal policies but still policy intervention to respond to the pandemia is preferable to no intervention. Moreover, transfers and lockdowns are substitutable to a degree and using either tool with sufficient strength can get reasonably close to the gains attained by the optimal policies. The reason is that either a large increase in transfers or a strict lockdown weakens significantly the strong adverse effects of the pandemia on inequality. For the same reason, however, combining weak lockdowns with small transfers programs is the worst policy choice. Unfortunately, this seems to be what is occurring in emerging and least developed countries, which on average responded to COVID-19 with weaker lockdowns and smaller fiscal interventions than advanced economies. Using the data

Covid Economics 70, 25 February 2021: 1-48

from Section 2 and from the IMF's *Fiscal Monitor*, we found that income per capita has a correlation with COVID lockdown effectiveness of roughly -0.2 but its correlation with Covid-related transfers is 0.5. Through September 2020, advanced economies increased transfers by nearly 10 percentage points of GDP on average while the increases in emerging and least developed countries averaged 4.4 and 3 percentage points, respectively.

The model and the quantitative findings also have important implications for the analysis of cross-country or cross-region responses to COVID-19. The model predicts that the pandemia has been more damaging for countries with higher wealth inequality and/or weaker pre-pandemia conditions in characteristics such as quality or capacity of health systems, income per capita, etc. Weaker pre-pandemia conditions can be thought of as implying higher elasticities of subsistence health demand to utilized capital which the model associates with larger optimal lockdowns and output drops. The relative size of the health sector also reflect cross-country differences in health systems. For a given elasticity, the model predicts larger effects of pandemias in countries with smaller health sectors or smaller shares of non-health expenditures.

This paper is related to the growing COVID-19 macro literature. Most of this literature emphasizes the probabilistic dynamics of contagion, infection and death (or recovery) from the disease itself, by incorporating them into macro models using the canonical SIR/SEIR models from epidemiology. The contribution of our work is the focus on resource scarcity and the saturation of the health sector as the drivers of the output-pandemia tradeoff and its distributional implications.[4] In SIR/SEIR-based models, decentralized equilibria are inefficient because the planner internalizes these disease dynamics and the social welfare function depends negatively (positively) on the death (recovery) rates. In contrast, in the model proposed here social welfare is a standard aggregation of individual preferences over consumption and labor, and the adverse implications of a pandemia for efficiency and inequality result from the surge in subsistence demand for health that it causes, which is larger at higher utilization and affects workers more severely than entrepreneurs. Moreover, this framework also accounts for large increases in the relative price of health goods during a pandemia.

Alvarez et al. (2020), Atkeson (2020) and Eichenbaum et al. (2020) initiated the literature on quantitative SIR-based macro models. In these models, the pandemia affects macroeconomic outcomes through demand and supply effects. Infections and mortality increase with consumption and hours worked. Sick workers become less productive or work less and consume less, and consumption and labor have feedback effects on infections. In addition, contagion causes externalities as agents do not internalize how their individual actions affect the SIR dynamics. Lockdowns improve efficiency by tackling this externality. Alvarez et al. (2020), Favero et al. (2020) and Jones et al. (2020) introduce also a congestion externality by modeling the COVID-19 fatality rate as an increasing function of total infections above a constant rate. This externality is similar to the utilization externality resulting from the adverse effect of utilization on the health subsistence demand in our model, but it differs in that in the SIR models congestion increases fatalities, which the planner is

[4]This is in parallel with the public health literature on pandemias, in which a branch focusing on resource scarcity and saturation of hospitals (e.g. Ajao et al., 2015, Halpern and Tan, 2020) coexists with the SIR/SEIR epidemiology branch (see the survey by Britton, 2010).

Covid Economics 70, 25 February 2021: 1-48

assumed to dislike. Hence, although both models predict that lockdowns are desirable because of health-system congestion, the mechanism driving the result is different. In particular, in our setup lockdowns are desirable because the pandemia brings all agents closer to their subsistence level of health regardless of whether they are infected and of the COVID-19 fatality rate, and redistribution is desirable because this effect hits workers more severely than entrepreneurs.

The macro-SIR/SEIR framework has also been used in models with agent and sectoral heterogeneity, as in the studies by Acemoglu et al. (2020), Baqaee et al. (2020), Bodenstein et al. (2020), Azzimonti et al. (2020), Glover et al. (2020), Guerrieri et al. (2020), Hur (2020), Kaplan et al. (2020), Krueger et al. (2020) and Rampini (2020). These studies suggest that lockdowns should be targeted differentially across sectors, with their severity depending on how contact-intensive sectors are, the composition of workers in the sector (age, susceptibility, health), how essential and easy to substitute are the goods produced by the sector, and how connected agents are in a production network. In most of these articles, agent and/or sectoral heterogeneity drive the policies due to their effect on aggregate outcomes and on the dynamics of infection, recovery and death rates.

SIR models with wealth and income inequality have also been used to study the optimal redistributive policy during a pandemia. Glover et al. (2020) find that the optimal policy involves redistribution from agents that continue working towards those who cannot or who lost their jobs. Bloom et al. (2020) argue that lockdowns and transfers should consider dimensions of income and wealth inequality, because low-income or low-wealth workers typically are more affected by lockdowns since their occupations are less suitable for teleworking (see also Galasso, 2020, Mongey et al., 2020 and Palomino et al., 2020). Thus, economies with a larger fraction of low-wealth agents require milder lockdowns and/or larger transfers. Chetty et al. (2020) examine heterogeneous effects on consumption. Using high-frequency data, they find that COVID-19 has had negative effects on consumption, with lower-income agents being affected disproportionately.

The SIR framework has also been used in open economy models. Arellano et al. (2020) embed SIR dynamics into an Eaton-Gersovitz sovereign default model. The sovereign cares about the fatality rate and can impose lockdowns in order to mitigate the magnitude of the health crisis. Since lockdowns depress output, the sovereign has the incentive to borrow abroad to smooth consumption, but this increases default risk and hence limits the planner's ability to impose aggressive lockdowns as its borrowing capacity is restricted, costing additional lives. Cakmakli et al. (2020) study a multi-sector model with sectoral supply and demand shocks that vary with infections depending on lockdowns. The openness of the economy matters via external demand shocks and input-output linkages.

There are other influential macro models of COVID-19 that do not use the SIR setup and consider the role of financial frictions on firms. Gourinchas et al. (2020) study effects on small and medium enterprises using a model in which the virus causes labor supply constraints that vary by sector and also causes sectoral and aggregate demand shocks and business failures. They find that firm bailouts are better than labor subsidies for reducing bankruptcies and saving jobs, and that targeted bailouts have sizable benefits at lower GDP costs. Céspedes et al. (2020) and Fornaro and Wolf (2020) show that financial frictions combined with a negative productivity shock during the pandemia can pro-

Covid Economics 70, 25 February 2021: 1-48

duce equilibria with long-lasting crises and slow recoveries. Elenev et al. (2020) study a setup in which firms can go bankrupt due to the pandemia, and study how bailouts can help save firms that are experiencing financial distress. Faria e Castro (2020) models the pandemia as a shutdown of the contact-intensive services sector (caused by a utility shock) that is transmitted to other sectors in the economy, while Guerrieri et al. (2020) model it as a shock on the labor supply of a productive sector that requires physical interactions (a fraction of workers becomes unable to work in this sector). In turn, reduced consumption of goods from this sector reduces the households' health. These studies find that transfer payments to workers in sectors affected by the pandemia are socially optimal.

The rest of the paper is organized as follows. Section 2 provides empirical evidence on the relevance of healthcare saturation and important empirical regularities of the macro effects of the COVID-19 pandemia. Section 3 describes the model. Section 4 presents the quantitative results of the calibrated model. Section 5 provides some conclusions.

Covid Economics 70, 25 February 2021: 1-48

2 Empirical Evidence

In this Section, we review the empirical evidence on COVID-19 that motivates the theoretical model. The discussion is divided into four parts: 1) a review of the resource shortages and constraints on medical systems for managing the pandemia, 2) the impact of the pandemia on prices of critical medical services and equipment, 3) international evidence on the severity and duration of lockdowns, and 4) a cross-country analysis of the determinants of output collapse during the pandemia.

2.1 Resource shortages and capacity constraints for COVID-19

Saturation of the health system caused by COVID-19 has three important components. The first is the capacity of hospitals to treat COVID patients, particularly to provide them with ventilation therapy. The second is the closure of non-Covid related medical and hospital services, as hospitals are dedicated to COVID patients and medical practices and elective procedures are shut down. The third are the shortages of medical and cleaning supplies as the healthcare and non-healthcare sectors as well as households aim to build up subsistence inventories.

Consider first hospital capacity to treat patients. Evidence from COVID-19 projections and existing studies from the public health literature shows that pandemias pose a serious risk to cause health systems to collapse. On March 26, 2020, the Institute for Health Metrics and Evaluation (IHME) of the University of Washington issued a forecast of the likely stresses on the U.S. medical system due to COVID-19. Their analysis, based on a state-by-state assessment of medical facilities, warned that in the absence of large-scale public health interventions, particularly mitigation measures (i.e. lockdowns) the demand for intensive care facilities would outstrip existing supply in a matter of days.

IHME's analysis focused on ICU beds, but health systems can collapse well before running out of regular and ICU hospital beds as they run out of medical specialists, nursing staff, equipment and materials needed to treat patients in respiratory distress. Ajao et al. (2015) assessed the capacity of the U.S. healthcare system to respond to increased demand for ventilation therapy due to a hypothet-

ical influenza pandemic outbreak under three levels of stress on the health system: (i) conventional capacity (usual and normal patient care); (ii) contingency capacity (minor adaptation of treatment approaches) and (iii) crisis capacity (fundamental, systematic change in which standards of care are significantly altered to allow treatment of a greater number of patients). Their study identified four key components necessary to provide ventilation therapy:

1. Supplies, such as ventilators, ancillary supplies, and equipment.
2. Space, namely hospital beds equipped for ventilation and critical care.
3. Staff, consisting of specialized medical personnel to manage patients on ventilators.
4. Systems, namely accessible, exercised plans to rapidly increase ventilation therapy capacity.

Hence, the provision of ventilation therapy is akin to a Leontief technology that requires complementary inputs in relatively fixed proportions. As a result, hitting a constraint on one input limits the ability to provide ventilation therapy. Taking as given the estimated number of ventilators availabe in 2010 and assuming that they would not be the constraining factor, Ajao et al. (2015) showed that at the peak of the hypothetical influenza pandemia in the United States, the constraining factor for ventilation therapy in scenario (iii) would be the number of respiratory therapists, not the number of beds. The maximum number of additional patients that could be put in a ventilator would range from 56,300 to 135,000, which would fall short of the number of available beds enabled for ventilation therapy. In fact, 32,300 to 42,300 beds would go unused.

Halpern and Tan (2020) assess U.S. capacity for treating COVID-19 patients under current conditions. Based on surveys of U.S. hospitals, they report that acute care hospitals own 62,188 full-featured mechanical ventilators. Adding other equipment that can be diverted to ventilator use (e.g. from operating rooms and the U.S. stockpile) has the potential to bring the total up to 200,000 devices nationally. Recent projections suggest that approximately 960,000 patients in the US would require ICU ventilatory support, though not all patients would be treated at the same time. But even if the number of patients could be optimally staggered, they conclude the critical factor is staffing. According to the BLS there are approximately 130,000 respiratory therapists in the labor force. However, there are far fewer respiratory intensivists, physicians certified to provide care for critically ill patients. The American Hospital Association estimates that there are roughly 29,000 intensivists nationwide, and about half of acute care hospitals have no intensivists on their staff. Halpern and Tan (2020) conclude, "At forecasted crisis levels, we estimate that the projected shortages of intensivists, critical care APPs, critical care nurses, pharmacists, and respiratory therapists trained in mechanical ventilation would limit the care of critically ill ventilated patients" (p. 1). "Moreover, even in the 50 percent of acute care hospitals with intensivists, the intensivist team may be overstretched as new ICU sites are created or experienced ICU staff become ill" (p. 8).

Li et al. (2020) apply the dynamics of the COVID-19 outbreak in Wuhan to the United States and reached similar conclusions as Ajao et al. (2015) and Halpern and Tan (2020). In their analysis, "the projected number of prevalent critically ill patients at the peak of a Wuhan-like outbreak in US cities was estimated to range from 2.2 to 4.4 per 10,000 adults, depending on differences in age distribution and comorbidity (ie, hypertension) prevalence" (p. 1). Based on a population of roughly 210 million

Covid Economics 70, 25 February 2021: 1-48

adults, this is an afflicted population of 460,000 to 920,000. "[I]f a Wuhan-like outbreak were to take place in a US city, even with social distancing and contact tracing protocols as strict as the Wuhan lockdown, hospitalization and ICU needs from COVID-19 patients alone may exceed current capacity... Plans are urgently needed to mitigate the consequences of COVID-19 outbreaks on local health care systems in US cities" (pp. 5-7).

The second aspect of health system saturation caused by COVID-19 is evidenced by the suspension or drastic reduction in provision of non-Covid-related medical services and treatments. Hospitals expanded capacity to treat COVID patients as envisaged in the critical scenario (iii) of Ajao et al. (2015), by reallocating physical and human resources normally dedicated to other uses to treat COVID patients. In addition, in many instances lockdowns implied closure of medical and dental practices, laboratories, and outpatient surgery facilities. These changes and restrictions caused a sharp increase in mortality, as measured by the standard excess mortality P-Score. We collected cross-country data for P-cores computed using the number of total deaths, COVID- and non-COVID-related, at a weekly frequency minus the average of deaths over the 2015–2019 period and divided by the same 2015–2019 average (the source was https://ourworldindata.org/excess-mortality-covid and some country-specific sources). Table 1 shows the highest weekly P-Scores for the January-June, 2020 period in 35 countries. The mean (median) reached 42.9 (23.8) percent, but in several cases it exceeded 50 percent (Belgium, Chile, Italy, Netherlands, Mexico, Peru, Spain, Turkey and the U.K.). Since P-scores combine COVID and non-COVID fatalities, they are a noisy measure of fatalities not caused directly by the disease, but in the analysis of cross-country output drops conducted below we will control for COVID fatalities to identify the effect of non-COVID excess mortality.

The third element of resource shortages due to COVID-19 relate to health goods and services and cleaning supplies for the economy as whole. We document the impact of these shortages by examining the evolution of the relative prices of the affected goods and services in the next subsection.

2.2 Rising prices of PPE and medical equipment

COVID-19 caused severe shortages of medical equipment and cleaning supplies that resulted in sharp price hikes. In the United States, spikes in prices for cleaning supplies, toilet paper and medical masks prompted consumer groups to complain of price gouging. Several states embarked on campaigns inviting consumers to send images of purported price gouging. A Google search of images of "COVID price gouging" yields pictures of 8 oz. bottles of hand sanitizer priced at $50 and Clorox wipes at over $40 per container. The U.S. PIRG consumer watchdog association reported inflation rates of COVID-19 related goods ranging from 200 percent for thermometers to 1,300 percent for anti-bacterial handwipes. These goods disappeared from store shelves where they were priced at regular prices, resulting in massive, prolonged stockouts of key items in retail chains. The prices of these goods facing severe shortages are mismeasured in aggregate price indexes, because these indexes rely on surveys of posted retail prices even for out-of-stock goods (e.g. on August 18, 2020, the posted but out-of-stock price for Clorox disinfecting wipes 75ct was $6.59 on the CVS website, but they were available on eBay for $29 plus $11.67 shipping; Lysol disinfectant spray 19oz was $5.97

Covid Economics 70, 25 February 2021: 1-48

at Home Depot but out of stock, while on eBay it was available for $12.50 plus $17.50 shipping).

Table 1: Excess Mortality P-Scores, Percent

Country	P-score	Country	P-score
Peru	163	Israel	20.3
Spain	154.5	South Africa	18
United Kingdom	108	Colombia	18
Belgium	104.4	Greece	16
Italy	96.8	Austria	16
Mexico	87	Germany	14.5
Netherlands	74.9	Russia	14
Chile	68.7	Finland	13.6
France	65.2	Ireland	12
Turkey	54	Australia	12
Indonesia	50	New Zealand	11.9
Sweden	47.1	Denmark	10.5
United States	44.9	South Korea	9.6
Switzerland	44	Norway	9.5
Brazil	42	Taiwan	9.2
Canada	26.2	Czech Republic	8.9
India	25	Poland	8.3
Portugal	23.8		

Notes: The scores shown are the maximum of weekly P-scores over the January-June, 2020 period computed as the number of total deaths in each week minus the average of deaths over the 2015-2019 period and divided by the same 2015-2019 average. For most countries, weekly P-scores were retrieved from https://ourworldindata.org/excess-mortality-covid on 12/2/2020. Data for Brazil, Indonesia, Mexico, Peru, Russia, South Africa, and Turkey are from https://www.economist.com/graphic-detail/2020/07/15/tracking-covid-19-excess-deaths-across-countries, for Colombia, India and Ireland from https://www.nytimes.com/interactive/2020/04/21/world/coronavirus-missing-deaths.html, and for Australia from the Australian Bureau of Statistics. Data for Indonesia and Turkey cover only Jakarta and Istanbul, respectively.

Covid Economics 70, 25 February 2021: 1-48

Similar price dynamics were observed for medical equipment as hospitals and even state governments competed for the limited supply of PPE and ventilators. On April 24, 2020, National Public Radio aired a report entitled "Are Illinois Officials Paying Hugely Inflated Prices For Medical Supplies?" A government audit revealed spending up to $174 million on COVID-related medical supplies and equipment, including $13 million for 200 ventilators, a 100 percent markup over the pre-COVID price. The governor stated that "A typical ventilator that's useful in an [intensive care unit] situation, the price starts at $25,000, maybe up to $35,000 or $40,000, ... When we're paying more than that, that's typically because the market has bid up the prices for any available ventilators. Let me be clear: There are very few ventilators available in the entire world. We are acquiring whatever we can so that we're ready in the event there's a spike in ICU beds and a need for ventilators..."

Wages for travel nurses responded to the increased demand for hospital staff. During peak COVID periods in the Spring and Summer of 2020, the weekly compensation rate for travel nurses roughly doubled, according to the Health IT website (HIT.net). The "Travel Nurse Compensation

Report" data from BLS show more modest salary increases for nurses in early 2020 of less than five percent, but these are somewhat misleading, however, as they aggregate the salaries of specialists in fields where medical services actually declined (e.g. voluntary medical care, private medical practices) along with the rising salaries of nurses that are ICU and respiratory specialists.

Table 2 shows evidence of the large price hikes caused by Covid-related shortages of essential health goods and services. The median price increase for transactions of thirteen key goods, including N95 masks, ventilators, thermometers and disinfectants, reached 259 percent from March to April, 2020. The Table also shows inflation rates for aggregate price indexes. Health-services prices rose at annualized rates ranging from 3.1 to 4.7 percent in the second quarter of 2020, while the price index for private goods-producing industries fell -16.1 percent.[5] Hence, prices of health services relative to those for goods-producing industries rose between 19.2 to 20.8 percent, and for the specific health goods listed in the Table, the median relative price hike exceeded 275 percent.

2.3 Duration and severity of lockdowns

Figure 1 illustrates the severity and duration of the lockdowns implemented in a group of sixteen advanced and emerging economies. The data correspond to the Government Response Stringency Index constructed as part of the Oxford COVID-19 Government Response Tracker (*OxCGRT*).[6] This index combines information from nine indicators including school and business closures, and travel bans in a scale from 0 to 100 (with 100 for the strictest). In countries where policies vary within the country, the index corresponds to the strictest area. The index is available for 180 countries.

The Figure shows that strict lockdowns were implemented in all countries by mid March, 2020. In most cases, the index peaked around 75-80 percent, except in Sweden, well-known for its less restrictive stance. Even in Sweden, however, the stringency index reached nearly 50 percent. Moreover, lockdowns have persisted from March to the latest available data as of the date of this paper. The severity of the lockdowns has fluctuated somewhat and in several cases declined (in some like France and New Zealand quite sharply), but as of the Dec. 2020 data all countries still maintained significant restrictions on economic activity relative to the pre-COVID-19 status. Even in Sweden, the stringency index fell slightly from its peak but it remains above 30 percent.

2.4 Economic activity

The strict lockdowns caused deep recessions, in many cases the largest recorded declines in quarterly GDP. Figure 2 shows year-on-year drops in GDP in the second quarter of 2020 for 48 advanced and emerging economies.[7] The mean (median) drop was a staggering -11.5 (-10.6) percent.

[5] Health services at this level of aggregation include some for which prices fell as a result of suspension of elective treatments, routine medical, dental and optical appointments, etc.

[6] Available at https://www.bsg.ox.ac.uk/research/research-projects/coronavirus-government-response-tracker

[7] Most of the data are from ourworldindata.org, fred.stlouisfed.org, and www.focus-economics.com. For China and Hong Kong, the Figure shows the GDP drop in the first quarter, because these countries entered the pandemia earlier.

Table 2: Price Changes of Key Health Goods & Services During the COVID-19 Pandemia

Item	Price Change	Source
N95 Masks	1513%	SHOPP
3M N95 Masks	6136%	SHOPP
Hand Sanitizer	215%	SHOPP
Isolation Gowns	2000%	SHOPP
Face Shields	900%	SHOPP
Soap	184%	SHOPP
Ventilators	80%	NY State
Clorox Disinfecting Wipes	660%	US PCW
Anti-Viral Facial Tissues	254%	US PCW
Bleach Cleaner	238%	US PCW
Thermometers	200%	US PCW
Face Masks	259%	US PCW
Anti-Bacterial Hand Wipes	1294%	US PCW
Aggregate Price Indexes (Q2:2020 v. Q1:2020 annualized)		
Physicians' Services	4.68%	BLS
Medical Care Services	4.40%	BLS
Hospital Services	3.14%	BLS
Health Care and Social Assistance	3.60%	BEA
Private Goods-Producing Industries	-16.10%	BEA

Notes: Personal protective equipment price changes are for April 2020 relative to pre COVID-19 levels (not annualized) reported by the Society for Healthcare Organization Procurement Professionals (SHOPP). Price changes (not annualized) for items reported by the US PCW (US PIRG Consumer Watchdog) correspond to the difference between the price listed in Amazon and the lowest price listed by other platforms during August 2020. BLS and BEA price indexes correspond to percent changes between 1st and 2nd quarter of 2020, annualized. Private goods-producing industries are: agriculture, forestry, fishing, and hunting; mining; construction; and manufacturing.

How much of the output declines was due to healthcare system saturation? To answer this question, we test for the relative importance of lockdowns, COVID case and mortality rates, and measures of the stress on healthcare systems in explaining cross-country differences in the magnitude of the decline in GDP.

The severity of lockdowns can be gauged with de-jure or de-facto measures. For the former, we use again the Oxford Stringency Index, and for the latter we use the components of the Google COVID-19 Community Mobility Reports that track movement to and from retail, recreational and work places. Mobility is reported as percent change relative to a pre-COVID baseline (the median for the five-week period Jan. 3rd-Feb. 6, 2020).[8] This indicator is useful because it captures the actual mobility of the population while the stringency index captures legal restrictions.

Unconditional scatter diagrams of both de-jure and de-facto lockdown severity indicators show a clear relationship with the observed quarterly GDP drops (see Figure 3). Output drops were larger in countries with stricter lockdowns, whether measured by a *higher* stringency index or *lower* community mobility. These scatter diagrams only tell part of the story, however, because other variables

[8]For both the Stringency Index and Community Mobility, we use 30-day averages as of the end of November, which were obtained from the components of Bloomberg's Covid Resilience Index, see https://www.bloomberg.com/news/articles/2020-11-24/inside-bloomberg-s-covid-resilience-ranking.

are likely to jointly affect economic activity and lockdowns, and we are interested in particular in determining whether variables that proxy for resource shortages and capacity constraints (i.e., health system saturation) play a role. To identify those effects, we conduct a panel regression analysis in a cross-section of 35 countries.

Figure 1: Lockdown Stringency Index for Selected Countries

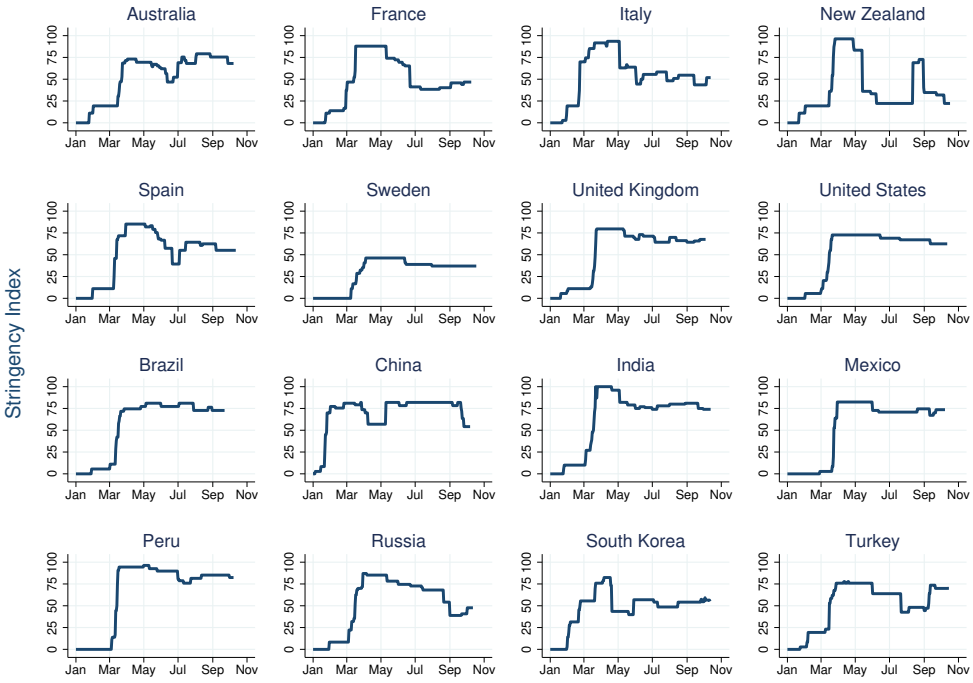

Source: Government Response Stringency Index available from the Oxford COVID-19 Government Response Tracker.

The dependent variable in this analysis is the contraction in GDP, as measured by the fall in the second quarter of 2020 relative to the same quarter in 2019. The independent variables include: the stringency index and community mobility changes described above, two variables to capture the infection and mortality rates of COVID-19 itself (COVID cases for November, 2020 and cumulative COVID deaths through the end of November), and four variables as proxies for health system resources and capacity limits. The latter include a proxy for the non-COVID excess mortality rate (defined as the residual from regressing the excess mortality P-scores on COVID deaths), hospital beds, the log of 2019 GDP per capita, and the UNDP's human development index (HDI) that combines life expectancy, educational attainment and gross national income per capita. COVID cases and fatalities and hospital beds are in units per one-million inhabitants and the rest of the variables are in percent. The data are available for 48 countries for most variables, but excess mortality P-scores are only available for 35, which sets the sample size of the regressions. The variables are expressed

Covid Economics 70, 25 February 2021: 1-48

in deviations from their means and the regressions are estimated using MM Robust Least Squares.[9] The coefficients for all variables but hospital beds and COVID cases and deaths are elasticities, since the data are all in percent, and hence they are comparable. Coefficients for hospital beds and COVID cases and deaths are comparable, because the data for each are per one-million inhabitants.

Figure 2: Year-on-Year 2020:Q2 GDP Declines

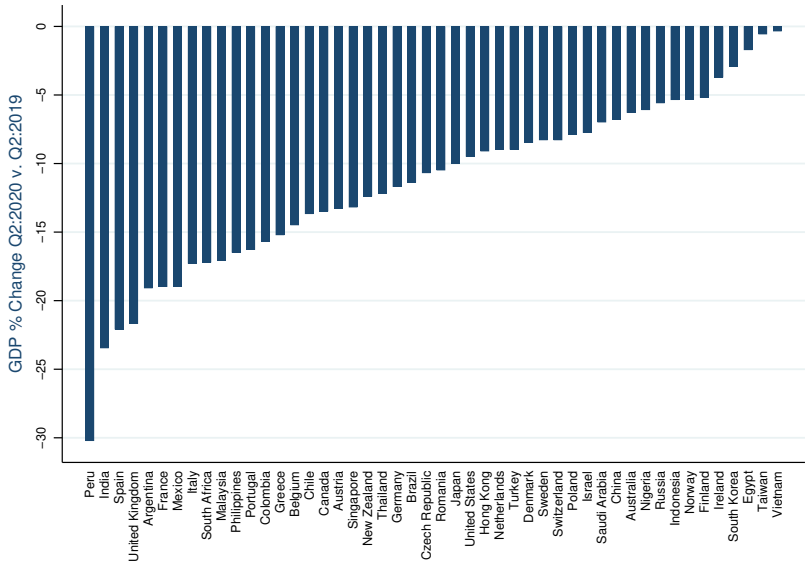

Source: http://ourworldindata.org/, https://fred.stlouisfed.org/, https://www.focus-economics.com/ and country sources.

Figure 3: Lockdown Severity and 2020:Q2 Output Declines

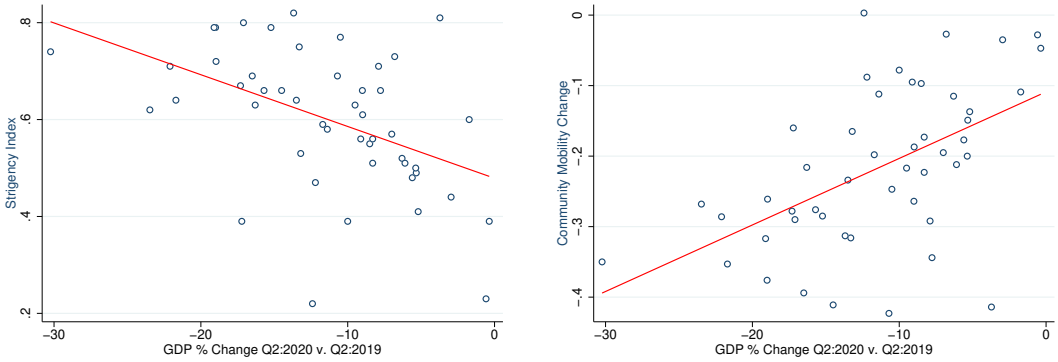

Notes: See footnotes to Figures 1 and 2 for sources of stringency index and GDP. Community mobility was retrieved from https://www.bloomberg.com/news/articles/2020-11-24/inside-bloomberg-s-covid-resilience-ranking on 11/29/2020.

[9] Leverage plots, influence statistics and histograms indicated outliers in Q2:2020 GDP and in several of the regressors.

Covid Economics 70, 25 February 2021: 1-48

The results are reported in Table 3. Column (1) shows the results with the highest overall significance ($R_n^2 = 99.2$) and explanatory power (robust $R_w^2 = 0.81$), and the lowest deviance coefficient (0.036). The regressors include the stringency index, non-covid excess mortality, (log of) GDP per capita, hospital beds and COVID cases. Using together a measure of lockdown severity, proxies for resource shortages and health system capacity, and COVID cases is important to avoid possible omitted variable bias (e.g. lockdown severity is likely to depend on COVID cases and deaths). Simultaneity bias is addressed by using lockdown severity and COVID variables with data up to November, 2020, which makes them less likely to be determined jointly with Q2:2020 GDP. All of the regression coefficients are significant at the 95-percent level or higher (hospital beds marginally) and have the expected signs. The regression explains roughly 81 percent of the cross-country variation in Q2:2020 GDP drops. In addition, an important result for the argument of this paper is that lockdown severity and the variables that proxy for health system resources and capacity are all significant, even after controlling for COVID infections. Non-covid excess mortality has the largest elasticity. A 100-basis-points increase in this variable reduces quarterly GDP growth by 1.12 basis points, compared with 0.9 for a 100-basis points rise in the stringency index and 0.65 for a cut in GDP per capita of the same magnitude. Moreover, hospital beds have a significantly larger effect on quarterly GDP than COVID cases. Adding one bed per one-thousand people improves GDP by roughly 58 basis points, whereas an extra COVID case per one-thousand inhabitants reduces GDP growth by 35 basis points.

Columns (2)-(8) explore the robustness of the above results to potentially important modifications. Column (2) shows that adding cumulative COVID deaths is not useful. The coefficient for this variable is not significant, the rest of the coefficients change slightly, and the explanatory power, significance and deviance statistics of the regression are slightly weaker. The coefficients on stringency and beds are estimated with less precision (they are marginally significant at the 90-percent confidence level). Column (3) shows that replacing cases for November, 2020 with cumulative COVID deaths throughout end November worsens the results. The regression explains about 10 percentage points less of the cross-country variation in GDP drops and has sharply lower R_n^2 and higher deviance than Columns (1) and (2). Beds are no longer significant. Columns (4) and (6) show that replacing the stringency index with community mobility makes little difference. Both are statistically significant (with opposite signs because higher mobility implies a weaker lockdown), and the other coefficients are similar to those in Columns (3) and (5), respectively. Column (5) shows that removing hospital beds also weakens the results, with sharply lower R_n^2 and R_w^2 and higher deviance. Column (7) compared with Column (5) shows that using either GDP per capita or HDI yields similar results. Finally, Column (8) shows that removing hospital beds from Column (1) yields slightly weaker results. The coefficient on the stringency index rises from -0.095 to -0.128, suggesting the possibility of omitted variable bias as lockdown severity may depend on hospital capacity.

In summary, Table 3 yields three key results: (a) non-SIR variables, particularly the proxies for differences in health system resources and capacity, are important determinants of the depth of the recessions caused by COVID-19, even after controlling for the direct effects of COVID transmission; (b) variables driving SIR dynamics also play a role, since the coefficients on COVID cases and/or deaths are statistically significant; and (c) the effects of non-SIR variables are stronger.

Table 3: Cross-Country Regressions for Output Collapse in Q2:2020

Dependent variable: year-on-year quarterly GDP growth as of Q2:2020								
Regressors	(1)	(2)	(3)	(4)	(5)	(6)	(7)	(8)
Stringency	-0.095	-0.084	-0.110		-0.115		-0.116	-0.128
	(*0.048*)	(*0.109*)	(*0.073*)		(*0.058*)		(*0.062*)	(*0.010*)
Mobility				0.186		0.168		
				(*0.025*)		(*0.044*)		
Non-covid excess	-0.112	-0.108	-0.081	-0.095	-0.084	-0.090	-0.089	-0.116
Mortality	(*0.000*)	(*0.000*)	(*0.004*)	(*0.000*)	(*0.002*)	(*0.001*)	(*0.002*)	(*0.000*)
ln(GDP pc)	0.065	0.063	0.047	0.052	0.050	0.051		0.071
	(*0.000*)	(*0.000*)	(*0.001*)	(*0.000*)	(*0.000*)	(*0.000*)		(*0.000*)
Human dev. index							0.361	
							(*0.000*)	
Hospital beds	5.801	5.262	1.649	2.766				
	(*0.053*)	(*0.100*)	(*0.644*)	(*0.410*)				
Covid cases	-3.51E-04	-3.11E-04						-2.98E-04
	(*0.001*)	(*0.013*)						(*0.005*)
Covid deaths		-1.49E-05	-6.00E-05	-3.85E-05	-6.06E-05	-5.15E-05	-5.84E-05	
		(*0.557*)	(*0.020*)	(*0.144*)	(*0.017*)	(*0.050*)	(*0.024*)	
# Observations	35	35	35	35	35	35	35	35
R^2_w	0.812	0.809	0.711	0.770	0.713	0.711	0.702	0.780
Adjusted R^2_w	0.812	0.809	0.711	0.770	0.713	0.711	0.702	0.780
R^2_n	99.151	93.737	55.515	69.026	56.655	61.942	54.073	82.747
Deviance	0.0363	0.037	0.0461	0.042	0.046	0.047	0.048	0.042

Notes: All regressions were estimated using Robust MM Least Squares. The variables are deviations from their respective country means in the common sample. Numbers in parenthesis are p-values. **Stringency** is the Oxford stringency index divided by 100. **Mobility** is Google's community mobility indicator. Both stringency and mobility are 30-day averages over a period ending in late November 2020. **Non-covid excess mortality** is the residual of regressing the excess mortality P-Scores in Table 1 on the cumulative deaths due to COVID-19 as of end November 2020. **Human dev. index** is the 2019 UNDP's human development index, which combines GNI per capita, life expectancy at birth, and mean years of schooling of adults older than 25. **Ln(GDP pc)** is the natural log of GDP per capita in 2019. **Hospital beds** are per 1 million inhabitants. **Covid cases** are the one-month COVID cases per 1 million population for the month ending in late November 2020. **Covid deaths** are cumulative deaths due to Covid-19 per 1 million inhabitants through late November 2020. **Q2:2020 GDP** data are from the sources reported in the note to Figure 2. Data on stringency, mobility, human development index, Covid cases and Covid deaths were retrieved from https://www.bloomberg.com/news/articles/2020-11-24/inside-bloomberg-s-covid-resilience-ranking on 11/29/2020. 2019 real GDP and hospital beds are from *World Bank Open Data* and population data are from *IMF World Economic Outlook*. Hospital beds data are based on WHO figures and is for the most recent year available, which is in the 2010-2015 range for most countries.

Covid Economics 70, 25 February 2021: 1-48

3 A Model of the Output-Pandemia Tradeoff

The key feature of the model is the characterization of a pandemia as a large, transitory shock to the subsistence level of demand for health goods and services ($\bar{h}_t$) in a Stone-Geary utility function that is directly related to the utilization rate (m_t). The value of $\bar{h}_t$ is given by:

$$\bar{h}_t = h^\star + z_t f(m_t K), \tag{1}$$

where $h^\star$ is the "normal" subsistence demand for h goods, z_t is a binary variable which equals 0 in normal times and 1 when there is a pandemia, and $f(\cdot)$ is a monotonically increasing function. A pandemia lasts j periods, so that $z_t = 1$ for $t = 0, ..., j$ and $z_t = 0$ for $t > j$, and is a fully

unanticipated, non-recurrent shock.[10] In addition, the supply of health goods H is assumed to be fixed, which is reasonable since the shock is unanticipated and key parts of the provision of health goods and services rely on forms of capital that are difficult to adjust in the short-run (e.g. hospitals, equipment, specialists, etc).

3.1 Decentralized Competitive Equilibrium

3.1.1 Households

There are two types of households, which together add up to a unit mass of agents. All agents have identical utility functions. A fraction γ_1 are type-1 agents (entrepreneurs) who own all the wealth, both the capital stock used to produce non-health goods and the stock of health goods and services.

The optimization problem of an individual of type 1 is to maximize this utility function:

$$\max_{\{c_t^1, l_t^1, h_t^1, d_{t+1}^1\}} \quad \sum_{t=0}^{\infty} \beta^t \left(a \ln \left(c_t^1 - \frac{(l_t^1)^\omega}{\omega} \right) + (1-a) \ln(h_t^1 - \bar{h}_t) \right), \tag{2}$$

subject to the following budget constraint,

$$c_t^1 + p_t^h h_t^1 = w_t l_t^1 - q_t d_{t+1}^1 + d_t^1 + \pi_t + p_t^h h - \tau_t. \tag{3}$$

In the above expressions, c_t^1 and h_t^1 are consumption of non-health and health goods by an agent of type-1, respectively, and l_t^1 is its labor supply. In addition, d_t^1 and d_{t+1}^1 are the agent's holdings of existing and newly-issued public debt. Non-health goods are the numeraire, so p_t^h is the relative price of health goods, w_t is the wage rate, and q_t is the price of government bonds, all in units of non-health goods. Type-1 agents are the only agents who purchase public debt. They own the endowment of health goods, with an amount h for each type-1 agent, and they also collect the profits paid by firms producing non-health goods and pay lump-sum taxes, with amounts π_t and τ_t for each type-1 agent, respectively, both in units of non-health goods.

The utility function is time-separable, with discount factor β, and period utility is a Stone-Geary utility function of consumption of h and c. The argument for utility of non-health consumption is of the Greenwood-Hercowitz-Huffman form (i.e. the subsistence level is determined by the disutility of labor, which removes the wealth effect on labor supply by making the marginal rate of substitution between l_t^1 and c_t^1 independent of the latter).[11] At equilibrium, the parameter a is the share of expenditure on non-health goods in excess of the disutility of labor relative to income net of the disutility of labor and subsistence expenditure on health goods. Similarly, $(1-a)$ is the share of excess health expenditure above its subsistence level relative to the same net income measure.

[10] The pandemia could also be modeled as a stochastic, non-insurable disaster shock, but modeling it as an unanticipated shock is a reasonable approximation to how COVID-19 arrived. Still, modeling it as a disaster shock is worthwhile, because it would alter precautionary saving behavior and incentivize the accumulation of buffer stocks of health goods.

[11] This assumption is essential for the result that aggregate allocations and the optimal lockdown are independent of agent heterogeneity, inequality and optimal transfers.

Simplifying the first-order conditions of the above problem yields these optimality conditions:

$$\frac{1-a}{a}\frac{c_t^1-\frac{(l_t^1)^\omega}{\omega}}{h_t^1-\bar{h}_t}=p_t^h \tag{4}$$

$$(l_t^1)^{\omega-1}=w_t \tag{5}$$

$$\frac{c_{t+1}^1-\frac{(l_{t+1}^1)^\omega}{\omega}}{c_t^1-\frac{(l_t^1)^\omega}{\omega}}=\beta R_t \tag{6}$$

where $R_t \equiv 1/q_t$. Condition (4) equates type-1's marginal rate of substitution between non-health and health consumption to the corresponding relative price. Condition (5) equates the marginal disutility of labor supply to the real wage. Condition (6) equates the intertemporal marginal rate of substitution in consumption to the real return on public debt.

The second type of agents are the workers who are a fraction $\gamma_2 \equiv 1-\gamma_1$ of the unit-mass of agents. The optimization problem of a single type-2 agent is given by:

$$\max_{\{c_t^2,l_t^2,h_t^2\}} \sum_{t=0}^{\infty}\beta^t\left(a\ln\left(c_t^2-\frac{(l_t^2)^\omega}{\omega}\right)+(1-a)\ln(h_t^2-\bar{h}_t)\right), \tag{7}$$

subject to this budget constraint,

$$c_t^2+p_t^h h_t^2=w_t l_t^2+tr_t. \tag{8}$$

Here, c_t^2 and h_t^2 are consumption of non-health and health goods by an agent of type 2, respectively, and l_t^2 is its labor supply. Type-2 agents collect income only from wages ($w_t l_t^2$) and from government transfers in the amount tr_t per agent.

The first-order conditions of the above problem reduce to the following optimality conditions:

$$\frac{1-a}{a}\frac{c_t^2-\frac{(l_t^2)^\omega}{\omega}}{h_t^2-\bar{h}_t}=p_t^h, \tag{9}$$

$$(l_t^2)^{\omega-1}=w_t. \tag{10}$$

Condition (9) equates type-2's marginal rate of substitution between non-health and health consumption to p_t^h. Condition (10) equates the marginal disutility of labor supply to the real wage.

3.1.2 Firms

All firms are identical and the representative firm's optimization problem is:

$$\max_{m_t,L_t} \quad \Pi_t=(m_t K)^{1-\alpha}L_t^\alpha-w_t L_t-\chi_0\frac{m_t^{\chi_1}}{\chi_1}K \tag{11}$$

subject to the technlogical constraint on utilization,

$$m_t \le \bar{m}, \tag{12}$$

Covid Economics 70, 25 February 2021: 1-48

where L_t is aggregate labor demand and $\bar{m}$ is the technologically-feasible maximum rate of utilization, which is assumed to be nonbinding. Since the capital stock is constant, utilization costs $\left(\chi_0 \frac{m_t^{\chi_1}}{\chi_1} K\right)$ can be seen as the standard cost associated to faster depreciation at higher utilization or as a rental cost that increases with utilization.

The first-order conditions of the above problem yield standard marginal-productivity conditions for labor demand and the utilization rate:

$$(1-\alpha)(m_t K)^{-\alpha} L_t^{\alpha} = \chi_0 m_t^{\chi_1 - 1}, \tag{13}$$

$$\alpha(m_t K)^{1-\alpha} L_t^{\alpha-1} = w_t. \tag{14}$$

The marginal products of utilization and labor equal their marginal costs. For the former, the cost is determined by the firm's utilization choice and for the latter the cost is the market wage rate.

3.1.3 Government Budget Constraint

The government budget constraint is the following:

$$T_t - TR_t = D_t - q_t D_{t+1}, \tag{15}$$

The left-hand-side is the primary balance, which equals aggregate tax revenue, T_t, minus total transfer payments, TR_t. The right-hand-side equals the repayment of existing debt net of the resources raised by selling new debt.

The fiscal structure could be simplified by abstracting from public debt so that transfers to type-2 agents are paid by lump-sum taxes paid by type-1 agents and the government's budget is balanced each period. Debt is introduced just so that we can highlight some implications of debt-financed transfers for fiscal solvency, but the two formulations are equivalent because the taxes are non-distortionary (i.e. debt is Ricardian). For a given policy of transfers funded with lump-sum taxes, the debt-equivalent formulation (without taxes) is given by the sequence of debt issuance $q_t D_{t+1} = D_t + TR_t$, starting from a given initial debt D_0. The debt formulation requires, however, that the intertemporal government budget constraint must hold, so the present discounted value of the primary balance as of any date t must match the outstanding debt as of that date. Hence, if it is optimal to increase transfers during a pandemia (as we show later) and the transfers are debt-financed, the debt accumulated during the j periods of the pandemia (D_{j+1}) is sustainable only if the stream of primary balances for $t > j$ increases so that their present value equals D_{j+1}, which can be accomplished by imposing lump-sum taxes on type-1 agents.

3.1.4 Competitive Equilibrium with and without Pandemia

The decentralized competitive equilibrium (DCE) is defined by sequences of individual allocations $\{c_t^1, c_t^2, h_t^1, h_t^2, l_t^1, l_t^2, d_{t+1}^1\}_{t=0}^{\infty}$, aggregate allocations $\{m_t, L_t, C_t, \Pi_t\}_{t=0}^{\infty}$, and prices $\{R_t, p_t^h, w_t\}_{t=0}^{\infty}$ such that: (a) the optimality conditions of type-1 and type-2 agents hold, (b) the optimality conditions

Covid Economics 70, 25 February 2021: 1-48

of the representative firm hold, (c) the following market-clearing conditions:

$$\gamma_1 l_t^1 + \gamma_2 l_t^2 = L_t, \tag{16}$$

$$\gamma_1 h_t^1 + \gamma_2 h_t^2 = H, \tag{17}$$

and (d) the following aggregation conditions hold:

$$\gamma_1 d_{t+1}^1 = D_{t+1}, \tag{18}$$

$$\gamma_1 \tau_t = T_t \tag{19}$$

$$\gamma_2 tr_t = TR_t, \tag{20}$$

$$\gamma_1 h = H, \tag{21}$$

$$\gamma_1 \pi_t = \Pi_t \tag{22}$$

$$\gamma_1 c_t^1 + \gamma_2 c_t^2 = C_t. \tag{23}$$

The budget constraints of the agents, the definition of profits and the above market-clearing and aggregation conditions yield the following resource constraint:

$$C_t = (m_t K)^{1-\alpha} L_t^{\alpha} - \chi_0 \frac{m_t^{\chi_1}}{\chi_1} K. \tag{24}$$

Since the only shock to the economy is the unanticipated, temporary hike in $\bar{h}_t$ during the pandemia, and since there are no endogenous mechanisms to induce dynamics, the DCE separates into pandemia (P) and no-pandemia (NP) phases, and within each prices and allocations are constant. The DCE has a closed-form solution. To characterize the DCE solution, consider first that, since preferences are identical, labor is homogeneous, and all agents are paid the same wage, conditions (5) and (10) imply that all agents offer the same labor supply, which must equal labor demand at equilibrium: $l_t^1 = l_t^2 = L_t$. Therefore, using the labor demand and supply conditions, considering that both must be equal at the equilibrium wage, yields this expression:

$$L_t^{\omega-1} = \alpha (m_t K)^{1-\alpha} L_t^{\alpha-1}, \tag{25}$$

This condition together with the firm's optimality condition for utilization yields the following expression for the labor allocation as a function of the utilization rate:

$$L_t = \left(\frac{\chi_0 \alpha K}{1-\alpha} \right)^{\frac{1}{\omega}} m_t^{\frac{\chi_1}{\omega}}. \tag{26}$$

Using the above result, factor allocations can be solved for using conditions (13) and (14):

$$m_t = m^{\star} = \left(\chi_0^{\alpha-\omega} \alpha^{\alpha} (1-\alpha)^{\omega-\alpha} K^{\alpha(1-\omega)} \right)^{\frac{1}{\chi_1 \omega + \alpha\omega - \omega - \chi_1 \alpha}} \tag{27}$$

Covid Economics 70, 25 February 2021: 1-48

$$L_t = l_t^1 = l_t^2 = L^\star = \left(\chi_0^{\alpha-1}\alpha^{\chi_1+\alpha-1}(1-\alpha)^{1-\alpha}K^{(1-\alpha)(\chi_1-1)}\right)^{\frac{1}{\chi_1\omega+\alpha\omega-\omega-\chi_1\alpha}}. \tag{28}$$

Given the above, it is straightforward to obtain equilibrium solutions for output, profits, wages and aggregate consumption using other optimality conditions and the resource constraint:

$$Y_t = Y^\star = (m^\star K)^{1-\alpha}L^{\star\alpha} \tag{29}$$

$$\Pi_t = \gamma_1\pi^\star = (1-\alpha)(1-\frac{1}{\chi_1})Y^\star > 0 \tag{30}$$

$$w_t = w^\star = (L^\star)^{\omega-1} \tag{31}$$

$$C_t = C^\star = Y^\star - \chi_0\frac{(m^\star)^{\chi_1}}{\chi_1}K. \tag{32}$$

Note two important properties of the aggregate DCE allocations, profits and wages solved above: First, they are independent of heterogeneity and inequality in wealth, income and consumption, as is evident by the fact that γ_1 and γ_2 do not enter in the solutions. Second, they are the same during the P and NP phases (i.e. for $t = 0, ..., j$ and for $t > j$).

In contrast with the aggregate allocations, *individual* consumption allocations of health and non-health goods and the relative price of those goods differ in the P and NP phases in the DCE. The equilibrium prices are:

$$p_t^{\star hP} = \frac{1-a}{a}\frac{C^\star - \frac{(L^\star)^\omega}{\omega}}{H - h^\star - f(m^\star K)} \quad \textit{for t=0, ..., j,} \tag{33}$$

$$p_t^{\star hNP} = \frac{1-a}{a}\frac{C^\star - \frac{(L^\star)^\omega}{\omega}}{H - h^\star} \quad \textit{for t>j.} \tag{34}$$

Prices are higher during the pandemia because of the direct effect on demand for health goods and services due to higher $\bar{h}_t$. In turn, this rise in $p_t^{\star hP}$ worsens income inequality because it increases the value of the endowment of health goods owned by type-1 agents.

The solutions of the consumption allocations across agents are straightforward applications of the linear expenditure system implied by the Stone-Geary preferences. In particular, using conditions (4) and (9) together with the budget constraints of the two types of agents and the above results for aggregate variables we can obtain solutions for the individual consumption allocations as functions of relative prices and the subsistence demand for health:

$$c_t^{\star 1}(p_t^{\star h}, \bar{h}_t) = a\left[\pi^\star + p_t^{\star h}h - \tau_t + (L^\star)^\omega - p_t^{\star h}\bar{h}_t - \frac{(L^\star)^\omega}{\omega}\right] + \frac{(L^\star)^\omega}{\omega} \tag{35}$$

$$c_t^{\star 2}(p_t^{\star h}, \bar{h}_t) = a\left[tr_t + (L^\star)^\omega - p_t^{\star h}\bar{h}_t - \frac{(L^\star)^\omega}{\omega}\right] + \frac{(L^\star)^\omega}{\omega} \tag{36}$$

$$h_t^{\star 1}(p_t^{\star h}, \bar{h}_t) = \frac{1-a}{p_t^{\star h}}\left[\pi^\star + p_t^{\star h}h - \tau_t + (L^\star)^\omega - p_t^{\star h}\bar{h}_t - \frac{(L^\star)^\omega}{\omega}\right] + \bar{h}_t \tag{37}$$

Covid Economics 70, 25 February 2021: 1-48

$$h_t^{\star 2}(p_t^{\star h}, \bar{h}_t) = \frac{1-a}{p_t^{\star h}} \left[tr_t + (L^\star)^\omega - p_t^{\star h}\bar{h}_t - \frac{(L^\star)^\omega}{\omega} \right] + \bar{h}_t \tag{38}$$

Expressing individual consumption allocations as functions of $(p_t^{\star h}, \bar{h}_t)$ is useful because these are the only two variables that cause the allocations to differ in the P and NP phases. Both $\bar{h}_t$ and $p_t^{\star h}$ are higher in the P phase, affecting individual consumption allocations as explained below.

Assume $tr_t = 0$ (i.e. a DCE without transfers either in normal times or during the pandemia), or alternatively, assume that transfers are unchanged when the pandemia hits. It follows from (36) that $c^{\star 2P}(p^{\star hP}, h^\star + f(m^\star K)) < c^{\star 2NP}(p^{\star hNP}, h^\star)$, because $p_t^{\star h}\bar{h}_t$ rises during the pandemia and the rest of the variables that determine non-health consumption of type-2 agents are unaffected by the pandemia. The intuition is that type-2 agents need to redirect some of their income to pay for the subsistence level of health, which increased both in quantity and in price. Since aggregate consumption $C^\star$ is unchanged, it must be that $c^{\star 1P}(p^{\star hP}, h^\star + f(m^\star K)) > c^{\star 1NP}(p^{\star hNP}, h^\star)$. For these agents, the rise in the value of the endowment of health goods exceeds the increase in the cost of the subsistence level of health. Hence, during a pandemia, non-health consumption of type-1 (type-2) agents rises (falls). The same applies to excess non-health consumption relative to the disutility of labor. It rises for type-1 agents and falls for type-2 agents.

The responses of health consumption differ from those of non-health consumption. In particular, h_t^2 rises but h_t^1 falls. The direct effect of higher $\bar{h}_t$ on demand for health goods is the same for both agents, but the income effect of higher p_t^h reducing the real value of income is stronger for entrepreneurs as the value of profits from the non-health sector in units of health goods falls. Excess health consumption (i.e., net of $\bar{h}_t$) falls for both agents, however, because even for type-2 agents the adverse income effects of higher prices imply that the increase in $\bar{h}_t$ exceeds that in h_t^2. Overall, type-2 agents suffer more with the pandemia, because they always consume less of all goods than type-1 agents and the pandemia causes their excess consumption of both health and nonhealth goods to fall, while for type-1 agents excess consumption of non-health goods rises.

The need to keep consumption of all goods above their subsistence levels imposes an upper bound on the set of $p_t^{\star hP}$ that can be supported as a DCE. In particular, the results in (36) and (38) imply that, in order for type-2 agents to keep $h_t^{\star 2}$ and $c_t^{\star 2}$ above $\bar{h}_t$ and L_t^ω/ω, respectively, their residual income must satisfy: $tr_t + (L^\star)^\omega - p_t^{\star h}\bar{h}_t - \frac{(L^\star)^\omega}{\omega} > 0$. Solving for $p_t^{\star hP}$ yields:

$$p_t^{\star hP} < \hat{p}^{\star hP} \equiv \frac{tr^P + (L^\star)^\omega \left(\frac{\omega-1}{\omega}\right)}{h^* + f(m^\star K)} \tag{39}$$

where tr^P is a given value of exogenous transfers provided during the pandemia. Hence, the jump in $p_t^{\star hP}$ caused by $f(m^\star K)$ during a pandemia cannot reach $\hat{p}^{\star hP}$, because otherwise type-2 agents hit their subsistence consumption levels triggering the Inada conditions of their preferences. The market price, which depends on the aggregate demand for health goods, would still be well-defined by condition (33), but it cannot be an equilibrium because type-2 agents saturate the health system.

Combining the above result with the pricing condition (33) implies that $f(\cdot)$ cannot exceed this

upper bound:

$$f(m^\star K) < \frac{H}{1+\frac{1-a}{a}\frac{c^\star-(L^{\star\omega})/\omega}{trP+(\omega-1)(L^{\star\omega})/\omega}} - h^*, \tag{40}$$

where $c^\star, L^\star, m^\star$ are the DCE allocations independent of $f(\cdot)$ (see eqns. (27), (28) and (32)).

If debt is used to pay for transfers, the real interest rate is solved for by plugging the solutions obtained above in the Euler equation of type-1 agents (eq. (6)). Since $L^\star$ is constant at all times, and since consumption of type-1 agents shifts from a higher level in the P phase to a lower level in the NP phase, the interest rate equals $1/\beta$ in all periods except between $t+j$ and $t+j+1$ (the transition from pandemia to non-pandemia). The interest rate on debt sold that period is:

$$R_{t+j} = \frac{c^{\star 1NP}_{t+j+1} - \frac{(L^\star)^\omega}{\omega}}{\beta\left(c^{\star 1P}_{t+j} - \frac{(L^\star)^\omega}{\omega}\right)}. \tag{41}$$

Hence, given that $c^{\star 1P} > c^{\star 1NP}$, the interest rate falls in the last period of the pandemia.

Finally, to characterize the effects of the pandemia on consumption inequality, it is useful to focus on the ratio of excess consumption of type-1 to type-2 agents denoted $\Omega^\star_t$. Dividing eq. (35) by (36), or (37) by (38), yields:

$$\Omega^\star_t = \frac{\pi^\star + p^{\star h}_t h - \tau_t + (L^\star)^\omega - p^{\star h}_t \bar{h}_t - \frac{(L^\star)^\omega}{\omega}}{tr_t + (L^\star)^\omega - p^{\star h}_t \bar{h}_t - \frac{(L^\star)^\omega}{\omega}} \tag{42}$$

Across the two types of agents in the DCE, this ratio is the same for non-health consumption or for health consumption, and the ratio itself satisfies $\Omega^\star_t > 1$. This is clearly true for the DCE without transfers, and when transfers are present it holds because we assume that $\tau_t < \pi^\star + p^{\star h}_t h$ (i.e. per-capita transfers never exceed the non-wage income of type-1 agents). Moreover, the ratio is constant at different levels with and without pandemia, and satisfies $\Omega^{\star P} > \Omega^{\star NP}$ so that consumption inequality worsens temporarily with a pandemia.

Since both agents supply the same labor, collect the same wages, and have the same $\bar{h}$, the movements in $\Omega^\star_t$ also capture the changes in income inequality due to the pandemia. Type-1 agents own the firms and the endowment of H, so their income includes, in addition to wages, the profits from non-health goods production and the sales of health goods. The adverse effect of the pandemia on income inequality occurs because the hike in the relative price of health goods induces regressive income redistribution as the income from sales of those goods that type-1 agents collect rises.

3.2 Social Planner's Problem

The social planner solves the following optimization problem:

$$\max_{\{c^j_t, l^j_t, h^j_t, m_t\}} \quad \phi\left\{\gamma_1 \sum_{t=0}^{\infty}\beta^t\left[a\ln\left(c^1_t - \frac{(l^1_t)^\omega}{\omega}\right) + (1-a)\ln(h^1_t - \bar{h}_t)\right]\right\}$$
$$+ (1-\phi)\left\{\gamma_2 \sum_{t=0}^{\infty}\beta^t\left[a\ln\left(c^2_t - \frac{(l^2_t)^\omega}{\omega}\right) + (1-a)\ln(h^2_t - \bar{h}_t)\right]\right\} \tag{43}$$

Covid Economics 70, 25 February 2021: 1-48

subject to resource constraints on labor, health goods, and non-health goods, the technological constraint on utilization, and the subsistence demand for health:

$$\gamma_1 l_t^1 + \gamma_2 l_t^2 = L_t,$$

$$\gamma_1 h_t^1 + \gamma_2 h_t^2 = H,$$

$$\gamma_1 c_t^1 + \gamma_2 c_t^2 \equiv C_t = (m_t K)^{1-\alpha} L_t^{\alpha} - \chi_0 \frac{m_t^{\chi_1}}{\chi_1} K,$$

$$m_t \leq \bar{m},$$

$$\bar{h}_t = h^{\star} + z_t f(m_t K).$$

The social welfare function is standard, with weight ϕ $(1-\phi)$ on type-1 (type-2) agents, and the ratio of these weights is denoted $\Omega^{sp} \equiv \phi/(1-\phi)$. As in the DCE, $\bar{m}$ is assumed to be nonbinding.

3.2.1 Socially Optimal Allocations

The social planner's equilibrium (SPE) can be characterized as the set of allocations that satisfy the constraints of the planner's problem and the following optimality conditions:

$$l_t^1 = l_t^2 = L_t = \left(\alpha (m_t K)^{1-\alpha}\right)^{\frac{1}{\omega-\alpha}} \tag{44}$$

$$(1-\alpha)\left(\frac{L_t}{m_t K}\right)^{\alpha} = \chi_0 m_t^{\chi_1 - 1} + \frac{1-a}{a}\frac{(C_t - \frac{L_t^{\omega}}{\omega})}{H - \bar{h}_t} z_t f'(m_t K). \tag{45}$$

$$\frac{h_t^1 - \bar{h}_t}{h_t^2 - \bar{h}_t} = \Omega^{sp} \tag{46}$$

$$\frac{c_t^1 - \frac{(l_t^1)^{\omega}}{\omega}}{c_t^2 - \frac{(l_t^2)^{\omega}}{\omega}} = \Omega^{sp} \tag{47}$$

The planner sets allocations at two different constant levels for the P and NP phases. As we show below, aggregate allocations are lower in the P phase. The conditions in (44) show that the planner aligns with the DCE in that it allocates the same labor supply to both agents, and the total labor allocation equates the marginal disutility of labor with the marginal product of labor.

Conditions (45)-(47) are essential to this paper's argument. Condition (45) determines the planner's optimal utilization choice and it drives the planner's incentive to lockdown the economy. It differs from its counterpart—equation (13) in the DCE—in that, during a pandemia, the social marginal cost of utilization in the right-hand-side of (45) exceeds its private counterpart by the amount $p_t^{h,sp} f'(m_t K)$ where $p_t^{h,sp} \equiv \frac{1-a}{a}\frac{(C_t - \frac{L_t^{\omega}}{\omega})}{H - \bar{h}_t}$ is the social price of health goods. Hence, utilization is inefficiently chosen in the DCE during a pandemia, because firms do not internalize the marginal social cost of utilization. This cost exceeds the private one because of the marginal social value of lowering utilization to relax the degree of saturation of the health system by hampering the increase in $\bar{h}_t$ due to the pandemia. As a result, the planner reduces utilization and this reduces

Covid Economics 70, 25 February 2021: 1-48

labor demand, output, profits and wages, giving rise to the output-pandemia tradeoff.

The SPE does not have a closed-form solution because of the non-linear nature of condition (45). Using this condition together with (44), the optimal utilization rate (i.e. the optimal lockdown) can be represented as the solution to the following non-linear equation in m_t:

$$(1-\alpha)\left(\frac{\left(\alpha(m_tK)^{1-\alpha}\right)^{\frac{1}{\omega-\alpha}}}{m_tK}\right)^{\alpha}-\chi_0 m_t^{\chi_1-1}= \\ \frac{1-a}{a}\left[\frac{(m_tK)^{1-\alpha}\left(\left(\alpha(m_tK)^{1-\alpha}\right)^{\frac{\alpha}{\omega-\alpha}}\right)-\chi_0\frac{m_t^{\chi_1}}{\chi_1}K-\frac{\left(\left(\alpha(m_tK)^{1-\alpha}\right)^{\frac{\omega}{\omega-\alpha}}\right)}{\omega}}{H-\bar{h}_t}\right]z_t f'(m_tK). \quad (48)$$

Without pandemia, $z_t=0$ and this equation collapses to the closed-form solution for utilization in the DCE, because there is no externality affecting the choice of m_t. Labor, output, and aggregate consumption are therefore the same as well. During the pandemia, utilization is lower because of its higher marginal social cost, but notice that it retains the property of the DCE that it is independent of individual allocations and now also of the planner's welfare weights. As a result, the planner's aggregate allocations for labor and production in the pandemia phase also retain this property.

The above results imply that in this model the utilization externality and the optimal lockdown do not interact with the planner's incentives to redistribute (i.e., with inequality and agent heterogeneity). The planner's utilization choice depends on $f'(m_tK)$ and $p_t^{h,sp}$, which are determined by aggregate variables. The planner determines first aggregate utilization and non-health GDP and then allocates health and non-health GDP to keep the ratios of excess consumption across agents equal to each other and equal to Ω^{sp}.[12] This also implies that the planner's aggregate allocations and the utilization externality are identical in a representative-agent version of the model (i.e., for $\gamma_1=1$).

Conditions (46) and (47) are important because they drive the planner's incentives to redistribute resources across agents during the pandemia. The planner sets the (inverse) ratios of marginal utilities of health and non-health consumption across agents equal to the ratio its welfare weights. The extent to which redistribution is relevant depends on the extent to which Ω^{sp} differs from $\Omega^{\star P}$ and $\Omega^{\star NP}$ (recall that in the DCE we showed that $\Omega^{\star P}>\Omega^{\star NP}>1$).

Consider three scenarios. First, a case with $\Omega^{sp}=1$ (i.e. $\phi=1/2$). This corresponds to a utilitarian social welfare function in which the planner weighs each agent equally.[13] The planner redistributes resources so as to equalize consumption of health and non-health goods across agents. Second, a case with $\Omega^{sp}=\Omega^{\star NP}$ (i.e. $\phi=\Omega^{\star NP}/(1+\Omega^{\star NP})$). This is an application of the First Welfare Theorem in which the DCE without pandemia is supported as an SPE.[14] The planner has no

[12] The resource constraints and conditions (46) and (47) imply also that $p_t^{h,sp}=(c_t^i-\frac{(l_t^i)^\omega}{\omega})/(h_t^i-\bar{h}_t)$ for $i=1,2$.

[13] In this case, ϕ can be ignored because it becomes a common factor for the utility of both agent types in the social welfare function, and the planner's allocations become independent of ϕ.

[14] This is evident because with $\Omega^{sp}=\Omega^{\star NP}$ and $z_t=0$ for all t the SPE's optimality conditions are identical to those of the DCE without pandemia.

Covid Economics 70, 25 February 2021: 1-48

incentive to redistribute without a pandemia, but will still want to redistribute during a pandemia because $\Omega^{sp} = \Omega^{\star NP} < \Omega^{\star P}$. Third, a case with $\Omega^{sp} > \Omega^{\star NP}$ (i.e. $\Omega^{\star NP}/(1+\Omega^{\star NP}) < \phi \leq 1$). This is a case with bias in favor of entrepreneurs, because the planner weighs type-1 agents by more than what the inequality implicit in $\Omega^{\star NP}$ indicates. We will show later that when this is the case it is possible for the optimal policies to be Pareto efficient (i.e. the lifetime utility of both agents increases relative to the DCE). In light of these results, the analysis that follows focuses on $\Omega^{sp} \in [1, \infty)$ (or $\phi \in [1/2, 1]$).

It is worth noting that if $\phi < \Omega^{\star NP}/(1+\Omega^{\star NP})$, the planner will engage in redistribution in favor of type-2 agents relative to the DCE even without pandemia. Still, the optimal transfers solely due to the pandemia can be separated from the those that are optimal in "normal times" so as to focus on the *additional* redistribution that is socially desirable when a pandemia hits.

Given the above intuition for the utilization externality and the distributional incentives of the planner, we can now characterize the solution of the planner's problem when the pandemia is present. The solution to the non-linear equation (48) yields the planner's optimal utilization rate m_t^{sp}, and once it is known it can be used to determine the rest of the SPE allocations: L_t^{sp}, C_t^{sp}, c_t^{1sp}, c_t^{2sp}, h_t^{1sp}, and h_t^{2sp}. It is evident that there are no distributional incentives affecting the utilization choice because ϕ, γ_1 and γ_2 do not enter in eq.(48). The higher social marginal cost of utilization leads the planner to reduce m_t^{sp}. Condition (44) then implies that aggregate and individual labor allocations fall, and since both labor and utilization fall, output and C_t also fall. This is again the output-pandemia tradeoff: The planner internalizes that by reducing utilization it weakens the pandemia, but it also takes into account that lowering utilization has output and consumption costs.

The drops in utilization, output and consumption chosen by the planner trigger distributional incentives, because as C_t^{sp} falls, the planner wants to keep consumption ratios aligned with Ω^{sp}. Given the SPE's aggregate allocations, the planner assigns to type-2 agents these consumption allocations:

$$c_t^{2sp} = \frac{C_t^{sp} - \frac{(L_t^{sp})^{\omega}}{\omega}}{1+\gamma_1(\Omega^{sp}-1)} + \frac{(L_t^{sp})^{\omega}}{\omega}, \tag{49}$$

$$h_t^{2sp} = \frac{H - h^* - z_t f(m_t^{sp} K)}{1+\gamma_1(\Omega^{sp}-1)} + h^* + z_t f(m_t^{sp} K). \tag{50}$$

The denominators of the first terms in the right-hand-side of the above expressions are equal to 1 for the utilitarian planner (since $\Omega^{sp} = 1$), and the solutions give the consumption levels that are common for all agents. For $\Omega^{sp} > 1$, these expressions yield consumption levels for type-2 agents that are lower than for type-1 agents. Type-2 (type-1) agents receive "below average" ("above average") consumption levels so that market-clearing in health and non-health goods holds. As explained earlier, the size of Ω^{sp} determines the degree of consumption inequality that is optimal for the planner. For $\Omega^{sp} = \Omega^{\star NP}$ (recall $\Omega^{\star NP} > 1$), this yields the same consumption allocations and the same inequality as in the DCE so that no redistribution is optimal without a pandemia.

Covid Economics 70, 25 February 2021: 1-48

Covid Economics 70, 25 February 2021: 1-48

3.2.2 Decentralization & Optimal Policies

The social planner's allocations can be implemented as a competitive equilibrium by imposing a lockdown (i.e. a binding limit on utilization) and providing transfers to type-2 agents. The optimal design of these two policies is characterized below.

Optimal Lockdown: The planner's optimal utilization rate can be decentralized using various instruments to correct the utilization externality. Since COVID-19 arrived as a large, unexpected shock that required an urgent response to the threat of saturation of health systems, it is reasonable to consider a lockdown as the policy instrument, instead of standard policy instruments (e.g. taxes) that would have been too slow and cumbersome to implement. The optimal lockdown is obtained by implementing the following policy rule:

$$m_t \leq m_t^{sp} \quad \textit{for t=0, ..., j,} \tag{51}$$

$$m_t \leq \bar{m} \quad \textit{for t>j.} \tag{52}$$

Since the utilization externality increases the marginal cost of utilization relative to the DCE and $\bar{m}$ is not binding in the DCE, it must be the case that $m_t^{sp} < m^\star < \bar{m}$ for $t = 0, ..., j$. Recall also that in the DCE, $m^\star$ is the optimal utilization rate with or without pandemia and that, since there is no utilization externality without pandemia, $m_t^{sp} = m^\star$ for $t > j$.

Optimal Transfers: By imposing the planner's health and non-health consumption allocations for type-2 agents (eqns. (49) and (50)) on these agents' budget constraint in the DCE solution (eq. (8)), it follows that the optimal policy rules for government transfers during and post the pandemia are

$$TR_t^{sp,P} = \gamma_2 \left[\left\{ \frac{C_t^{sp} - \frac{(L_t^{sp})^\omega}{\omega}}{1+\gamma_1(\Omega^{sp}-1)} + \frac{(L_t^{sp})^\omega}{\omega} + p_t^{h,sp} \left(\frac{H - h^* - f(m_t^{sp}K)}{1+\gamma_1(\Omega^{sp}-1)} + h^* + f(m_t^{sp}K) \right) \right\} - (L_t^{sp})^\omega \right] \quad \textit{for t= 0, ..., j,} \tag{53}$$

$$TR_t^{sp,NP} = \gamma_2 \left[\left\{ \frac{C^\star - \frac{(L^\star)^\omega}{\omega}}{1+\gamma_1(\Omega^{sp}-1)} + \frac{(L^\star)^\omega}{\omega} + p^{\star h} \left(\frac{H - h^*}{1+\gamma_1(\Omega^{sp}-1)} + h^* \right) \right\} - (L^\star)^\omega \right] \quad \textit{for t>j.} \tag{54}$$

In the expressions inside square brackets, the terms in braces represent the total value of nonhealth and health consumption of type-2 agents, and the term $(L_t^{sp})^\omega$ is these agents' wage income. Hence, the optimal transfer finances the gap between the planner's desired allocation of total consumption to type-2 agents and the wages they collect (all in units of nonhealth goods). The optimal transfers are constant at different levels in the P and NP phases, just like the SPE's allocations.

The planner takes into account that a pandemia always worsens income inequality (even with an optimal lockdown), as it increases the market income of type-1 agents relative to that of type-2 agents, since the latter only earn wages while the former collect profits and sales of H in addition

to wages. The planner internalizes that the relative price of health goods rises, making health-good purchases costlier and income from selling health goods larger, and that without policy intervention the overall result of these effects would move type-2 agents closer to their subsistence levels of health and non-health goods. To correct for this, the planner intervenes to redistribute income and consumption from type-1 to type-2 agents by more than it does in normal times without pandemia. If $\Omega^{sp} = \Omega^{\star NP}$, there is no redistribution in normal times ($TR^{sp,NP} = 0$), but the planner still redistributes during the pandemia. Hence, the planner has incentives to intervene in the DCE so as to both reduce utilization (to tackle the utilization externality) and redistribute resources across agents (to redistribute the decline in aggregate output across agents and maintain their ratio of excess consumptions equal to Ω^{sp}).

The planner chooses m_t^{sp} independently of inequality but it is critical to note that the lockdown itself contributes to mitigate the effects of the pandemia on inequality. This is because the lockdown reduces the spike in the price of health goods that drives the regressive effect on income and thereby mitigates the increase in consumption inequality too. As a result, the lower $p_t^{h,sp}$ that results from the lockdown reduces the size of the transfers that the planner needs to provide during the pandemia, as equation (53) shows.

As explained earlier, the planner can pay for the optimal transfers during the pandemia with lump-sum taxes on type-1 agents maintaining a balanced budget, or it can finance them by selling debt to those agents. Using debt, the equilibrium interest rates would be given by $R_t = 1/\beta$ for $t = 0, .., j-1$ or $t > j$ and $R_j = (c_{j+1}^{1sp} - \frac{(L_{j+1}^{sp})^{\omega}}{\omega}) / \left[\beta(c_j^{1sp} - \frac{(L_j^{sp})^{\omega}}{\omega})\right]$. Since transfers are constant during the pandemia and the interest rate differs from $1/\beta$ only in period j, the planner would arrive at the end of the pandemia with a debt stock $D_{j+1}^{sp} = (1/R_j)\left[TR^{sp,P}\sum_{i=0}^{j-1}\beta^i + \beta^{j-1}D_0\right]$. In order to maintain fiscal solvency after the pandemia (i.e. satisfy the intertemporal government budget constraint), the government can impose lump-sum taxes T_t for $t > j$ such that the present discounted value of tax revenue equals D_{j+1}^{sp}. The specific sequence of these taxes is undetermined. Any sequence that satisfies the solvency condition yields the same outcome because the taxes are non-distortionary. For instance, since $R_t = 1/\beta$ for $t > j$, a constant lump-sum tax $\bar{T} = (1-\beta)D_{j+1}^{sp}$ satisfies the solvency condition. A tax paying all the debt in one period ($T_{j+1} = D_{j+1}^{sp}$) is also consistent with solvency, but is akin to a default in which the government "pays" all the debt at $t = j+1$ by simply taxing away the entire debt repayment. The planner has no reason to prefer either debt or taxes to pay for transfers during the pandemia, or any particular sequence of taxes post-pandemia consistent with solvency, since they all yield identical allocations and welfare (i.e. there is Ricardian equivalence). In contrast, with distortionary taxes, given the pre-pandemia structure of tax rates, the planner's problem is more complex because it would consider the optimal structure and time-variation of tax rates. When further restricted to time-invariant tax rates, it would consider how dynamic Laffer curves limit sustainable debt levels (see D'Erasmo et al., 2016).

3.3 Social Welfare & Private Utility Gains:

In order to compare the utility that agents derive under the SPE relative to the DCE, define $\Delta U_i \equiv U_i^{SPE} - U_i^{DCE}$ for agents of type $i = 1, 2$ where U_1 and U_2 are the lifetime utility functions shown in (2) and (7). Then, denoting excess consumption levels as $\tilde{C}_t \equiv C_t - L_t^{\omega}/\omega$ and $\tilde{h}_t \equiv h_t - \bar{h}_t$ and using the results from the SPE and the DCE yields these expressions:

$$\begin{aligned}\Delta U_1 = &\sum_{t=0}^{j} \beta^t \left[a \left(\ln\left(\tilde{C}_t^{sp}\right) - \ln\left(\tilde{C}^{\star}\right) \right) + (1-a) \left(\ln\left(\tilde{h}_t^{sp}\right) - \ln\left(\tilde{h}_t^{\star}\right) \right) \right] \\ &+ \left[\sum_{t=0}^{j} \beta^t \left(\ln\left(\frac{\Omega^{sp}}{1+\gamma_1(\Omega^{sp}-1)} \right) - \ln\left(\frac{\Omega^{\star P}}{1+\gamma_1(\Omega^{\star P}-1)} \right) \right) \right. \\ &\left. + \frac{\beta^j}{1-\beta} \left(\ln\left(\frac{\Omega^{sp}}{1+\gamma_1(\Omega^{sp}-1)} \right) - \ln\left(\frac{\Omega^{\star NP}}{1+\gamma_1(\Omega^{\star NP}-1)} \right) \right) \right],\end{aligned} \tag{55}$$

$$\begin{aligned}\Delta U_2 = &\sum_{t=0}^{j} \beta^t \left[a \left(\ln\left(\tilde{C}_t^{sp}\right) - \ln\left(\tilde{C}^{\star}\right) \right) + (1-a) \left(\ln\left(\tilde{h}_t^{sp}\right) - \ln\left(\tilde{h}_t^{\star}\right) \right) \right] \\ &+ \left[\sum_{t=0}^{j} \beta^t \left(\ln\left(\frac{1}{1+\gamma_1(\Omega^{sp}-1)} \right) - \ln\left(\frac{1}{1+\gamma_1(\Omega^{\star P}-1)} \right) \right) \right. \\ &\left. + \frac{\beta^j}{1-\beta} \left(\ln\left(\frac{1}{1+\gamma_1(\Omega^{sp}-1)} \right) - \ln\left(\frac{1}{1+\gamma_1(\Omega^{\star NP}-1)} \right) \right) \right].\end{aligned} \tag{56}$$

Using these results, the change in social welfare (ΔW) under the SPE allocations with the optimal lockdown and transfer policies relative to the unregulated DCE allocations can be expressed as:

$$\Delta W = \phi\gamma_1 \Delta U_1 + (1-\phi)\gamma_2 \Delta U_2. \tag{57}$$

Thus, the change in social welfare attained by the optimal policies equals the valuation of the individual lifetime utility changes valued using the social welfare function.

To obtain a cardinal measure of ΔW, we follow the standard procedure of expressing welfare gains in terms of a compensating variation in consumption. In particular, we calculate the percentage increase in consumption of non-health goods common across households and time periods (Λ) that would be needed for the DCE to yield the same social welfare as under the SPE allocations. That is, we compute the value of Λ that solves this equation:

$$\begin{aligned}&\phi \sum_{t=0}^{\infty} \beta^t \gamma_1 \left(a \ln\left(c_t^{1\star}(1+\Lambda) - \frac{(L_t^{\star})^{\omega}}{\omega} \right) + (1-a)\ln(h_t^{1\star} - \bar{h}_t) \right) \\ &\quad + (1-\phi) \sum_{t=0}^{\infty} \beta^t \gamma_2 \left(a \ln\left(c_t^{2\star}(1+\Lambda) - \frac{(L_t^{\star})^{\omega}}{\omega} \right) + (1-a)\ln(h_t^{2\star} - \bar{h}_t) \right) = W^{sp}\end{aligned} \tag{58}$$

where W^{sp} is given by eq. (43) evaluated at the SPE allocations. Note that, while the duration of the pandemia does not alter allocations and prices in the DCE and SPE (it only determines when the

Covid Economics 70, 25 February 2021: 1-48

Covid Economics 70, 25 February 2021: 1-48

economy switches from the P to the NP phase), it does matter for the size of all of these individual utility and social welfare effects. In particular, the effects of the pandemia on social welfare and individual utility are larger for pandemias that last longer.

The term in the first row in the right-hand-side of equations (55)-(56) for ΔU_1 and ΔU_2 is the same, because it represents the aggregate effects of the planner's management of the output-pandemia tradeoff by neutralizing the utilization externality. Since, as we showed earlier, the SPE's aggregate allocations are independent of inequality, this term depends only on aggregate allocations and not on their distribution across agents. In the DCE, aggregate labor and consumption of non-health goods are constant at the same level in the P and NP phases, so that $\tilde{C}^{\star}$ is constant at all times. During the pandemia, however, aggregate excess health goods consumption ($\tilde{h}_t^{\star}$) falls because of the increase in $\bar{h}_t$ for $t = 0, .., j$. The utilization externality implies that these allocations are suboptimal. Hence, during the pandemia the planner lowers the utilization rate, which reduces $\tilde{C}_t^{sp}$ but props-up $\tilde{h}_t^{sp}$. The post-pandemia phase washes out from this term, because, as explained earlier, for all $t > j$ there is no utilization externality and hence the aggregate allocations of labor, non-health output and consumption of both goods are the same in the DCE and SPE.

The second and third rows in the right-hand-side of ΔU_1 and ΔU_2 reflect the distributional effects, with the parts due to the P and NP phases shown in the second and third rows, respectively. $\Omega^{\star P} > \Omega^{\star NP} \geq \Omega^{sp}$ is a sufficient condition for these effects to be negative for ΔU_1 and positive for ΔU_2. These distributional effects are determined by a collection of constant terms that depend on γ_1 and the marginal utility ratios of the planner (Ω^{sp}) vis-a-vis those in the DCE ($\Omega^{\star P}, \Omega^{\star NP}$).[15] The terms for the pandemia phase reflect the result justifying increased transfers to type-2 agents during the pandemia, because the distribution of resources for health and nonhealth consumption is suboptimal and worsens during the pandemia (since $\Omega^{\star P}$ rises). The terms for the post-pandemia phase show that, as explained earlier, the planner redistributes resources to type-2 agents even without a pandemia (as long as $\Omega^{sp} < \Omega^{\star NP}$).

For quantitative analysis, expressions (55) and (56) provide an intuitive way of separating the social welfare gain into key components: First, the gains due to correcting the efficiency loss affecting aggregate allocations via the utilization externality. Second, the gains due to the socially optimal redistribution during a pandemia (which also depend partially on the utilization externality, since a larger externality implies more inequality in the DCE). Third, the gains due to redistribution even without a pandemia, because of the planner's dislike for inequality in general.

Evaluating ΔU_1 and ΔU_2 separately from social welfare is also helpful for assessing whether the optimal policy is Pareto efficient (i.e. $\Delta U_1, \Delta U_2 \geq 0$). For this to be the case, the utility gain for type-1 agents from correcting the aggregate effects of the utilization externality must exceed their loss due to the redistribution in favor of type-2 agents. A heuristic argument suggests that, for given social welfare weights, the SPE can be Pareto efficient if γ_1 is sufficiently high. Start with some γ_1 that yields a particular $\Omega^{*NP}(\gamma_1)$ and assume we set $\Omega^{sp} = \Omega^{*NP}(\gamma_1)$. As we increase γ_1 keeping Ω^{sp} fixed, the

[15] In the $[1, \infty)$ interval of Ω^{sp}, the utilitarian planner ($\Omega^{sp} = 1$) has the strongest desire for reallocating resources. All the terms that include Ω^{sp} vanish from $\Delta U_1, \Delta U_2$, which implies that the second and third rows of ΔU_1 (ΔU_2) take their most negative (positive) values. In particular, comparing the second rows of the two expressions shows that the planner has the strongest desire to redistribute when the pandemia hits, relative to scenarios with $\Omega^{sp} > 1$.

utility of type-1 agents rises (locally) because the cost of redistribution falls, since the second row of ΔU_1 increases (becomes less negative) and the third row is zero (since $\Omega^{sp} = \Omega^{*NP}(\gamma_1)$). The result is not general, however, because the redistribution costs and ΔU_1 are nonlinear functions of γ_1, but as we verify in the numerical example below, it is possible to have a paremeterization such that for given Ω^{sp} there is an interval of γ_1 values such that $\Delta U_1, \Delta U_2 \geq 0$.

4 Quantitative Analysis

In this section, we study the model's quantitative predictions by examining numerical solutions based on a calibration to U.S. data.

4.1 Calibration

Table 4 lists the model's calibrated parameter values. The values of all of the parameters, except those of the Stone-Geary utility and the $f(mK)$ function, are easy to set following a conventional calibration approach. The model is set to a quarterly frequency with a standard discount factor of $\beta = 0.99$. The Frisch elasticity of labor supply is set to 2, which is also a standard value in the literature, and since the Frisch elasticity in the model is $1/(\omega - 1)$, we obtain $\omega = 1.5$. The labor share in production is set to $\alpha = 0.7$, which is a common value based on historical U.S. data. Utilization is normalized so that $m = 1$ without pandemia, which is equivalent to full capital utilization. The depreciation (or utilization cost) function is modified slightly to adopt a formulation typical of dynamic macro models (see Mendoza et al., 2014): $\delta(m_t) = \chi_0 \frac{m_t^{\chi_1}}{\chi_1}$. Without pandemia, since $m_t = 1$, the capital depreciation rate satisfies $\delta = \frac{\chi_0}{\chi_1}$, where δ is set to a depreciation rate of 0.0164 per quarter, consistent with the calibration to U.S. data in Mendoza et al. (2014) and D'Erasmo et al. (2016). The capital stock is set to $K = 6.04$, which is consistent with a capital-GDP ratio of 3. The value of χ_0 then follows from the DCE optimality condition for capital utilization, which yields $\chi_0 = (1-\alpha)(L(K,m)/K)^{\alpha} = 0.10$, where $L(K,m)$ is the solution to eq. (25) for $K = 6.04$ and $m = 1$, and then the condition that $\delta = \frac{\chi_0}{\chi_1}$ yields $\chi_1 = 6.10$. Finally, $\gamma_1 = 0.2$ because the top quintile of the U.S. wealth distribution owned nearly 90 percent of the wealth in 2017 (Leiserson et al., 2019), and for simplicity we focus on the case in which $\Omega^{sp} = \Omega^{\star NP}$, so that the SPE supports the DCE without pandemia and there is no incentive to redistribute except when a pandemia hits.

To calibrate the Stone-Geary preferences, we normalize the endowment of health goods so that $H = 1$. Hence, $h^\star$ represents the percent of the available supply of health goods that constitutes subsistence demand in normal times. The value of $h^\star$ is set by estimating a standard linear-expenditure-system regression of nominal expenditures of health goods and services on nominal expenditures of non-health goods and services and the price of health goods. This regression follows from the pricing condition for the NP phase, eq. (34), using the resource constraint for non-health goods and the market-clearing condition for health goods.[16] The value of $h^\star$ corresponds to the coefficient on

[16] After simplifying terms, combining these expressions yields $p^h H = \frac{1-a}{a}\left(1 - \frac{\delta(\cdot)K}{Y} - \frac{\alpha}{\omega}\right) Y + h^\star p^h$.

Covid Economics 70, 25 February 2021: 1-48

p_t^h, which yields $h^\star = 0.0948$ with a standard error of 0.0235 and a p-value of 0.0002.[17]

Table 4: Calibration to U.S. Data

Parameter	Value	Reference
β	0.99	Standard for quarterly frequency
ω	1.5	Frisch Elasticity of labor supply equals 2
α	0.7	Standard labor share
K	6.04	Capital stock to match K/GDP=3
$m^\star$	1	Normalization
χ_0	0.10	Optimality condition for utilization with $m^\star = 1$
χ_1	6.10	1.64% depreciation rate, Mendoza et al. (2014)
γ_1	0.2	Top quintile owns 90% of U.S. wealth in 2017, Leiserson et al. (2019)
H	1	Normalization
$h^\star$	0.0948	Linear-expenditure-system regression
a	0.756	Average nonhealth-to-health consumption and GDP ratios, 2009-2018
θ	0–0.1069	Interval that supports DCE solutions

The share of non-health expenditures a is determined by imposing on the same pricing condition (34) the estimated value of $h^\star = 0.0948$ and the average ratios of non-health to health consumption and non-health to health GDP for the period 2009-2018, which are 5.01 and 4.73, respectively. We use 2009-2018 data because they yield stable averages for these ratios, after several years in which both fell steadily. This yields $a = 0.756$.

The last item that needs to be specified is the function $f(m_t K)$ that maps utilization into subsistence health demand during a pandemia. As noted earlier, the function is assumed to be monotonically increasing. A concave (convex) $f(\cdot)$ would represent an economy in which reductions in utilization are less (more) effective at reducing the stress on the health system during a pandemia. For simplicity, we assume a linear function $f(m_t K) = \theta m_t K$, so that the elasticity of $\bar{h}$ with respect to mK is equal to θ. We know little about θ, but given the value of K, equation (40) yields an upper bound $\tilde{\theta}$ at which health demand of type-2 agents equals their subsistence demand and there is no DCE solution with pandemia. Hence, we will study model solutions for $\theta \in [0, \tilde{\theta})$. Moreover, within this interval, we examine detailed solutions for the value of θ that makes the drop in U.S. non-health GDP observed during the pandemia consistent with an optimal lockdown. Matching the decline of 8.8 percent in U.S. non-health GDP in the second quarter of 2020 relative to the first quarter as part of the SPE solution requires $\theta = 0.0918$. The corresponding utilization rate is 0.848 and hence $f(mK) = 0.0918 \times 0.848 \times 6.04 = 0.47$. Thus, accounting for the observed non-health GDP drop as the result of an optimal lockdown implies a sharp increase in subsistence demand for health from 9.48 to $9.48 + 47 = 56.4$ percent of the available supply.

[17] The regression uses data for 1960-2018. Expenditures are proxied by GDP of health and non-health goods. The price index corresponds to the GDP deflator for the health sector (obtained from the BLS). Expenditures are expressed as indexes with the same base year as the deflator. Other time series used are Total National Health Expenditures, Health Investment, Health Consumption Expenditures, obtained from the National Health Expenditure database of the Centers for Medicaid and Medicare Services (CMS), and Nominal GDP and Gross Private Domestic Investment, obtained from the BLS and BEA, respectively. The regression is estimated in second differences, because non-health expenditures are integrated of order two, reflecting the sharp growth of the health sector relative to the rest of the U.S. economy.

Covid Economics 70, 25 February 2021: 1-48

4.2 Results

Table 5 shows a set of results for the calibration with $\theta = 0.0918$. Column (I) shows the equilibrium without pandemia, for which $\text{DCE}_{NP} = \text{SPE}_{NP}$ since DCE and SPE are the same in normal times. Column (IV) is the SPE solution for the pandemia that rationalizes the observed output drop as resulting from an optimal lockdown (SPE_P). Columns (II) and (III) show two DCE solutions: Column (II) is the NL case studied in Section 3, in which utilization is unaffected by the pandemia ($\text{DCE}_{P,NL}$), and Column (III) is the OL case with an ad-hoc lockdown of the same size as the optimal lockdown ($\text{DCE}_{P,OL}$). Tr is unchanged from the normal-times level in both DCE solutions. Column (I) is in levels and the rest are percent changes relative to NP levels, except m and Tr/GDP for which we show percentage points changes and Ω and $\bar{h}$ which are always in levels.

Table 5: Competitive & Social Planner's Equilibria for $\theta = 0.0918$

Variable	(I) Normal Times (*levels*) $\text{DCE}_{NP} = \text{SPE}_{NP}$	(II) No Lockdown (*percent changes*) $\text{DCE}_{P,NL}$	(III) Observed Lockdown (*percent changes*) $\text{DCE}_{P,OL}$	(IV) Social Planner (*percent changes*) SPE_P
Aggregate variables:				
Ω	3.46	16.46	9.54	3.46
$\bar{h}$	0.09	0.65	0.56	0.56
GDP^{NH}	2.01	0	-8.84	-8.84
m	1	0	-15.18	-15.18
l	1.26	0	-5.99	-5.99
π	0.5	0	1.85	1.85
c	1.91	0	-6.02	-6.02
w	1.12	0	-3.04	-3.04
p^h	0.35	157.76	101.1	101.1
Individual variables:				
c_1	3.2	51.91	30.54	-4.93
c_2	1.59	-26.07	-24.38	-6.57
h_1	2.19	-6.02	-4.35	-28.25
h_2	0.7	4.71	3.4	22.08
$\tilde{c}_1$	2.26	73.49	46.92	-3.3
$\tilde{c}_2$	0.65	-63.55	-46.73	-3.3
$\tilde{h}_1$	2.1	-32.69	-26.94	-51.92
$\tilde{h}_2$	0.61	-85.86	-73.51	-51.92
Transfers & Welfare				
Tr/GDP (%)	14.5	-2.74	-1.00	10.85
Welfare Gain (%)	n.a.	n.a.	n.a.	0.82 (0.33)
ΔU_1	n.a.	n.a.	n.a.	-2.06 (-1.65)
ΔU_2	n.a.	n.a.	n.a.	4.08 (2.35)

Notes: The "Normal Times" column shows the equilibrium without pandemia (DCE and SPE are identical because the calibration assumes $\Omega^{sp} = \Omega^{\star NP}$). Allocations and prices in the Observed Lockdown and No Lockdown scenarios are reported as percent changes relative to Normal Times, except $\bar{h}$ and Ω are shown in levels and m and Tr/GDP are differences in percentage points relative to their normal-times values. Welfare gains, ΔU^1 and ΔU^2 are as defined in the text. Welfare gains assume the pandemia lasts four quarters and are relative to the No Lockdown scenario with values in parenthesis relative to the Observed Lockdown scenario.

The aggregate allocations for $\text{DCE}_{P,OL}$ and SPE_P show that the 8.8 percent output drop during the pandemia is associated with a cut in m of 15 percentage points and declines in consumption

Covid Economics 70, 25 February 2021: 1-48

and labor of about 6 percent. For the planner, the cut in m is the optimal response to the utilization externality. Profits of the non-health sector rise 1.9 percent because of reduced utilization costs. Subsistence health demand climbs from 0.09 to 0.56, as explained earlier, and the relative price of health goods rises 101.1 percent, because aggregate excess consumption of health goods falls much more than for non-health goods. Without lockdown, the results for aggregate allocations in the DCE$_{P,NL}$ differ from the NP phase only in that the relative price rises sharply, by nearly 158 percent. This is larger than in the OL and planner's solutions because there is no cut in utilization moderating the spike in subsistence health demand, which climbs to 0.65 instead of 0.56.

Regarding individual allocations, recall that the planner has weights set so as to match the ratio of excess consumptions across agents without pandemia ($\Omega^{sp} = 3.46$). Hence the planner cuts excess consumptions of each agent by the same percentage relative to the NP state (-3.3 and -51.9 percent for non-health and health goods, respectively). In levels, however, the planner reduces entrepreneurs' consumption of both goods (-4.9 and -28.3 percent for non-health and health goods, respectively), while for workers it reduces non-health consumption by -6.6 percent but increases health consumption by 22.1 percent. The planner spreads the drop in the aggregate supply of non-health goods triggered by the optimal lockdown relatively evenly across agents, while the contrast of the large drop it assigns to health consumption for entrepreneurs v. the large increase for workers is in response to the planner's strong incentive to redistribute so as to keep $\Omega^{sp} = 3.46$. This redistribution requires an increase in the ratio of transfers to GDP of nearly 11 percentage points, which would be even larger without the strong valuation effect driving up the relative value of health GDP. Assuming the pandemia lasts four quarter, the optimal lockdown and transfers policies increase welfare by 0.82 percent, which is a sizable gain.

Inequality worsens sharply in the NL scenario, with Ω^{*P}_{NL} rising to 16.5. This large increase in excess consumption inequality results from $\tilde{c}$ increasing (falling) by 73.5 (-63.6) percent for type-1 (type-2) agents. Since labor supply and labor disutility are the same for both agents, this implies that nonhealth consumption also rises sharply for type-1 agents and falls sharply for type-2 agents. Regarding excess health consumption, $\tilde{h}$ falls much less for type-1 than type-2 agents (-32.7 v. -85.9 percent, respectively). Hence, the pandemia moves workers closer to the subsistence demand for health at a much faster pace than entrepreneurs. Income inequality also worsens sharply as result of the large increase in the value of the endowment of health goods that type-1 agents own. Transfers are unchanged in levels from the NP state, but since the value of GDP rises with p^h, transfers as a share of GDP fall by -2.7 percentage points.

The OL equilibrium with the ad-hoc lockdown (Column (III)) performs better than the NL case but it is still inferior to the optimal policy scenario. The ad-hoc lockdown yields the same aggregate allocations and prices as for the planner. Importantly, it also moderates the adverse effects of the pandemia on inequality. The ratio of excess consumptions rises to $\Omega^{*P}_{OL} = 9.5$, instead of 16.5 in the NL case, and this is possible because both $\bar{h}$ and p^h increase less. The latter implies that income inequality also worsens less in the OL than the NL case.[18] The implied weaker valuation effect also

[18]Note that wage income falls by the same amount for both agents, since they supply the same labor at the same wage, and that the small increase in profits worsens income inequality but it is dwarfed by the effect of the smaller hike in p^h.

implies that transfers (which are constant at the NP level) fall less as a share of GDP, by 1 percentage point instead of 2.7. The SPE yields a welfare gain of 0.33 percent relative to this OL case, and since the gain relative to the NL case was 0.82, it follows that the lockdown alone yields a welfare gain of about 50 basis points and the transfers add 32. Thus, roughly 3/5ths of the total welfare gain produced by the optimal policies is due to the lockdown. Keep in mind, however, that the lockdown has effects both on aggregate efficiency (by tackling the utilization externality) and on inequality (by moderating the hikes in $\bar{h}$ and p^h). Thus, the ad-hoc lockdown does help mitigate the adverse inequality effects of the pandemia but not nearly enough as is socially optimal.

The results in Table 5 are for $\theta = 0.0918$, which was targeted to match the observed 2020Q2 fall in U.S. non-health GDP. We acknowledge, however, that there is substantial parameter uncertainty regarding the value of θ. Hence, we turn now to examine the full spectrum of solutions for the interval of θ values that support competitive equilibria. As noted earlier, this is possible for $\theta \in [0, \tilde{\theta})$ where $\tilde{\theta}$ is the upper bound at which health consumption of workers hits the subsistence level. Under the calibration to U.S. data, the DCE with no lockdown yields $\tilde{\theta} = 0.1069$.

Figure 4 shows utilization and non-health GDP. The blue curves show the SPE solutions, the black lines show the DCE under the NL case (for which aggregate allocations are invariant in θ), and the red lines show the OL solutions for the DCE with an ad-hoc lockdown of the same size as the optimal lockdown that matches the drop in U.S. non-health GDP. The black and red dots denote the solutions shown in Table 5. By construction, the red dots must be at the intersection of the blue curves with the red lines (i.e., an ad-hoc lockdown of the same size as the optimal lockdown). The dashed, red vertical lines identify $\tilde{\theta}$. The DCE lines are discontinuous at that point because there is no DCE solution when $\theta = \tilde{\theta}$.

Figure 4: Utilization and Non-Health Output in Pandemia as θ Varies

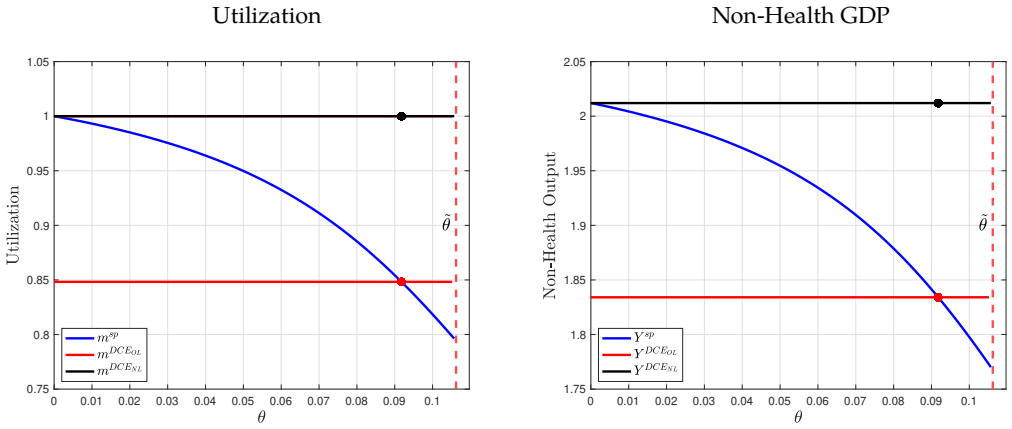

Figure 4 shows that the planner's optimal reductions in utilization and non-health GDP are concave in θ. Hence, as the elasticity of subsistence health demand to utilized capital rises, the optimal lockdown in response to a pandemia increases with θ at a faster rate. Scenarios with low θs are un-

likely to be relevant. They represent weak pandemias for which $\bar{h}$ varies little in response to cuts in m (i.e., social distancing is not that important to alter contagion) and as a result small cuts in utilization and output, namely weak lockdowns, would suffice to address the utilization externality. This is captured in the Figure by the small gap between the black lines that correspond to the NL solutions and the blue curves of the planner's solutions for $\theta < 0.05$.

Pandemias become relevant as θ rises above 0.05. In this region, the concavity of the planner's choices has a key implication: Small "errors" in measuring θ result in non-trivial errors in the utilization and output cuts adopted to respond to a pandemia. The gaps between the blue and red curves illustrate how these errors vary as the "true" value of θ varies if the lockdown that would be optimal for $\theta = 0.0918$ is adopted. If θ is in fact slightly smaller (larger) the lockdown would be too strict (weak) and non-health GDP would be allowed to fall too much (little) relative to what is truly optimal. For example, if $\theta = 0.08$, the ad-hock lockdown of the OL line would cut utilization and output by 3.2 and 2.3 percentage points more than what is optimal, respectively. Relative to pre-pandemia levels, utilization and output would fall by 15.2 and 8.8 percentage points, respectively, compared with optimal drops of 12 and 6.5 percentage points each.

An alternative interpretation of Figure 4 is as indicative of the implications of cross-country or cross-region heterogeneity in health systems and other relevant pre-pandemia conditions (like income per capita, life expectancy, etc.). Countries with weaker pre-pandemia conditions can be viewed as countries with higher θ, and hence faced with a pandemia they require larger optimal lockdowns which imply larger output drops. The relative size of the health sector also captures cross-country differences in health systems. Equation (48) implies that the utilization externality is weaker in countries where H is larger, and hence for the same θ the optimal lockdown and output drop would be smaller in these countries. The same applies to countries where a is larger.

The two plots in Figure 5 show how the rise in p^h and the worsening consumption inequality due to a pandemia vary with θ in the SPE (in blue) and in the DCE cases for no-lockdown (in black) and the ad-hock lockdown (in red) that matches the observed decline in non-health GDP. Black and red dots denote again the NL and OL outcomes in Table 5. The planner chooses higher prices for θ values that would make the optimal lockdown of Table 5 excessive ($\theta < 0.0918$), and lower prices when the opposite occurs. In contrast, the SPE price hikes are always smaller than those for the no-lockdown DCE case, because the planner reduces utilization and this moderates the increase in the relative price. Prices are nearly linear in θ for the planner but they are convex for both DCE cases, and hence small errors in assessing the value of θ to implement lockdowns would result in large differences in price hikes during pandemias.

The price hikes are quite large overall, except for θ values that result in negligible drops in utilization and output. In line with the argument that pandemias are weak for $\theta < 0.05$, prices in the no-lockdown DCE scenario are negligibly different from those produced under the optimal policies for those θ values. For $\theta > 0.05$, the optimal policy yields price hikes of at least 45 percent and as much as 105 percent. Price hikes in the no-lockdown DCE case are uniformly higher, ranging from 50 to 230 percent. Hence, the model predicts large relative price movements during pandemias.

The graph for the ratios of excess consumption (plotted in a logarithmic scale) shows a constant

CEPR PRESS

Ω^{sp} for the planner, which follows from the welfare weights calibrated to match the value of Ω in the DCE without pandemia (3.46). During the pandemia, consumption inequality is sharply higher in the DCEs for the NL and OL scenarios than for the planner, and it worsens at an increasing rate as θ rises driven by the rising p^h and the worsening income inequality. For θ ranging between 0.05 and 0.1, the values of Ω in the NL (OL) scenario are in the 6-37 (5-12.5) range, much larger than the 3.46 ratio in normal times. Consumption inequality is higher in the NL than the OL case because the NL case lacks the effect of the ad-hoc lockdown moderating the increase in p^h and the rise of income inequality in the OL case.

The left panel of Figure 6 shows the optimal transfers and the social welfare gain of the optimal lockdown and transfers policies as θ varies. Transfers are plotted as the change in the transfers-GDP ratio relative to normal times ($\Delta Tr/GDP$) and welfare is measured relative to the no-lockdown DCE assuming a 4-quarter pandemia. $\Delta Tr/GDP$ rises monotonically because consumption inequality increases with θ (see Figure 5) and strengthens the incentives to redistribute income and consumption across agents so as to maintain the ratio of excess consumptions at $\Omega^{sp} = 3.46$. $\Delta Tr/GDP$ is small for weak pandemias but for $\theta > 0.05$ increases in transfers from 5 to 13 percentage points of GDP are optimal.[19] Similarly, weak pandemias yield negligible welfare gains from implementing the optimal policies, but for $\theta > 0.05$ the welfare gains are a sharply convex function of θ and grow infinitely large as θ approaches $\tilde{\theta}$, because at that point workers hit the Inada condition for health consumption in the Stone-Geary preferences. This plot also shows that the nonlinear effects of implementing policies with measurement error in θ discussed earlier have nonlinear welfare implications. For instance, around $\theta = 0.0918$, which is the value that renders the observed GDP decline consistent with the optimal policy, if the "true" θ is slightly lower (higher) the welfare gain is much smaller (larger).

Figure 5: Relative Prices and Consumption Inequality in Pandemia as θ Varies

Relative Price of Health Goods

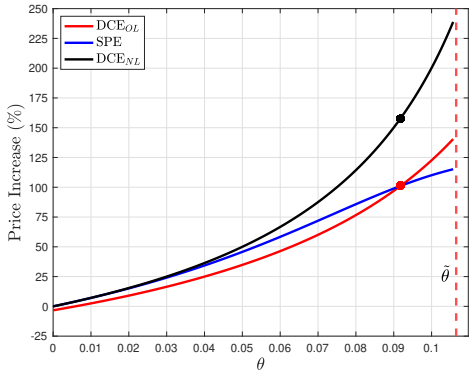

Excess Consumption Ratios

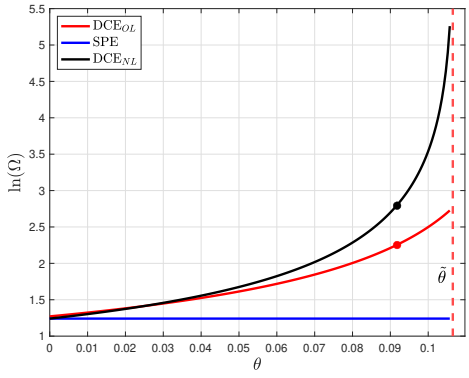

[19] Recall that $\Delta Tr/GDP$ captures both the effect of the exogenous change in transfers and the endogenous response of GDP to the optimal policies. The valuation effect of higher p^h reduces the ratio.

Covid Economics 70, 25 February 2021: 1-48

The right panel of Figure 6 shows a decomposition of the welfare gains in terms of the fractions due to changes in aggregate allocations and redistribution across agents. The contribution of removing the inefficiency in aggregate allocations is always much smaller than the contribution due to redistribution, which highlights again the relevance of the effects of pandemias on inequality in the model. As θ rises, the contribution from changes in aggregate allocations shrinks and that from redistribution rises, because inequality is also increasing in θ. The aggregate inefficiencies account at most for about 11 percent of the welfare gains, and that is for very small welfare gains corresponding to weak pandemias. Redistribution accounts for 88 to 96 percent of the welfare gains. This is again because type-2 agents move closer to their subsistence level of health consumption as θ rises and as this happens they approach the Inada condition that makes the marginal utility of allocating health consumption to them infinitely large. For the optimal policy reported in Table 5, the contribution of redistribution is close to 92 percent. This result is not inconsistent with the previous finding showing that for that same optimal policy the gains from reducing m are larger than those from increasing Tr, because, as noted earlier, reducing m contributes to both improve aggregate efficiency and reduce inequality.

Figure 6: Transfers & Welfare Gains as θ Varies

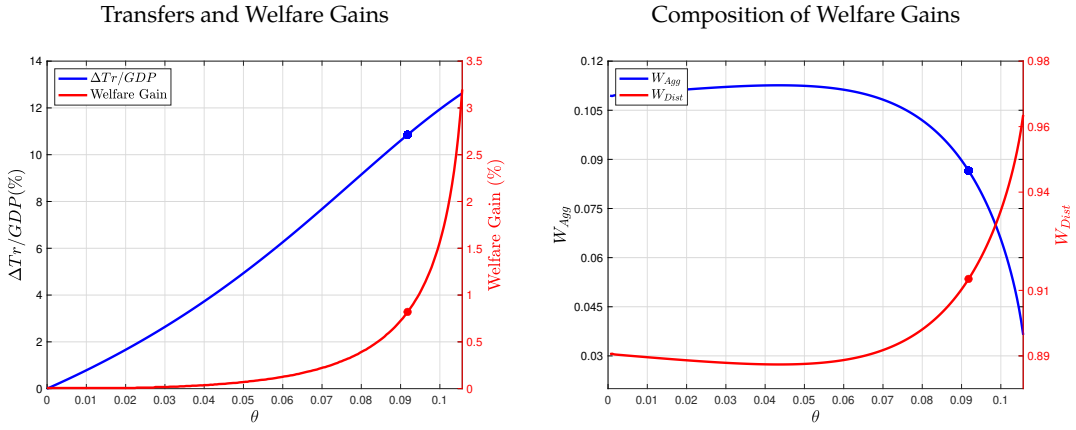

The role of inequality in these results can be illustrated further by examining the welfare implications of agent heterogeneity. Figure 7 compares social welfare gains of the optimal policies (relative to the no-lockdown DCE) as θ varies for the calibrated economy with $\gamma_1 = 0.2$ and the comparable representative-agent economy with $\gamma_1 = 1$. In the latter, the welfare gains are only due to the removal of the utilization externality. The DCE (SPE) aggregate allocations are the same as in the DCE (SPE) with two agents. Both welfare gains display the convex, asymptotic behavior as θ reaches $\tilde{\theta}$. The value of $\tilde{\theta}$, however, is about 60 percent bigger in the representative-agent model that has no inequality (since $\gamma_1 = 1$). This occurs because, as explained earlier, the pandemia moves workers

Covid Economics 70, 25 February 2021: 1-48

toward their subsistence health demand at a much faster pace than entrepreneurs, and hence the health system saturates at lower θ when inequality is present. At values of θ for which both models can be solved, the welfare gains of the optimal policies are negligible for the representative-agent model. A much stronger utilization externality, driven by higher θ values (above 0.14), would be needed in order to yield non-trivial welfare gains. At those values, however, the model would predict much larger falls in output than what has been observed (since the higher θ values would yield much larger utilization cuts).

Figure 7 also indicates that a pandemia of identical characteristics in terms of the elasticity of health subsistence to utilized capital is much more damaging for countries with higher levels of wealth inequality pre-pandemia (lower γ_1). The welfare implications of wealth inequality are also nonlinear, because the upper bound $\tilde{\theta}$ at which the health system saturates and the welfare gains of the optimal policies grow infinitely large is decreasing in γ_1.

Figure 7: Welfare Gains as θ Varies with Representative and Heterogeneous Agents

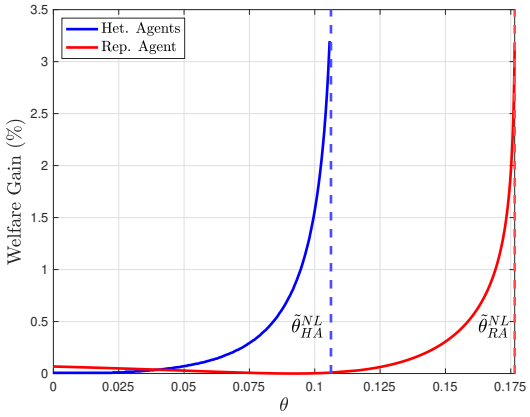

Notes: Welfare gains are computed relative to the no-lockdown DCE .

We discussed the implications of suboptimal policies resulting from parameter uncertainty or country heterogeneity related to the values of θ, H and a. We consider next policy errors due to ad-hoc deviations from the optimal transfers and lockdown policies that could be the result of political economy considerations, institutional flaws, or other frictions outside the model.

Figure 8 shows welfare costs from policies that deviate from the planner's optimal policies in the calibrated model (i.e., those reported in Table 5). To construct this Figure, we solve the DCE for arbitrary pairs of mandated utilization rates and increases in transfers, calculate the welfare gain that would be obtained by shifting to the planner's optimal policies, and plot the negative of that gain as the welfare cost of each arbitrary policy pair. The transfers policies span the 0-28% interval, defined in terms of increases relative to transfers in normal times in percent of the GDP of normal times ($\Delta Tr/GDP_{NP}$). We use a common value of GDP to scale Tr_P and Tr_{NP} in order to isolate

Covid Economics 70, 25 February 2021: 1-48

the change in transfers per-se (which is the policy instrument) from endogenous changes in GDP. The Figure shows curves for welfare costs as a function of $\Delta Tr/GDP_{NP}$ for four utilization rates $m = 0.6, 0.7, 0.85, 1$. The percent drops in non-health GDP associated with these utilization rates are 25, 18.2, 8.8 and 0, respectively. The curves are discontinuous because transfers that are too large would make excess consumption of type-1 agents negative. The SPE's optimal policies correspond to $m^{sp} = 0.85$ and $\Delta Tr/GDP_{NP}{}^{sp} = 12.7\%$. By construction, the maximum value for the curve corresponding to $m = m^{sp} = 0.85$ is $\Delta Tr/GDP_{NP}{}^{sp} = 12.7\%$ and there is zero welfare cost, because this point in the curve matches the SPE. Any deviation from this policy pair reduces welfare. As before, the red and blue dots correspond to the DCE solutions for the NL and OL cases in Table 5. The horizontal line identifies the welfare cost if there is no policy change when the pandemia hits.

Figure 8: Welfare Costs of Deviating from Optimal Policies

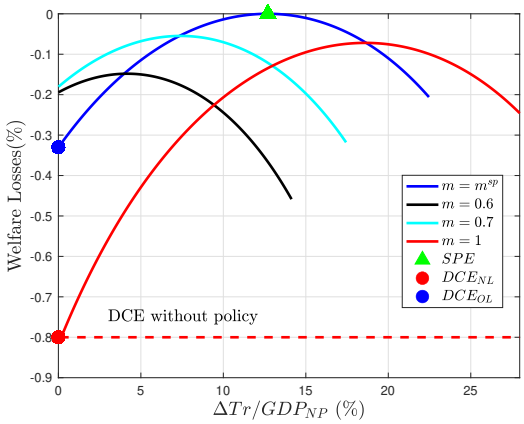

Note: The associated drops in nonhealth output with respect to the no-pandemia level are 8.84% for $m = m^{sp}$, 18.2% for $m = 0.7$ and 25% for $m = 0.6$.

This Figure yields two important results. First, deviating from the optimal policies can have non-trivial welfare costs but, for the set of policy pairs considered, policy intervention is always preferable to no intervention and mostly by a sizable margin. Relative to the DCE without policy intervention, welfare is at least 0.35 percent higher with all policy pairs except those with no lockdown ($m = 1$) and small transfer hikes (below 5 percentage points).[20] Note, however, that the ranking of the policies is not monotonic, as the crossing of the curves indicates: With low transfers, stricter lockdowns are better but as transfers increase stricter lockdowns are undesirable.

The second result is that transfers and lockdowns can be traded off widely at a small welfare cost. For instance, a no-lockdown policy with a transfers hike of 18 percentage points yields about the same welfare as one pairing a hike in transfers of about 5 percentage points with a strict lockdown

[20]Policies that reduce welfare below the DCE without policy changes require unrealistically large lockdowns ($m \leq 0.3$).

Covid Economics 70, 25 February 2021: 1-48

that reduces m to 0.7 and output by 25 percent, and both policy pairs are only about 0.08 percent below the SPE in terms of welfare. Even in a scenario in which only one instrument can be used, a hike in transfers of 18 percentage points without a lockdown is only about 0.1 of percent better than a lockdown setting $m = 0.6$ without increasing transfers. This is possible because either a large increase in transfers or a strict lockdown reduce the strong adverse effects on inequality caused by the pandemia. For the same reason, policies that combine weak lockdowns with small hikes in transfers are undesirable and the interaction of the two is nonlinear. For instance, the welfare loss resulting from changing from the optimal lockdown to no lockdown (i.e., the gap between the blue and red curves) grows larger as the size of the increase in transfers is reduced. This is again because both less strict lockdowns and weaker transfers programs allow the pandemia to worsen inequality more.

These results have important policy implications, because the data show that countries with high income per-capita have implemented much larger transfers policies and stricter lockdowns in response to COVID-19 than those with lower income. Data from the *IMF Fiscal Monitor* show that, through September 2020, the average increase in transfers for advanced economies reached 9.9 percent while for emerging and less developed countries the averages were 4.4 and 3 percent, respectively.[21] For the 53 countries included in the Bloomberg resilience indicator, the log of income per-capita has a correlation with the community mobility measure of -0.2 while the correlation with Covid-related transfers is 0.5. Hence, on average, poorer countries responded to COVID-19 with both weaker lockdowns and smaller fiscal interventions, which is the worst combination in the model.

The last graph, Figure 9, shows an important result regarding Pareto efficiency of the optimal policies. The plot shows how the lifetime utilities of type-1 and type-2 agents change under the SPE vis-a-vis the no-lockdown DCE as the fraction of type-1 agents rises. For each value of γ_1, we obtain the SPE and no-lockdown DCE solutions, keeping social welfare weights and θ at the levels used in Table 5 (i.e., $\Omega^{sp} = 3.46$ and $\theta = 0.0918$), and we plot ΔU_1 and ΔU_2. At the calibrated value of $\gamma_1 = 0.2$, the SPE yields $\Delta U_1 < 0$ and $\Delta U_2 > 0$. However, if γ_1 is slightly higher so that it falls within the shaded area in the Figure, both agents are better off under the SPE. Thus, as suggested in the previous section, given social welfare weights, the SPE can be Pareto efficient if γ_1 is sufficiently high so as to reduce the per-agent cost of redistribution for type-1 enough to make them better off but also not too high so that redistribution is insufficient to make type-2 agents better off. The per-agent cost of redistribution for type-1 agents falls with γ_1 because there are more agents of this type to share the cost and the SPE allocates less consumption of health and non-health goods to type-2 agents as γ_1 rises (see equations (49)-(50)).

[21] These data include additional and accelerated spending plus foregone and deferred revenue and exclude business liquidity support (equity injections, loans, asset purchases, debt assumptions, guarantees and quasi-fiscal operations).

Figure 9: Lifetime Utility Changes and Fraction of Type-1 Agents
(SPE relative to no-lockdown DCE)

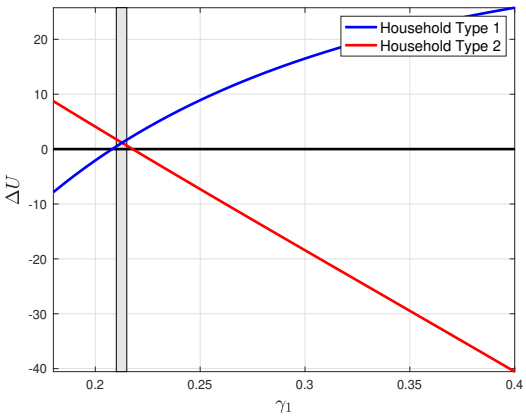

Notes: Utility changes under the SPE allocations relative to the no-lockdown DCE scenario.

5 Conclusions

This paper proposed a model of the macroeconomic effects of pandemias in which the saturation of the health system is the key driving force. This approach is motivated by evidence we provided on resouce shortages and capacity constraints of hospitals, sharp increases in the relative prices of key health goods and services, spikes in excess mortality beyond that explained by COVID-19, and a cross-country analysis showing that proxies for healtcare system saturation and the stringency of lockdowns are significant determinants of differences in the size of GDP drops caused by COVID-19, even after controlling for the effects of COVID infection and mortality.

Healthcare saturation is modeled by introducing Stone-Geary preferences with a jump in the subsistence demand for health goods and services during pandemias that is positively related to capital utilization. The model features entrepreneurs and workers in order to capture the effects of pandemias and lockdowns (i.e., mandated reductions in utilization) on consumption and income inequality. An output-pandemia tradeoff emerges because firms do not internalize that reducing utilization during a pandemia moves the healthcare system away from its saturation point. The pandemia moves workers closer and faster to the subsistence demand for health than entrepreneurs and it causes a sharp increase in the relative price of health goods and in the excess consumption ratio of entrepreneurs relative to workers. Lockdowns mitigate these adverse effects on inequality by mitigating the shock on subsistence health demand and its impact on the relative price of health. A planner with a standard social welfare function reduces utilization (to tackle the utilization externality) and redistributes consumption and income from entrepreneurs to workers (to keep the excess consumption ratio unchanged). Hence, the optimal policy that decentralizes the planner's allocations includes a lockdown and increased transfers to workers.

Covid Economics 70, 25 February 2021: 1-48

We examined the quantitative predictions of the model using numerical solutions for a calibration to U.S. data. Two key pieces of this calibration related to the subsistence demand for health are its level in normal times and its elasticity with respect to utilized capital. The former was determined using a linear-expenditure-system regression with pre-COVID-19 data, and for the latter we examined results for the interval of elasticity values that support competitive equilibria, since the elasticity has an upper bound at the level that drives workers to reduce their demand for health to the subsistence level. Within this interval, we also studied a set of results for which the elasticity is such that the observed decline in U.S. non-health GDP results from an optimal lockdown, which requires an elasticity of 0.09. This planner's solution was then compared with competitive equilibria in which policies are unchanged (the no-lockdown, NL, case) and in which a lockdown equal to the optimal one is implemented but transfers remained unchanged (the observed-lockdown, OL, case).

The results are indicative of the potential relevance of the proposed approach to study pandemias as a problem of health-system saturation and resource shortages and shed light on the challenges facing the design of lockdown and transfer policies to deal with pandemias. The effects of the pandemia on both aggregate efficiency and inequality are significant. For the scenario that rationalizes the observed output drop as an optimal policy, the welfare gains relative to the NL and OL cases are 0.82 and 0.33 percent, respectively. The optimal policy requires a cut in utilization of 15 percentage points (which yields a non-health output drop of 8.8 percent) and an increase in the transfers-GDP ratio of 10.9 percentage points. The relative price of health rises 101 percent under the optimal policies and the OL case, and 158 percent in the NL case. Inequality worsens very sharply during the pandemia, with the excess consumption ratio increasing by factors of 4.8 and 2.8 in the NL and OL cases, respectively. The difference between the two shows that lockdowns have strong effects on inequality, because even without transfers, a lockdown reduces the hike on subsistence health demand, which reduces the rises in relative prices and the excess consumption ratio.

Examining the set of solutions for the entire interval of feasible elasticities of subsistence health demand to utilized capital shows that the effects of pandemias on macro aggregates and inequality start to become relevant at elasticities higher than 0.05. The output-pandemia tradeoff yields concave, negative relationships between either the planner's optimal utilization or non-health output and that elasticity. Relative prices and excess consumption ratios in the NL and OL solutions, and the welfare gains under the optimal policies are increasing, convex functions of the elasticity. Hence, small measurement error in the value of this elasticity results in non-trivial differences on the magnitude of optimal lockdown and transfer policies and their effects.

The planner undoes the large negative effect of the pandemia on inequality through the direct effect of the transfers and the indirect effect of the lockdown (which mitigates the relative price hike and the rise of the excess consumption ratio). The two effects combined contribute over 90 percent of the welfare gains of the optimal policies. The aggregate effect of the lockdown removing the utilization externality accounts for the other 10 percent. Inequality also makes the model more plausible. A planner in a representative-agent version of the model only gains by removing the utilization externality and thus needs larger elasticities of subsistence health demand to utilized capital (above 0.13) in order to yield nontrivial welfare gains. But these elasticities would yield

Covid Economics 70, 25 February 2021: 1-48

unrealistically large output drops.

Deviating from the optimal policies has nontrivial welfare costs. However, policy intervention is preferable to no intervention for a large set of lockdown and transfer policy pairs. Moreover, transfers and lockdowns can be traded off widely at a small welfare cost, because either a large increase in transfers or a strict lockdown reduce the strong adverse effects of the pandemia on inequality. For the same reason, policies that combine weak lockdowns with small hikes in transfers are the worst choice. This result has important policy implications, because emerging and least developed countries responded to COVID-19 with both weaker lockdowns and smaller fiscal interventions than advanced economies. Income per capita has a correlation with lockdown effectiveness of roughly -0.2 whereas its correlation with Covid-related transfers is 0.5. The mean increase in transfers in advanced economies has been at least 2.25 times larger than in emerging and least developed countries.

Our results also have important implications for the analysis of cross-country or cross-region responses to COVID-19. The model predicts that a pandemia is more damaging for countries with higher wealth inequality and/or weaker health systems or other pre-pandemia conditions (e.g., income per capita, life expectancy, etc.). Weaker pre-pandemia conditions can be viewed as implying higher elasticities of subsistence health demand to utilized capital which imply larger optimal lockdowns and output drops. The relative size of the health sector also captures cross-country differences in health systems. For a given elasticity, the model predicts weaker effects of pandemias in countries with larger health sectors or larger shares of non-health expenditures.

This study is a first step in a research agenda exploring the saturation of the healthcare system as the mechanism driving macroeconomic models of pandemias. The model we presented is streamlined with the intent of highlighting the essential elements of this mechanism, leaving for further research enriching the model to explore dynamic and cross-country propagation, particularly in models with capital accumulation and financial frictions, and to study the interaction of optimal lockdown and transfer policies with optimal taxation and public debt sustainability.

Covid Economics 70, 25 February 2021: 1-48

References

Acemoglu, D., Chernozhukov, V., Werning, I., and Whinston, M. D. (2020). 'A Multi-Risk SIR Model with Optimally Targeted Lockdown'. NBER Working Paper No 27102.

Ajao, A., Nystrom, S., Koonin, L., Patel, A., Howell, D., Baccam, P., Lant, T., Malatino, E., Chamberlin, M., and Meltzer, M. (2015). 'Assessing the Capacity of the Healthcare System to Use Additional Mechanical Ventilators During a Large-scale Public Health Emergency'. *Disaster Medicine and Public Health Preparedness*, vol. 9, no. 6, 634–641.

Alvarez, F. E., Argente, D., and Lippi, F. (2020). 'A Simple Planning Problem for COVID-19 Lockdown'. NBER Working Paper No 26981 and *Covid Economics*, vol. 14, 1-32.

Arellano, C., Bai, Y., and Mihalache, G. P. (2020). 'Deadly Debt Crises: COVID-19 in Emerging Markets'. NBER Working Paper No 27275.

Atkeson, A. (2020). 'What Will Be the Economic Impact of COVID-19 in the US? Rough Estimates of Disease Scenarios'. NBER Working Paper No 26867.

Azzimonti, M., Fogli, A., Perri, F., and Ponder, M. (2020). 'Pandemic Control in ECON-EPI Networks'. NBER Working Paper No 27741.

Baqaee, D., Farhi, E., Mina, M., and Stock, J. (2020). 'Reopening Scenarios'. NBER Working Paper No 27244.

Bloom, D. E., Kuhn, M., and Prettner, K. (2020). 'Modern Infectious Diseases: Macroeconomic Impacts and Policy Responses'. NBER Working Paper No 27757.

Bodenstein, M., Corsetti, G., and Guerrieri, L. (2020). 'Social Distancing and Supply Disruptions in a Pandemic'. Finance and Economics Discussion Series 2020-031 and *Covid Economics*, vol. 19, 1-52.

Britton, T. (2010). 'Stochastic Epidemic Models: A Survey'. *Mathematical Biosciences*, vol. 225, 24–35.

Cakmakli, C., Demiralp, S., Kalemli-Ozcan, S., Yesiltas, S., and Yildirim, M. A. (2020). 'COVID-19 and Emerging Markets: An Epidemiological Model with International Production Networks and Capital Flows'. NBER Working Paper No 27191.

Céspedes, L. F., Chang, R., and Velasco, A. (2020). 'Macroeconomic Policy Responses to a Pandemic'. Working Paper.

Chetty, R., Friedman, J. N., Hendren, N., Stepner, M., and Team, T. O. I. (2020). 'How Did COVID-19 and Stabilization Policies Affect Spending and Employment? A New Real-Time Economic Tracker Based on Private Sector Data'. NBER Working Paper No 27431.

D'Erasmo, P., Mendoza, E., and Zhang, J. (2016). 'What is a Sustainable Public Debt?' *Handbook of Macroeconomics*, vol. 2, 2493–2597.

Eichenbaum, M. S., Rebelo, S., and Trabandt, M. (2020). 'The Macroeconomics of Epidemics'. NBER Working Paper No 26882.

Elenev, V., Landvoigt, T., and Van Nieuwerburgh, S. (2020). 'Can the Covid Bailouts Save the Economy?' NBER Working Paper No 27207 and *Covid Economics*, vol. 17, 101-153.

Faria e Castro, M. (2020). 'Fiscal Policy during a Pandemic'. Federal Reserve Bank of St. Louis Working Paper No 2020-006E and *Covid Economics*, vol. 2, 67-101.

Favero, C. A., Ichino, A., and Rustichini, A. (2020). 'Restarting the Economy While Saving Lives'. CEPR Discussion Paper No 14664.

Fornaro, L. and Wolf, M. (2020). 'Covid-19 Coronavirus and Macroeconomic Policy'. CEPR Technical Report.

Galasso, V. (2020). 'Covid: Not a Great Equaliser'. *Covid Economics*, vol. 19, 241–255.

Glover, A., Heathcote, J., Krueger, D., and Ríos-Rull, J. (2020). 'Health versus Wealth: On the Distributional Effects of Controlling a Pandemic'. NBER Working Paper No 27046 and *Covid Economics*, vol. 6, 22-64.

Gourinchas, P.-O., Kalemli-Ozcan, S., Penciakova, V., and Sander, N. (2020). 'COVID-19 and SME Failures'. NBER Working Paper No 27877.

Guerrieri, V., Lorenzoni, G., Straub, L., and Werning, I. (2020). 'Macroeconomic Implications of COVID-19: Can Negative Supply Shocks Cause Demand Shortages?' NBER Working Paper No 26918.

Halpern, N. A. and Tan, K. (2020). 'United States Resource Availability for COVID-19'. Society of Critical Care Medicine Report.

Hur, S. (2020). 'The Distributional Effects of COVID-19 and Optimal Mitigation Policies'. Federal Reserve Bank of Dallas Working Paper and *Covid Economics*, vol. 47, 130-161.

Jones, C. J., Philippon, T., and Venkateswaran, V. (2020). 'Optimal Mitigation Policies in a Pandemic: Social Distancing and Working from Home'. NBER Working Paper No 26984.

Kaplan, G., Moll, B., and Violante, G. (2020). 'The Great Lockdown and the Big Stimulus: Tracing the Pandemic Possibility Frontier for the U.S.' NBER Working Paper No 27794.

Krueger, D., Uhlig, H., and Xie, T. (2020). 'Macroeconomic Dynamics and Reallocation in an Epidemic'. NBER Working Paper No 27047 and *Covid Economics*, vol. 5, 21-55.

Leiserson, G., McGrew, W., and Kopparam, R. (2019). 'The Distribution of Wealth in the United States and Implications for a Net Worth Tax'. Washington Center for Equitable Growth.

Covid Economics 70, 25 February 2021: 1-48

Li, R., Rivers, C., Tan, Q., Murray, M., Toner, E., and Lipsitch, M. (2020). 'Estimated Demand for US Hospital Inpatient and Intensive Care Unit Beds for Patients With COVID-19 Based on Comparisons With Wuhan and Guangzhou, China'. *JAMA Network Open*, vol. 3, no. 5.

Mendoza, E., Tesar, L., and Zhang, J. (2014). 'Saving Europe?: The Unpleasant Arithmetic of Fiscal Austerity in Integrated Economies'. NBER Working Paper No 20200.

Mongey, S., Pilossoph, L., and Weinberg, A. (2020). 'Which Workers Bear the Burden of Social Distancing Policies?' NBER Working Paper No 27085 and *Covid Economics*, vol. 12, 69-86.

Palomino, J., Rodríguez, J., and Sebastian, R. (2020). 'Wage inequality and poverty effects of lockdown and social distancing in Europe'. *European Economic Review*, vol. 129, 103564.

Rampini, A. (2020). 'Sequential Lifting of COVID-19 Interventions with Population Heterogeneity'. NBER Working Paper No 27063.

Will Schumpeter catch Covid-19?[1]

Mathieu Cros,[2] Anne Epaulard[3] and Philippe Martin[4]

Date submitted: 20 February 2021; Date accepted: 21 February 2021

We estimate the factors predicting firm failures in the COVID crisis based on French data in 2020. Although the number of firms filing for bankruptcy was much below its normal level (-36% compared to 2019) the same factors that predicted firm failures (primarily productivity and debt) in 2019 are at work in a similar way as in 2020. Hence, the selection process, although much reduced, has not been distorted in 2020. At this stage, partial hibernation rather than zombification characterises the selection into firm survival or failure. We also find that the sectoral heterogeneity of the turnover COVID shock (proxied by the change in credit card transactions) has been largely (but not fully) absorbed by public policy support because it predicts little of the probability of bankruptcy at the firm level. Finally, we sketch some potential scenarios for 2021-2022 for different sectors based on our empirical estimates of predictors of firm failures.

Covid Economics 70, 25 February 2021: 49-69

1 We thank Pierre Olivier Gourinchas, David Sraer and David Thesmar as well as members of the French National Productivity Board for helpful comments. Philippe Martin is grateful to the Banque de France-SciencesPo partnership for its financial support. We also thank the Groupement des Cartes Bancaires CB for its help in providing data within the partnership of the French Council of Economic Analysis and the Digital Finance Chair.

2 Graduate student, Paris Dauphine - PSL University.
3 Professor of Economics, Paris Dauphine - PSL University; Research Fellow, France Stratégie.
4 Professor of Economics, SciencesPo; CEPR Research Fellow.

Covid Economics 70, 25 February 2021: 49-69

1 Introduction

The COVID-19 crisis, a global shock 'like no other', has had dire consequences on several economic variables: consumption, production, employment, trade, productivity, business and consumer confidence etc... However, one economic impact that was anticipated very early on (see for example the simulations by Gourinchas et al....) did not materialise so far: firm bankruptcies. Indeed, the number of bankruptcy filings has decreased significantly. In France for example, as illustrated in graph 1 the number of firms filling for bankruptcy is much below its normal level: - 36% at the end of 2020 (week 52) compared to 2019. The last time the French economy experienced a large downturn was in 2009 with the GDP contracting by 2.9%. That year, the number of firms filing for bankruptcy jumped by 14% compared to 2008 (and 23% compared to 2007). This paradoxical situation is observed in other countries. Even if international comparisons are not easy on bankruptcy filings, the UK and German situations are similar. In the UK for the third quarter of 2020, filings are 39% below the same period in 2019 and 9% below the second quarter of 2020[2]. In Germany, where the obligation to declare insolvency has been suspended on March 1st, the number of firms filing for bankruptcy has decreased by 10% in the first semester of 2020 relative to 2019. In both Germany and France, no catching up in the past few months is observed. In the US, a recent study (Wang et al. (2020)) shows that although there is a sizeable decrease in direct bankruptcies there is still a substantial increase of Chapter 11 filings by large corporations but which are a small share of overall bankruptcies.

The main explanation of this unexpected observation is that governments have provided ample liquidity to firms most affected by the pandemic. They have reduced their wage bill (in Europe through short time work schemes) and made direct transfers for example to pay for some fixed costs. The objective was clearly to freeze the economy during the crisis and put firms most at risk in hibernation. The sharp reduction in bankruptcies in France and Germany suggests this objective was attained. But did governments go too far? Some concerns in the public debate [3]have emerged that these policies may create zombies by reducing the exit of non productive firms. According to Schumpeter, the least productive firms are more likely to go bankrupt during recessions and Schumpeterian creative destruction may therefore be put into danger by an over generous policy response. If so this may have dire consequences on productivity in the following years as exit of unproductive firms is likely to be a substantial share of aggregate productivity growth. Foster et al. (2001) find that entry and exit of plants account for around 25 percent of US

[2]see *UK Insolvency Service Quarterly* (2020)
[3]see The-Economist (September 26,2020) or Financial-Times (December 3, 2020)

Covid Economics 70, 25 February 2021: 49-69

Figure 1: Cumulative number of bankruptcy filings (2008-2020)

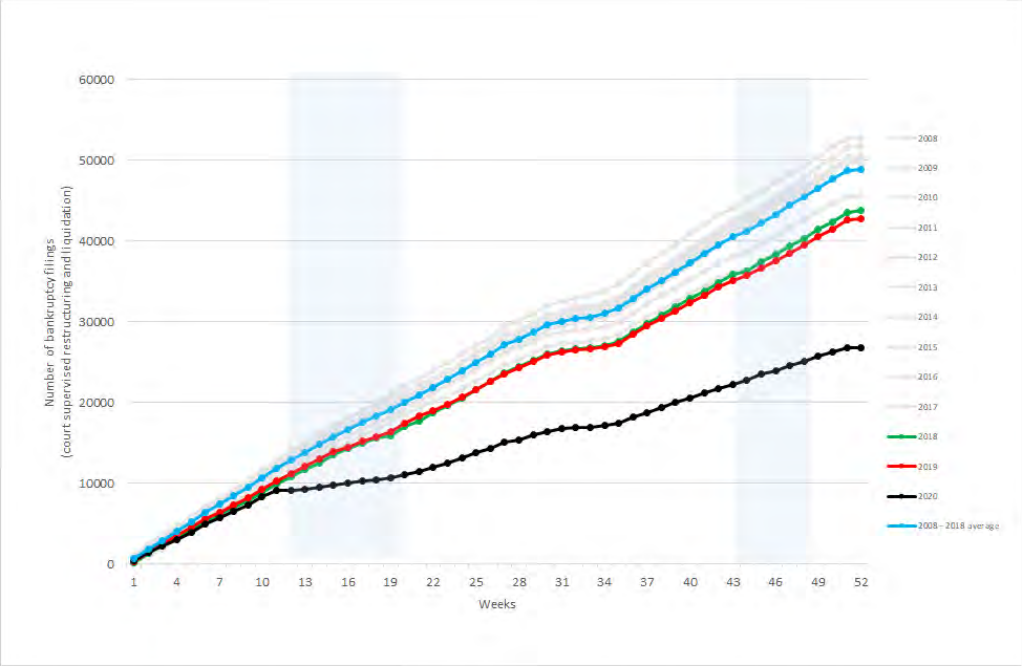

Reading note: At the end of 2020 the cumulative number of bankruptcy filings had reached 26,779, while at the end of 2019, the cumulative number of bankruptcy filings had reached 42,687.
Source: BODACC data up to December 2020

manufacturing productivity growth over the period 1977 - 1992 and that the impact of net entry is probably larger in the service sector. This effect comes from exiting firms that are less productive - and/or less innovative - than both continuing and entering firms (see Syverson (2011). As in other countries, entry and exit of firms is a sizeable component of labour productivity growth in France: David et al. (2020) show that more than 60 percent over the period 2011 - 2017 is caused by creative destruction [4]. This is so even though net entry is a small component of TFP growth volatility[5] . This accounting decomposition of productivity growth does not take into account the potential negative additional impact of low productivity firms (zombie firms) on the growth of continuing firms. Adalet-McGowan et al. (2018) find that zombie firms reduce the growth of more productive firms and might also reduce entry. This further increases the potential burden of surviving low productivity firms on aggregate productivity. However, Laeven et al. (2020) argue

[4]see also Turner (2013) who shows that 40% of hourly productivity growth in the retail sector in France over the period 1997 - 2007 comes from entry and exit of firms.
[5]see Osotimehin (2019)

that "the different nature of the crisis means that many firms that normally would be classified as zombie firms are in fact viable firms".

The concern that public policies to support firms may impair the cleansing effect of the recession by saving unproductive firms from exit is therefore legitimate. But the opposite concern that productive firms may go bankrupt because of the COVID crisis is also legitimate. The cleansing effect is based on the implicit assumption that markets efficiently select the most productive firms. However, several studies show that the probability of firm failure depends not only on their productivity but also on their access to credit. Barlevy (2002) studies the consequences of credit frictions on resource allocation during recessions and shows that credit frictions can lead to the opposite of the cleansing effect during recessions. Fougère et al. (2013) confirm the fundamental role of credit constraints on the probability of bankruptcy. They find that payment delays and cash flow difficulties disproportionately affect SMEs. During recessions, these delays are longer, commercial credit between companies is more risky and SMEs are the first to suffer from this via a considerable increase in their probability of bankruptcy. However, Osotimehin & Pappadà (2017) find that there is a cleansing effect of recessions in the presence of credit frictions, despite their effect on the selection of exiting and entering firms.

The impact of the COVID crisis on productivity through its effect on the firm bankruptcy process is therefore ambiguous. In this paper, we analyse whether there is early evidence that the selection process of firms bankruptcies is not only partially frozen but also distorted. We offer a preliminary answer to this question based on French data. At this stage the answer is only tentative because the dynamics of firm bankruptcies in 2021-2022 is difficult to anticipate. Although, firm bankruptcies have been sharply reduced we still observe some (more than 60% of the "normal" level) and we can therefore analyse whether the determinants of the mechanism of firm destruction has been sharply distorted by the crisis. Two risks co-exist that both would reduce aggregate productivity: that low productivity firms are unduly protected and that high productivity firms are not protected enough. In both cases, this would point to misguided public policies. Our results, again at an early stage, are relatively reassuring:

- The risk of an increase in productive firms going bankrupt during the pandemic did not materialise: in 2020 the firms filing for bankruptcy were in 2018 already less productive and/or had higher debt. A logit model shows that the main predictors of bankruptcy are at work in 2020 as in 2019 and 2018: productivity, debt, age are still associated with bankruptcy probability. Moreover, the coefficients for these variables are not statistically different from

Covid Economics 70, 25 February 2021: 49-69

one year to another. Creative destruction has been partially frozen but not distorted.

- Not surprisingly, the reduction in the number of bankruptcies comes from lower bankruptcy filing of less productive firms. In the short run however, the impact on the aggregate productivity gain is likely to be small. This is only true if the process of creative destruction is unfrozen once the crisis is over.

- The COVID shock has been very heterogeneous across sectors. This is particularly true for the commerce sector (e.g. restaurants versus food-stores). We measure the shock for these sectors by the change in credit card transactions. We find that sectors more affected by the COVID shock are more likely to file for bankruptcy. However, the predictive power of the sectoral COVID shock on bankruptcy is much smaller than that of firm productivity or debt. This suggests that public policies did compensate, in the short term, a very large part of the sectoral nature of the COVID shock.

- The legacy of the pandemic on firm balance sheets will likely be large. The reduction of bankruptcies thanks to generous liquidity measures comes at the cost of an increase in corporate debt especially in sectors that are most affected by the pandemic. For firms in these sectors, a return to normal of the bankruptcy process would predict a large increase in bankruptcies from 1.1% in 2019 to 1.8% in 2021 (and after 0.7% in 2020). This is large but most of the increase comes from a catch up process of bankruptcies that did not take place in 2020. One political economy issue for the government is that this return to normal through catch-up may be interpreted as a policy failure.

Covid Economics 70, 25 February 2021: 49-69

In section 2, we provide an empirical estimate of the determinants of bankruptcies in the French COVID crisis. Section 3 sketches some potential scenarios for 2021-2022 based on these estimates. In section 4, we conclude with a discussion of some policy implications.

2 The determinants of bankruptcies in the Covid-19 crisis

2.1 Data sources and summary statistics on bankruptcy filings in the pandemic

We follow bankruptcy filings in France from 2009 to 2020. Our database is based on daily electronic files of BODACC[6], an official online publication that reports all commercial court decisions relative to French firms and notably all bankruptcy filings. We then merge this database with SirenE, an

[6]Bulletin Officiel des Annonces Civiles et Commerciales

INSEE database that gives information regarding the geographical location of firm headquarter and their industry. Attrition between these two database is negligible (with a loss of around 4000 firms for an initial database of 600 000 bankruptcy filings over the period 2009 - 2020). In a second step, this database is matched with the FARE database, which contains firms accounting information (balance sheet and income statement). We use this information to compute labour productivity (EBITDA per worker) and leverage (total debt over total assets).

Since, the crisis (and the reduction of bankruptcies) only started in March 2020, we only account for the companies that went bankrupt from March 1 to September 30. In order to be able to compare our results to previous years and since there may be seasonality in insolvency bankruptcies or commercial court activity, we do the same for all the years in our study. Hence, all firms that filed for bankruptcy in January, February, October, November or December of any year are systematically excluded from the sample. Moreover, since we want to analyse what drives bankruptcy in SMEs (small and medium-size enterprises), we focus on companies with at least one employee[7] and less than 250 employees. Moreover, we exclude from the sample all the companies that we consider not being in our framework because they have odd debt ratio below 0 or over 1, or because their labour productivity is above 300 thousand euros per worker or under -100 thousand euros. Therefore, the sample consists of 863,162 observations in 2013 and has 1,118,379 observations in 2020. Summary statistics for the 2019 and 2020 samples are presented in Table 1. Since the last income statements and balance sheet available are from 2018, we report labour productivity, debt ratios, age and number of employees with a two year lag. That is, 2018 firm characteristics are used for the 2020 sample and 2017 firm characteristics are used for the 2019 sample.

Except for bankruptcy rate, which we comment below, the two samples (2019 and 2020) are quite similar. This is normal since most firms appear in the two samples and do not change drastically from one year to the next. The average firms is 15 year old, has 8 employees and an annual labour productivity slightly below 70 000 euros. The average debt to assets ratio is around 45%. Bank debt is on average around 14% of total asset, supplier debt on average around 12%. For these firms "Other debt", which consist mainly in tax and social security debt is almost 20% of total assets.

As mentioned in the introduction, bankruptcy filings in 2020 was dramatically lower than in 2019. The default being calculated over March to September was respectively 1.1% in 2013, 0.7% in 2019 and only 0.4% in 2020. Liquidations and court supervised restructurings in 2020 are 36%

[7]Self-employed workers and auto-entrepreneurs are excluded from the sample

Covid Economics 70, 25 February 2021: 49-69

CEPR PRESS

Table 1: Summary statistics - 2019 and 2020 samples

	N	Mean	St. Dev.	Median	D1	D9	Min.	Max.
2019 sample								
Bankruptcy (0/1)	1,097,795	0.007	0.084	0.000	0.000	0.000	0.000	1.000
Labour productivity ('000 euros)	1,097,795	67	50	56	19	130	-100	300
Total debt (/assets)	1,097,795	0.451	0.237	0.426	0.152	0.802	0.000	1.000
Bank debt (/assets)	1,097,795	0.137	0.170	0.072	0.000	0.383	0.000	1.000
Supplier debt payable (/assets)	1,097,795	0.122	0.126	0.083	0.011	0.285	0.000	1.000
Other debts (/assets)	1,097,795	0.192	0.175	0.135	0.034	0.435	0.000	1.000
Age (in years)	1,097,795	15	14	12	3	32	2	119
Nb of employees	1,097,795	8	20	3	1	18	1	249
2020 sample								
Bankruptcy (0/1)	1,118,379	0.004	0.066	0.000	0.000	0.000	0.000	1.000
Labour productivity ('000 euros)	1,118,379	68	52	57	19	135	-100	300
Total debt (/assets)	1,118,379	0.440	0.238	0.412	0.144	0.792	0.000	1.000
Bank debt (/assets)	1,118,379	0.137	0.170	0.072	0.000	0.384	0.000	1.000
Supplier debt payable (/assets)	1,118,379	0.119	0.125	0.080	0.010	0.279	0.000	1.000
Other debts (/assets)	1,118,379	0.184	0.174	0.127	0.031	0.422	0.000	1.000
Age (in years)	1,118,379	15	14	12	4	32	2	127
Nb of employees	1,118,379	8	20	3	1	18	1	249

Source: BODACC, FARE 2017, FARE 2018.

Covid Economics 70, 25 February 2021: 49-69

below their 2019 levels. Both the number of direct liquidations and court-supervised restructuring stands well below year 2019 levels which was already low. Nevertheless, the reduction in court-supervised restructuring filings is even greater than that of liquidations: reorganisations are 49% below their 2019 level while liquidations decreased only by 31%. When compared to the 2008-2018 average, liquidations are down by 41% and reorganisations by 53%.

To measure the size of the demand shock that hit firms in the retail and personal service sectors, we use data from Cartes Bancaires CB, the leading consortium of payment service providers, banks and e-money institutions. These data have been exploited by Bounie et al. (2020) to measure the consumption behaviour of French households during and after the first lockdown. Here we use this data set from the merchant perspective. We have access to the weekly total of CB payments by merchant category code (MCCs). These MCCs are used by payment brands to classify merchants and businesses by the type of goods or services provided. Based on the available data, we created an association between sectors codes of the MCC nomenclature (Merchant Category Code) and the French NAFRév2 nomenclature (INSEE) to be able to match the credit card spending changes to the companies of our sample.

2.2 Empirical estimates

There are two potential effects on productivity of the very unusual dynamics of bankruptcies of 2020. First, if this drop was persistent it could affect the productivity level because more firms (and among them low productivity) would be allowed to remain active. Second, the very process

of bankruptcy may be distorted by the mix of the financial difficulties faced by firms and the very large policy response to support firms. It is possible indeed that high productivity firms (but with high levels of debt) may go more into bankruptcy than in normal circumstances, at the same time as low productivity firms are allowed to remain active. The answer to the first question "will a lower number of bankruptcies generate lower productivity?" depends on whether the drop is persistent or not. The answer to the second question "is the bankruptcy process distorted ?" depends on the characteristics of firms that are still going into bankruptcy.

The second question is the one we focus on. To do this we compare the determinants of bankruptcies since the COVID crisis and the years before.

Comparing distributions of labour productivity and leverage debt of companies filing for bankruptcy in different years is a first way to assess whether the characteristics of the Schumpeterian process have changed. We use labour productivity (added value per worker) and a debt ratio (overall debt divided by total assets) to measure whether companies that filed for bankruptcy in 2020 were more or less productive and indebted than those that went bankrupt in 2019 and companies that neither went bankrupt in 2019 nor 2020 (Figure 2 and 3). Since 2018 is the last year of available companies' balance sheet data, we look at 2018 balance data for companies that filed in 2020 and for companies that never filed for bankruptcy, and 2017 data for companies that filed for bankruptcy in 2019. We observe that bankrupt companies of 2019 and 2020 had a very similar productivity and debt ratio distribution two years before whereas non-bankrupt firms were both more productive and less indebted.

To analyse further this issue we estimate a Logit model to identify the main predictors of business failures. Logit models are better suited than standard OLS to estimate the probability of occurrence of rare events, which is the case for bankruptcy as less than 1% of firms filing for bankruptcy in a given year.

The benchmark model explains the probability of bankruptcy in year t for firm i on the base of the firm characteristics in year $t-2$. The explanatory variables are labour productivity (measured as it added value by worker), the overall leverage of the firm (measured by the ratio of the firm's total debt to its total assets), the age of the firms (a dummy for each subcategory: 0 to 5 years, 6 to 10 years, 10 to 30 years and more than 30 years), its size (measured by the log of the number of employees) and its industry (with 15 industry dummies - see Figure **??**). The equation is the following:

Covid Economics 70, 25 February 2021: 49-69

Covid Economics 70, 25 February 2021: 49-69

Figure 2: Labour productivity distribution

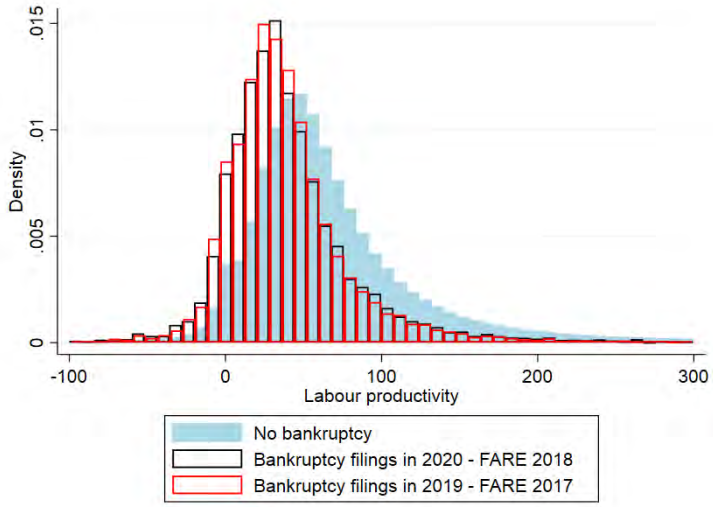

Reading note: the companies that respectively filed for bankruptcy in 2020 and 2019 had a labour productivity distribution two years before that was on the left of the distribution for firms that neither filed for bankruptcy in 2020 nor before. Around 12.5% of the companies that filed for bankruptcy had a labour productivity comprised between 16 and 24 thousand euros per worker while it represented only a little more than 5% of the companies that never filed for bankruptcy.

Figure 3: Debt ratio distribution

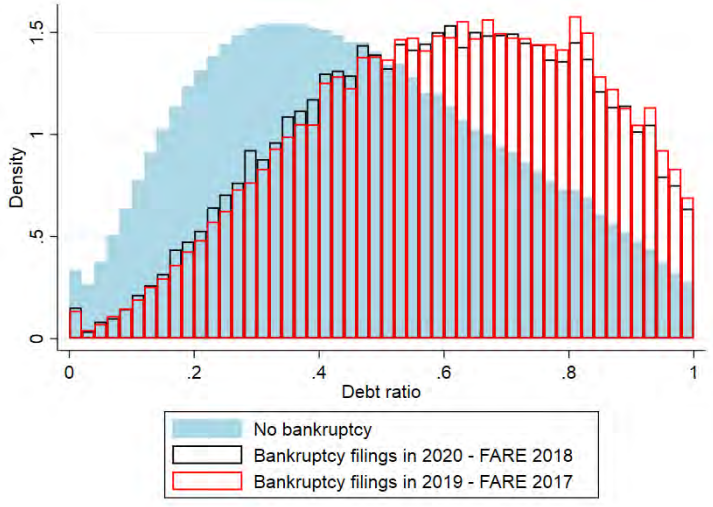

Reading note: the companies that respectively filed for bankruptcy in 2020 and 2019 had a debt ratio distribution two years before that was on the right of the distribution for firms that neither filed for bankruptcy in 2020 nor before. Around 7% of the companies that filed for bankruptcy had a debt ratio comprised between 0.98 and 1 whereas it represented only around 2.5% of the companies that never filed for bankruptcy.

$$Y_t = \frac{1}{1 + e^{-(\alpha + X_{it-2}\beta + \mu_s)}} \quad (1)$$

where μ_s is the industry fixed effect and X_{it-2} contains all other firm characteristics. There is no time fixed effect as we estimate this equation for each year separately from 2013 to 2020. In a given year t, the sample considered for the estimation contains all firms for which we have the balance sheet and income information in the year $t-2$ and for which a bankruptcy process was not started in the year $t-1$.

This model is estimated every year since 2013 on the firm sample described above. Results of these year by year estimations are reported in Tables 2 and 3, the later table presenting an empirical model with leverage being divided between bank debt, supplier debt and "other debts" (mainly fiscal and social security debt).

Table 2: Predictors of the bankruptcy probability (2013-2020) - All sectors - Total debt

VARIABLES	(1) 2013	(2) 2014	(3) 2015	(4) 2016	(5) 2017	(6) 2018	(7) 2019	(8) 2020
Labour Productivity	-0.0124***	-0.0134***	-0.0132***	-0.0142***	-0.0147***	-0.0114***	-0.00956***	-0.00919***
	(0.000354)	(0.000380)	(0.000388)	(0.000402)	(0.000436)	(0.000376)	(0.000318)	(0.000382)
Debt / Assets	2.588***	3.061***	3.115***	2.963***	2.821***	2.804***	2.488***	2.469***
	(0.0527)	(0.0560)	(0.0573)	(0.0583)	(0.0617)	(0.0572)	(0.0529)	(0.0653)
ln(Number of employees)	-0.00998	0.00567	-0.0480***	-0.0237**	-0.0526***	-0.0495***	-0.160***	-0.154***
	(0.0107)	(0.0110)	(0.0116)	(0.0119)	(0.0129)	(0.0124)	(0.0112)	(0.0142)
Constant	-5.181***	-5.603***	-6.024***	-5.143***	-5.195***	-6.347***	-5.222***	-6.328***
	(0.359)	(0.323)	(0.384)	(0.310)	(0.361)	(0.505)	(0.359)	(0.582)
Observations	863,162	854,087	847,743	859,037	847,294	925,521	1,097,795	1,118,379
Sector FE	Yes	Yes	Yes	Yes	Yes	Yes	Yes	Yes
Age class FE	Yes	Yes	Yes	Yes	Yes	Yes	Yes	Yes
Pseudo-R2	0.0782	0.0892	0.0867	0.0907	0.0843	0.0843	0.0713	0.0588
Bankruptcy percentage	0.0110	0.0104	0.00963	0.00900	0.00766	0.00792	0.00709	0.00434

Standard errors in parentheses
*** p<0.01, ** p<0.05, * p<0.1

Table 3: Predictors of the bankruptcy probability (2013-2020) - All sectors - Debt components

VARIABLES	(1) 2013	(2) 2014	(3) 2015	(4) 2016	(5) 2017	(6) 2018	(7) 2019	(8) 2020
Labour productivity	-0.0124***	-0.0131***	-0.0130***	-0.0140***	-0.0144***	-0.0112***	-0.00926***	-0.00895***
	(0.000354)	(0.000383)	(0.000392)	(0.000408)	(0.000441)	(0.000379)	(0.000321)	(0.000386)
Bank debt / assets	2.258***	2.567***	2.631***	2.285***	2.251***	2.223***	1.816***	1.875***
	(0.0656)	(0.0693)	(0.0716)	(0.0741)	(0.0806)	(0.0753)	(0.0729)	(0.0899)
Supplier debt / assets	3.108***	3.492***	3.489***	3.421***	3.285***	3.220***	3.004***	3.029***
	(0.0723)	(0.0756)	(0.0788)	(0.0799)	(0.0854)	(0.0793)	(0.0762)	(0.0952)
Other debt / assets	2.488***	3.169***	3.249***	3.180***	2.892***	2.895***	2.590***	2.502***
	(0.0653)	(0.0668)	(0.0681)	(0.0690)	(0.0730)	(0.0668)	(0.0636)	(0.0789)
ln(Number of employess)	-0.0188*	0.00291	-0.0489***	-0.0230*	-0.0537***	-0.0477***	-0.156***	-0.154***
	(0.0108)	(0.0111)	(0.0117)	(0.0120)	(0.0130)	(0.0125)	(0.0114)	(0.0143)
Constant	-5.181***	-5.603***	-6.024***	-5.143***	-5.195***	-6.347***	-5.222***	-6.328***
	(0.359)	(0.323)	(0.384)	(0.310)	(0.361)	(0.505)	(0.359)	(0.582)
Observations	863,162	854,087	847,743	859,037	847,294	925,521	1,097,795	1,118,379
Sector FE	Yes	Yes	Yes	Yes	Yes	Yes	Yes	Yes
Age class FE	Yes	Yes	Yes	Yes	Yes	Yes	Yes	Yes
Pseudo-R2	0.0794	0.0909	0.0882	0.0936	0.0862	0.0863	0.0737	0.0607
Bankruptcy percentage	0.0110	0.0104	0.00963	0.00900	0.00766	0.00792	0.00709	0.00434

Standard errors in parentheses
*** p<0.01, ** p<0.05, * p<0.1

The ability of the model to explain the individual heterogeneity in bankruptcy is - not surpris-

Covid Economics 70, 25 February 2021: 49-69

ingly - low. The Pseudo-R2 varies between 0.094 in 2014 and 0.061 in 2020. The lower explanation power in the year 2020 model suggests that the usual bankruptcy predictors (size, age, productivity, leverage) are less informative on individuals' propensity for bankruptcy in 2020 than in other years. However, the key finding in these tables is that coefficients for these predictors are very stable over time, notably when comparing 2019 and 2020.

The main take away from this estimation is that the COVID crisis and the policy measures put in place by the government have not changed drastically the determinants of bankruptcy, except the size of the process itself (see the fall in the constant in 2020). Firms that failed in 2020 are less productive and more financially fragile, just as in 2019. The difference in coefficients across types of debt (to suppliers, banks and social and fiscal administrations) is also very stable in 2019 and 2020.

2.3 The COVID shock and the role of emergency measures

We cannot directly assess the impact of public emergency measures on the bankruptcy in 2020. However, we know that both the COVID turnover shock on turnover and the policy measures that were put into place were heterogeneous across sectors. These policy measures are described in detail in appendix. Several- but not all - were targeted to firms in sectors most affected by the COVID crisis. The most important ones are the State-guaranteed loan, short-time work the solidarity fund for small business, and deferral of payment for social and/or fiscal charge.

The support of public policy to firms lies between two potential extremes. At one extreme, if public support to firms had not absorbed the COVID shock, bankruptcy rates would be much larger for firms in sectors hit more strongly by the COVID shock. At the other extreme, if public policy support had fully absorbed the COVID turnover shock, this shock at the sectoral level would not have any predictive power on bankruptcies. The net effect of the COVID shock and of the support measures to absorb the shock would be zero. In this section, we analyse how much of the sectoral heterogeneity due to COVID was absorbed by the French public policy support.

Our measure of the shock on turnover is based on credit card payments received by firms that serve consumers/households (as opposed to businesses, for which credit card receipts are not a large part of their overall receipts). Thus we focus on the retail sectors in the broadest sense (it includes for example car dealerships, restaurants, hairdressers, beauty salons and funeral services - amongst others - that are not included in the narrow retail sector). Summary statistics for this broadly defined retail sector sample for the year 2020 are in Table 4. For the year 2020, there are 377,334 firms in the retail sector. With an average of 6 employees, firms in this sector smaller

Covid Economics 70, 25 February 2021: 49-69

than the whole sample used in previous section, the labour productivity is also below that of the whole sample and these firms have marginally lower debt ratio. The default rate from March to September was 0.44% in 2020, while it was 0.65% in the same months of 2019, a drop of nearly 33% in business bankruptcies.

Table 4: 2020 - Retail sector

	N	Moyenne	St. Dev.	Median	D1	D9	Min.	Max.
Bankruptcy (0/1)	377,334	0.004	0.066	0.000	0.000	0.000	0.000	1.000
Labour productivity ('000 euros)	377,334	60	44	50	18	113.	-100	300
Total debt (/assets)	377,334	0.458	0.247	0.434	0.146	0.822	0.000	1.000
Bank debt (/assets)	377,334	0.177	0.194	0.111	0.000	0.473	0.000	1.000
Supplier debt (/assets)	377,334	0.113	0.112	0.079	0.017	0.250	0.000	0.985
Other debt (/assets)	377,334	0.168	0.171	0.105	0.028	0.405	0.000	1.000
Age	377,334	15	12	11	4	31	2	120
Nb of employees	377,334	6	15	2	1	11	1	249

Source: BODACC, FARE 2018.

We proxy the Covid turnover shock by the change in credit card payments (Groupement des Cartes CB) received by these sectors between 2020 and 2019. As one would expect, the COVID shock was very heterogeneous across sectors[8] depending on the type business: some were very affected (-61% of credit card transactions for travel agencies for example) and others actually benefited (+23% for tobacco shops and +18% for bakeries for example). (see table 5).

We include this Covid turnover shock (in a way such that a higher shock means lower turnover) in the regression for bankruptcy in addition to other predictors of bankruptcy. The regression now estimated on the sub-sample of firms operating in the retail sectors as defined above[9]. Results are shown in Table 6.

The COVID shock as measured by the sectoral decrease in credit card transactions is a very significant predictor of the probability for a firm to fail. From this point of view we can conclude that public policy measures did not fully absorb the sectoral heterogeneity of the COVID shock. However, note that the other predictors of bankruptcy are not much affected by the introduction of the size of the COVID shock and are not very different either from the recent years without COVID shock. The comparison between regressions (3) and (4) in table 6 shows a slight increase in the model accuracy (the pseudo-R2 increased by 0.018). However, the quantitative impact of the COVID shock on the probability of default compared to the other traditional factors is minor.

[8]Although this indicator should give us an idea of how the sectors were actually affected at a very fine level, shopkeepers in some sectors may have adopted new strategies that may have fostered the use of credit cards, among which pick-and-collect strategies including full credit card payments. For this reason, there may be sectors which have increased their credit card income while their actual sales level is still below 2019 level. Nevertheless, we cannot take into account the sectors' true turnover since we only have high-frequency data on credit card, but we make the assumption that this indicator provides a good proxy of the heterogeneity of the COVID shock across sectors.

[9]Summary statistics for this subsample the year 2020 are presented in Table

Covid Economics 70, 25 February 2021: 49-69

Table 5: Change in credit card receipts par sub-sector in retail

Sector	change in CB receipts
Activities of travel agencies	-61%
Passenger transportation by cab	-48%
Beauty care	-40%
Retail sales of leather goods and travel goods	-29%
Body maintenance	-28%
Hotels and similar accomodation	-26%
Retail sale of fuel in sepcialized stores	-23%
Laundry and dry cleaning	-23%
Fast food restoration	-21%
Traditional catering	-18%
Retail sales of clothing in specialized stores	-16%
Retail sale of perfume and cosmetics in specialized stores	-15%
Haidressing	-15%
Repair of shoes and leather goods	-14%
Catering services	-12%
Retail sale of watches, clocks and jewelry in specialized stores	-11%
Foowear retailing	-9%
Repair of watches and jewelry items	-7%
Motor vehicle maintenance and repair	-2%
Retail sale of automotive equipment	-1%
Campground and parks for caravans or recreational vehicles	1%
Repair ofof househod appliance and equipment for home and garden	2%
Beverage outlets	2%
Repair of consumer electronic products	2%
Trade and repair of motorcycles	2%
Retail sale of books in specialized stores	3%
Retail sale of other household equipment in specialized store	3%
Retail sale of of beverages in specialized stores	4%
Trade in motor vehiccles	4%
Retail sale of flowers, plants, seeds, fertilizers, pets and pet food in specialized stores	6%
Optical retail business	9%
Repair of computers an peripheral equipment	10%
Retail sale of information and communication equipment in specialized stores	12%
Retail of pharmaceutical producy in specialized stores	13%
Retail sale in non-specialized stores	15%
Retail sale of bread, pastry and confectionnery in speciaized stores	16%
Funeral services	17%
Other food retailing in specialized stores	18%
Retail sale of tobacco products in specialized stores	23%
Retail sale of medical and orthopaedic articles in sepcialized stores	24%
Retail sale of newspapers and stationery in specialized stores	28%

Reading note: according to credit card data, the funeral services has increased its sales by 17% in 2020.
Source: Groupement Cartes Bancaires CB, authors' calculations

Figure 4 shows the influence of the different predictors on the pseudo-R2. Quantitatively, debts, labour productivity and size of the company are much more important predictors of the probability of failure than the COVID sectoral shock. Hence, we conclude that although public support to the retail sector in France has not fully absorbed the COVID shock, our estimates suggest that it has

Covid Economics 70, 25 February 2021: 49-69

Table 6: Predictors of the bankruptcy probability + credit card shock (2018-2020) - Retail

VARIABLES	(1) 2018	(2) 2019	(3) 2020	(4) 2020 + Shock
Credit card shock				1.576***
				(0.253)
Labour productivity	-0.0169***	-0.0127***	-0.0146***	-0.0141***
	(0.000818)	(0.000695)	(0.000839)	(0.000844)
Bank debt / Assets	2.551***	2.247***	2.132***	2.143***
	(0.121)	(0.120)	(0.143)	(0.143)
Supplier debt / Assets	3.960***	3.987***	3.651***	3.669***
	(0.150)	(0.144)	(0.175)	(0.174)
Other debt / Assets	2.541***	2.429***	2.167***	2.128***
	(0.125)	(0.121)	(0.144)	(0.144)
ln(Number of employees)	-0.307***	-0.340***	-0.327***	-0.329***
	(0.0267)	(0.0248)	(0.0301)	(0.0302)
Constant	-5.889***	-5.012***	-5.641***	-5.404***
	(0.116)	(0.114)	(0.147)	(0.152)
Observations	324,602	374,856	377,334	377,334
Sector FE	Yes	Yes	Yes	Yes
Age class FE	Yes	Yes	Yes	Yes
Pseudo-R2	0.0831	0.0795	0.0687	0.0705
Bankruptcy percentage	0.00712	0.00655	0.00433	0.00433

Standard errors in parentheses
*** p<0.01, ** p<0.05, * p<0.1

absorbed a very large share given that the shock explains little of the risk of failure. This suggests that a large part of the sectoral heterogeneity in turnover variation between 2020 and 2019 has been compensated by symmetric heterogeneity in public support.

Figure 4: Contributions of different predictors to bankruptcy risk in 2019 and 2020

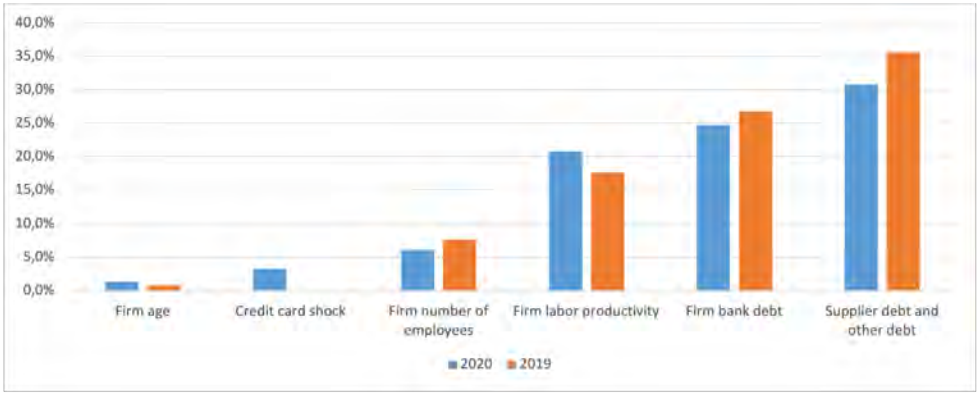

Reading note: In 2019, including the ratio of bank debt to corporate assets among the explanatory variables for default increases the explanatory performance of the econometric model by 25% compared to a model where all the other variables listed here are present, as well as sector fixed effects.

3 The expected rise in firm failures

Micro simulations (Gourinchas et al. (2020), Guerini et al. (2020), Demmou et al. (2021), predict a sharp increase in SME failures compared to 2018 and 2019, up to 25% for example in the accommodation and food sector. However, these simulations do not take into account all the public support measures.

Our empirical model can shed light on this question although it is too simple and incomplete to offer a forecast of firm failures in 2021-2022. Rather we estimate three scenarios to analyse how different sectors could be affected. We propose a simple method based on our econometric model by considering that the increase in insolvencies to be expected in the trade sector for 2021 would be the sum of 2 effects: 1) the catching up on bankruptcies that did not take place in 2020 and 2) the turnover fall over the period 2020-2021 and additional debt accumulated by firms.

We focus on the broadly defined retail trade firms and consider 3 plausible scenarios depending on the impact of the COVID-19 shock on productivity on the two year period (2020-2021) and debt of companies.

- The least affected firms would experience a 3% drop in labour productivity, but their debt levels would remain unchanged.
- The intermediate firms would experience a 6 percent drop in labour productivity and a 2.5 point increase in their debt ratio (all debts combined, i.e. bank debt, tax and social security debt, and supplier debt).
- The most affected firms would see labour productivity decrease by 12 percent and their debt ratio increase by 5 points.

These scenarios are not meant to be precise but indicative and are based on the following assumptions:

- Concerning the drop in productivity, the assumption is that all retail trade firms have faced a drop in labour productivity, if only because of periods of mandatory closure, social distancing measures and the drop in demand. For companies moderately affected by the shock, the drop in labour productivity would be 6%, which corresponds roughly to the cumulative annual growth decline expected over the period 2020-2021[10]. For the least affected companies, the

[10]In the draft amending finance bill presented at the end of November 2020, the government forecasts a negative growth rate for the French economy in 2020 (-11%) followed by a rebound of around 6% in 2021, i.e. an average annual growth rate over the two years of around -3%.

Covid Economics 70, 25 February 2021: 49-69

impact on labour productivity would be half as large (-3%) and twice as large (-12% for the most affected companies).

- Concerning the increase in indebtedness, to calibrate a plausible shock we observed the distribution of state-guaranteed loans at the end of November 2020 as published on the government website Etatlab on public data. This information is then used to compute the relative change in the ratio of overall debt to the total assets at a sectoral level based on balance sheets data of firms. According to our calculations, the state guaranteed loan corresponds to an increase in the debt ratio up to 2.7 points (see Table 7). From there we constructed three scenarios. In the worst-case scenario, the debt ratio at the end of the second lockdown (December 2020) would increase by 5 points compared to the situation at the end of 2019 due not only to the state-guaranteed loan scheme, but also to the tax and social security arrears accumulated thanks to government measures and possible moratorium in supplier invoice payments. For the companies least affected, the debt ratio would not increase due to the combination of lockdown periods and strong catching up in post lockdown periods. Finally, the moderately affected companies would see their debt ratio (all debts combined) increase by 2.5 points compared to the level at the end of 2019. To give an idea of the magnitude of the simulated debt shocks, the debt ratio in the wider retail trade sector, which averaged 40 percent at the end of 2019, would remain unchanged for the least affected retail trade companies and would rise to 45 percent for the most affected companies.

From the baseline model, we simulate the different scenarios described above on retail trade companies. We keep the 2019 baseline estimation as the closest to the conditions that would be those of year 2021 without government support measures. Based on three different scenarios for the three types of sectors, we estimate the increase in bankruptcy based on the logit estimation where we estimate the in-sample individual probability to go bankrupt using the actual characteristics of each company. We then simulate the individual changes in debt and labour productivity depending on the three scenarios explained above, and we measure how the probability of each individual is affected by those changes according to the model. We finally compute the variation of the average probability of bankruptcy before and after the simulated changes in characteristics. These are shown in table 8

The impact is quantitatively large for the most affected sectors but is small for the other sectors. Note also that the productivity fall has a larger quantitative impact than the increase in debt. In table 9 we translate this increase in failure probability in failure rates for the year 2021-2022. As

Covid Economics 70, 25 February 2021: 49-69

Table 7: Bank debt ratio increase by sector

Sector	State Guaranteed Loan over Total Assets
Extraticves Indsutries	0.17
Manufacturing	0.57
Construction	1.43
Wholesale and Retail Trade; Repair of Motor Vehicles and Motorcycles	1.38
Transportation and Warehousing	0.72
Lodging and Catering	2.71
Information and Communication	0.32
Financial and Insurances Activities	0.39
Real Estates Activities	0.10
Specialized, Scientific and Technical Activities	0.52
Administrative and Support Service Activities	0.62
Education	2.51
Human Health and Social Action	1.92
Arts, Entertainment and Recreation	2.05
Other Service Activities	2.09

Reading note: the take up of the state-guaranteed in the construction sector amounts to an increase of 1.43 point of the debt ratio.
Source: FARE 2018, Etalab

Table 8: 3 plausible scenarios for retail trade companies and bankruptcy increase

Sector shock	low	intermediate	high
Shock 1 : Labour productivity fall	-3%	-6%	-12%
Impact on bankruptcy	+2,3%	+ 4,8%	+9,9%
Shock 2 : Debt ratio increase	+0pt	+2,5pt	+5pt
Impact on bankruptcy	0%	+6,9%	+14,4%
Combined shocks			
Impact on bankruptcy	+2,3%	12,1%	25,7%

Table 9: COVID-19 crisis and bankruptcy catch-up : Predicted bankruptcy rate in 2021-2022

Sector shock	low	intermediate	high
Bankruptcy rate in 2019 (1)	1,1%	1,1%	1,1%
Bankruptcy rate in 2020 (2)	0,7%	0,7%	0,7%
Bankruptcy rate in 2021 = (1) + (3) + (4)	1,53%	1,63%	1,78%
2020 catch-up (3) = (1) - (2)	0,4%	0,4%	0,4%
Covid combined shocks (4)	0,03%	0,13%	0,28%

a starting point, in 2019, 1.1% of the firms in those sectors filed for bankruptcy. For example, in the most affected sectors the 25% increase in failure rate due to the combined effect of lower productivity and higher debt would translate into 0.28% of firms failing in the next two years.The catch-up effect (firms that would normally have failed in 2020 but did not and would normally fail in 2021-2022) would actually be much larger as it would involve 0.4% of firms. Overall the bankruptcy rate would increase from 1.1% to almost 1.8% in the most affected sectors an increase

Covid Economics 70, 25 February 2021: 49-69

that would be due in majority (around 60%) to the catch-up effect. These scenarios should be taken with great caution given the huge uncertainty on the validity of our assumptions. They suggest however that the policy challenge in 2021-2022 may be to manage as much the wave of "normal" failures that did not occur in 2020 as the failures due to the COVID shock itself. Another challenge will be for commercial courts to deal with the wave of bankruptcies. Iverson (2018) shows that in the US, the insolvency framework becomes less efficient when courts are congested with a higher risk for viable firms to be liquidated.

The limitations of our scenarios should however be stressed:

- Our scenarios for retail trade companies implicitly assume that there will be no further deterioration of the economic situation nor additional public support.
- Our econometric model used lacks crucial features.
  - It does not take into account general equilibrium effects. In the case of business failures, these can be of two kinds: on the one hand, an increase in bankruptcies can lead to the weakening of other businesses through supply chain effects; on the other hand - and this has the opposite impact - a business can benefit from the difficulties of its competitors.
  - It does not take into account the endogeneity issue that potentially leads to overestimate the increase in insolvencies due to the COVID crisis. A firm with low productivity is likely to make low or negative profit and to accumulate debt because of low productivity. In this case, the accumulation of debt is more the symptom than the cause of the firm's problems. However, in the COVID crisis, the increase in debt is of different nature. This debt is a result of the shock suffered and not a symptom of the deterioration of the firm's ability to generate profits. Taking into account firms' labour productivity helps reduce this endogeneity, but we may still exaggerate the role of debt on firm failure in the present crisis. However, remember that our estimates of productivity and debt as predictors of firm failures in 2020 were very similar to those of 2019.

4 Conclusion

This paper is the first, to our knowledge, to estimate the factors predicting firm failures in the COVID crisis based on actual data in 2020. Although we are very aware of the limits of our exercise, we believe that several interesting messages emerge from it. First, at this stage Schumpeter has not catched COVID in the sense that the normal selection process in firm failure has not been distorted

Covid Economics 70, 25 February 2021: 49-69

in 2020. The same factors that predicted firm failures (productivity and debt) in 2019 are at work and in a similar way in 2020. The reduction of firm failures is very large and is due to policy measures to support firms but it has so far generated a partial "hibernation" of the destructive creation process rather than a massive "zombification" of the French economy. Of course, this early reassuring message should be taken with caution. The catch-up of failures in 2021-2022 will be large and will constitute a policy issue as it may be interpreted as a policy failure rather than a return to normal. The policy challenge will therefore be to continue support to productive and viable firms (but with potentially high debt due to the COVID shock) while at the same time progressively discontinue support to firms that are not viable.

Covid Economics 70, 25 February 2021: 49-69

References

Adalet-McGowan, M., Andrews, D., & Millot, V. (2018). The Walking Dead? Zombie Firms and Productivity Performance in OECD Countries. *Economic Policy*, *33*(96), 685–736.

Barlevy, G. (2002). The sullying effect of recessions. *Review of Economic Studies*, *69*(1).

Bounie, D., Camara, Y., Fize, E., Galbraith, J., Landais, C., Lavest, C., ... Savatier, B. (2020). Consumption Dynamics in the COVID Crisis: Real Time Insights from French Transaction Bank Data. *Covid Economics, Issue 59*, *69*.

David, C., Faquet, R., & Rachiq, C. (2020). Quelle contribution de la destruction créatrice aux gains de productivité en France depuis 20 ans ? *Document de Travail, DG Trésor*, *05*.

Demmou, L., Calligaris, S., Franco, G., Dlugosch, D., McGowan, A., & Sakha, S. (2021). Insolvency and Debt Overhang Following the COVID-19 Outbreak: Assessment of Risks and Policy Responses . *Covid Economics, Issue 69*.

Financial-Times. (December 3, 2020). European Zombification becomes even scarier.

Foster, L., Haltiwanger, J. C., & Krizan, C. J. (2001). Aggregate Productivity Growth: Lessons from Microeconomic Evidence. In C. R. Hulten, E. R. Dean, & M. J. Harper (Eds.), *New Developments in Productivity Analysis* (p. 303-372). University of Chicago Press.

Fougère, D., Golfier, C., Horny, G., & Kremp, E. (2013). What was the impact of the 2008 crisis on business failure. *Economics and Statistics*, *69*(97).

Gourinchas, P. O., Kalemli-Özcan, S., Penciakova, V., & Sander, N. (2020). COVID-19 and SME Failures. *NBER Working Paper*, *27877*.

Guerini, M., Nesta, L., Ragot, X., & Schlavo, S. (2020). Dynamique des défaillances d'entreprises en France et crise de la Covid-19. *OFCE Policy Brief*, *73*.

Iverson, B. (2018). Get in Line: Chapter 11 Restructuring in Crowded Bankruptcy Courts . *Management Science*, *64*(11), 5370-5394.

Laeven, L., Schepens, G., & Schnabel, I. (2020). Zombification in Europe in times of pandemic. *Vox EU*.

Osotimehin, S. (2019). Aggregate Productivity and the Allocation of Resources over the Business Cycle. *Review of Economic Dynamics*, *32*, 180-205.

Osotimehin, S., & Pappadà, F. (2017, June). Credit Frictions and The Cleansing Effect of Recessions. *The Economic Journal*, *127*(602), 1153-1187.

Syverson, C. (2011). What Determines Productivity? *Journal of Economic Literature*, *49*(2), 326-65.

The-Economist. (September 26,2020). Why covid-19 will make killing zombie firms off harder.

Turner, L. (2013). La productivité dans le commerce : l'impact du renouvellement des entreprises, de l'innovation et de l'appartenance à un réseau. In *Les entreprises en France* (p. 29-42). INSEE.

UK Insolvency Service Quarterly. (2020, October).

Wang, J., Yang, Y., Iverson, B., & Kluender, R. (2020). Bankruptcy and the Covid-19 Crisis. *Harvard Business School WP*, *21*.

Covid Economics 70, 25 February 2021: 49-69

CEPR PRESS

Appendix

Economic support measures for companies during Covid-19 crisis

- **State-guaranteed loan (SGL)**: it allows firms to ask for a credit to commercial banks that is guaranteed from 70% up to 90% by the French public investment bank (BPIFrance) in case of default. All companies are eligible since May and they can ask for a SGL until June, 30th of 2021 with low interest rates going from 1% to 2.5% according to the duration of the repayment (from 1 to 5 years). The amount obtained cannot exceed 25% of the 2019 sales of the company or two years of payroll. Firms have been granted access to such loans 638 034 times since the beginning of this aid, for a total amount of 130 040 million euros credited until now. For firms that do not find any bank willing to lend, some loans can directly be granted by the state. The idea behind such an economic measure is that SGL provides incentive to banks to lend and allows to enhance access to credit for financially distressed firms and to smooth the shock on liquidity, avoiding chain defaults.
- **Short time work measures**: it offers firms the possibility to a subsidy for temporary reductions in the number of hours worked in case the activity of the company is subject to temporary closure, significant decrease or difficulties to supply access or impossibility to prevent the employees from being exposed to the virus. This support mechanism allows that the employee to receive 70% of his gross wage (85% of net salary), and the firm receives an amount of 85% of the employee cost, up to an amount equivalent to 4.5 minimum wages. In some sectors (tourism, hotels, restaurants, sports, culture, air transport and entertainment), the firm could receive full compensation. An overall number of 189 455 requests have been compensated, accounting for 936 960 employees and more than 49 million hours.
- **Solidarity fund**: This fund changed several times since the beginning of the crisis. It is aimed at supporting small businesses, micro-entrepreneurs and self-employed workers particularly affected by the economic consequences of Covid-19. Initially, only companies below 10 employees could request this fund up to a 1500€ threshold whenever they justified administrative closure or decrease in sales of more than 50%. However, it evolved by increasing the employee threshold up to 20 employees first and 50 then for some sectors, while also raising the amount possibly received from 1500 up to 10 000 and 200 000 at the group level. Although the eligibility requirements is sector dependent, the support is a transfer without any need to be paid back for all the beneficiaries. Until now, the overall amount of the aid account for 11 870 million euros given to more than 1.9 million businesses.
- **Deferrals of payment of social and/or fiscal charges**: this deferral of employer contributions was available for all self-employed workers and auto-entrepreneurs belonging to sectors considered to be affected by the crisis according to a list defined by the URSSAF, companies of less than 250 employees in sectors highly affected, and to companies in other sectors employing less than 10 people but that were forced to close. The conditions for eligibility were then loosened in October. In addition, other fiscal contributions also benefited from deferrals such as the property tax, or corporate income tax, or value-added tax credits. The deferral of payment amounted to 3 199 million euros by January 13th, 2021.

Covid Economics 70, 25 February 2021: 49-69

Covid Economics Issue 70, 25 February 2021

The association of opening K-12 schools and colleges with the spread of Covid-19 in the United States: County-level panel data analysis[1]

Victor Chernozhukov,[2] Hiroyuki Kasahara[3] and Paul Schrimpf[4]

Date submitted: 21 February 2021; Date accepted: 21 February 2021

This paper empirically examines how the opening of K-12 schools and colleges is associated with the spread of COVID-19 using county-level panel data in the United States. Using data on foot traffic and K-12 school opening plans, we analyze how an increase in visits to schools and opening schools with different teaching methods (in-person, hybrid, and remote) is related to the 2-weeks forward growth rate of confirmed COVID-19 cases. Our debiased panel data regression analysis with a set of county dummies, interactions of state and week dummies, and other controls shows that an increase in visits to both K-12 schools and colleges is associated with a subsequent increase in case growth rates. The estimates indicate that fully opening K-12 schools with in-person learning is associated with a 5 (SE = 2) percentage points increase in the growth rate of cases. We also find that the positive association of K-12 school visits or in-person school openings with case growth is stronger for counties that do not require staff to wear masks at schools. These results have a causal interpretation in a structural model with unobserved county and time confounders. Sensitivity analysis shows that the baseline results are robust to timing assumptions and alternative specifications.

1 We are very grateful to Emily Oster for her helpful comments. All mistakes are our own.
2 Department of Economics and Center for Statistics and Data Science, MIT.
3 Vancouver School of Economics, University of British Columbia.
4 Vancouver School of Economics, University of British Columbia.

Covid Economics 70, 25 February 2021: 70-108

1. Introduction

Does opening K-12 schools and colleges lead to the spread of COVID-19? Do mitigation strategies such as mask-wearing requirements help reduce the transmission of SARS-CoV-2 at school? These are important policy relevant questions. If in-person school openings substantially increase COVID-19 cases, then local governments could promote enforcing mitigation measures at schools (universal and proper masking, social distancing, and handwashing) to lower the risk of COVID-19 spread. Furthermore, the government could prioritize vaccines for education workers in case of in-person school openings. This paper uses county-level panel data on K-12 school opening plans and mitigation strategies together with foot traffic data to investigate how an increase in the visits to K-12 schools and colleges/universities is associated with a subsequent increase in the growth rates of COVID-19 cases in the United States.

We begin with simple suggestive evidence. Fig. 1 provides visual evidence for the association of opening K-12 schools with the spread of COVID-19 as well as the role of school mitigation strategies. Fig. 1(a) and (b) plot the evolution of average weekly cases and deaths per 1000 persons, respectively, against days since school opening across different teaching methods as well as mask requirements for staff. In Fig. 1(a), the average number of weekly cases starts increasing after 2 weeks of opening schools in-person or hybrid, especially for counties with no mask mandates for staff. This possibly suggests that mask mandates at school reduce the transmissions of SARS-CoV-2. In Fig. 1(b), the number of deaths starts increasing after 3 to 5 weeks of opening schools, especially for counties that adopt in-person/hybrid teaching methods with no mask mandates. Alternative mitigation strategies of requiring mask-wearing to the student, prohibiting sports activities, and promoting online instruction also appear to help reduce the number of cases after school openings (see SI Appendix, Fig. S1(i)-(p)).

Fig. 1(c) shows that opening K-12 schools in-person or hybrid increases the number of per-device visits to K-12 schools more than opening remotely, especially when no mask mandates are in place. Fig. 1(d) and SI Appendix, Fig. S1(e)-(f) show that visits to full-time and part-time workplaces increase after school openings with in-person teaching, suggesting that the opening of schools allow parents to return to work. On the other hand, we observe no drastic changes in per-device visits to restaurants, recreational facilities, and churches after school openings (SI Appendix, Fig. S1(b)-(d)).

Fig. 2 and SI Appendix, Fig. S2 provide further descriptive evidence that opening colleges and universities with in-person teaching lead to the spread of COVID-19 in counties where the University of Wisconsin(UW)-Madison, the University of Oregon, the University of Arizona, the Michigan State University, the Pennsylvania State University, the Iowa State University, and the University of Illinois-Champaign are located.

What happened in Dane county, WI, is also illustrative. The left panel of Fig. 2 presents the evolution of the number of cases by age groups, the number of visits to colleges and universities, and the number of visits to bars and restaurants in Dane county, WI. The first panel shows that the number of cases for age groups of 10-19 and 20-29 sharply increased

Covid Economics 70, 25 February 2021: 70-108

FIGURE 1. The evolution of cases, deaths, and visits to K-12 schools and restaurants before and after the opening of K-12 schools

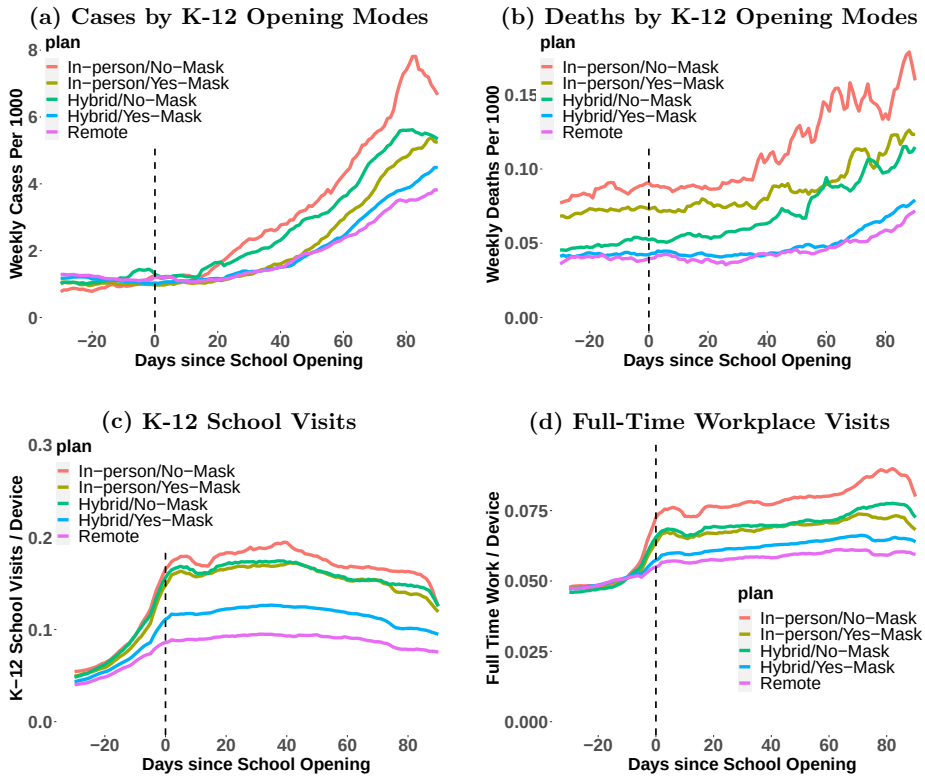

Notes: (a)-(b) plot the evolution of weekly cases or deaths per 1000 persons averaged across counties within each group of counties classified by K-12 school teaching methods and mitigation strategy of mask requirements against the days since K-12 school opening. We classify counties that implement in-person teaching as their dominant teaching method into "In-person/Yes-Mask" and "In-person/No-Mask" based on whether at least one school district requires staff to wear masks or not. Similarly, we classify counties that implement hybrid teaching into "Hybrid/Yes-Mask" and "Hybrid/No-Mask" based on whether mask-wearing is required for staff. We classify counties that implement remote teaching as "Remote." (c) and (d) plot the evolution of per-device visits to K-12 schools and full-time workplaces, respectively, against the days since K-12 school opening using the same classification as (a) and (b).

in mid-September while few cases were reported for other age groups. The second to the fourth panels suggest that this sharp increase in cases among the 10-29 age cohort in mid-September is associated with an increase in visits to colleges/universities, bars, and restaurants in late August and early September. The fall semester with in-person classes at the UW-Madison began on September 2, 2020, when many undergraduates started living together in residential halls and likely visited bars and restaurants. This resulted in increases

CEPR PRESS

in COVID-19 cases on campus; according to the letter from Dane County Executive Joe Parisi to the UW-Madison Parisi (2020), nearly 1,000 positive cases were confirmed on the UW-Madison campus by September 9, 2020, accounting for at least 74 percent of confirmed cases from September 1 to 8, 2020 in Dane county.

FIGURE 2. The number of cases by age groups and the number of visits to colleges/universities and bars in Dane county, WI, and Lane county, OR

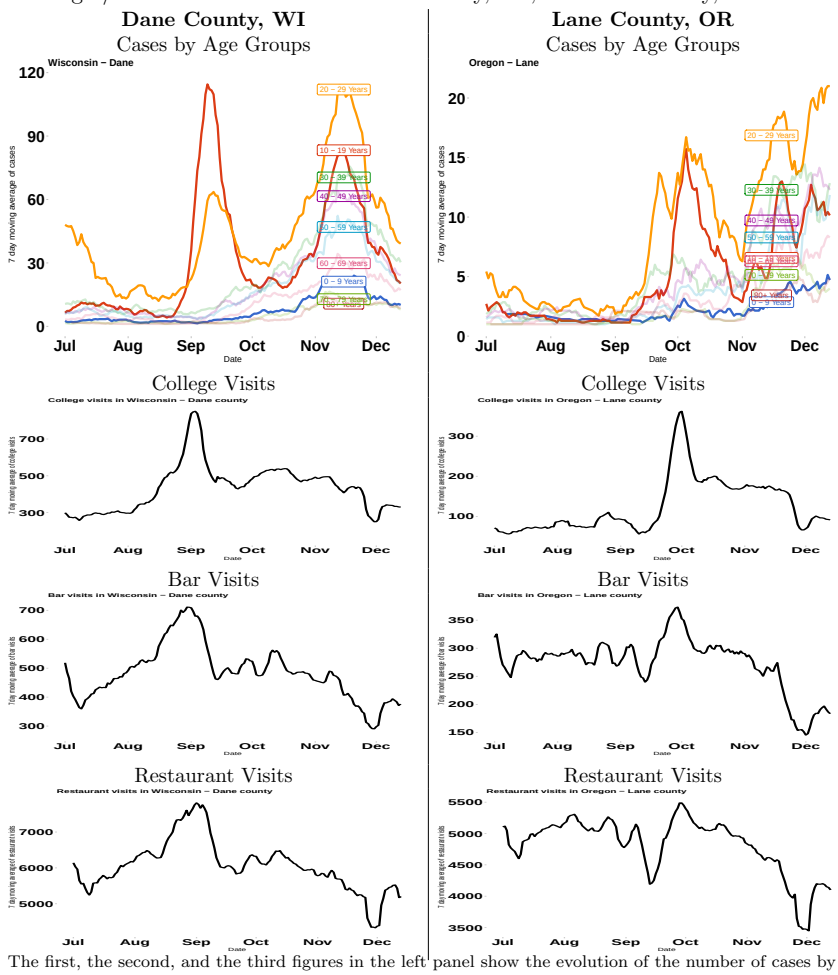

Notes: The first, the second, and the third figures in the left panel show the evolution of the number of cases by age groups, the number of visits to colleges/universities, and bars, respectively, in Dane County, WI. The right panel shows the corresponding figures for Lane County, OR.

Covid Economics 70, 25 February 2021: 70-108

Covid Economics 70, 25 February 2021: 70-108

While Fig. 1-2 as well as SI Appendix, Fig. S1-S2 are suggestive, the patterns observed in them may be driven by a variety of confounders. Therefore, we analyze the effect of opening K-12 schools and colleges/universities by panel data regression analysis with fixed effects to capture unobserved confounding.

We conduct the analysis using county-level data in the United States. As an outcome variable, we use the weekly growth rate of confirmed cases approximated by the log-difference in reported weekly cases over two weeks, where the log of weekly cases is set to be -1 when we observe zero weekly cases. The main explanatory variables of interest are 2-weeks lagged per-device visits to K-12 schools and colleges/universities from SafeGraph foot traffic data (SI Appendix, Fig. S3. (3)(6)).

We also consider the variable for school openings with different teaching methods (in-person, hybrid, and remote) from MCH Strategic Data (SI Appendix, Fig. S3(11)). Foot traffic data has the advantage over school opening data in that it provides more accurate information on the actual visits to schools over time, possibly capturing unrecorded changes in teaching methods and school closures beyond the information provided by MCH Strategic Data. Furthermore, foot traffic data covers all counties while there is missing information for some school districts in MCH Strategic Data, which may possibly cause sample selection issues.

To investigate the role of mitigation strategies at school on the transmission of SARS-CoV-2, we examine how the coefficients of K-12 school visits and K-12 school opening depend on the mask-wearing requirement for staff by adding an interaction term, for example, between K-12 school visits and mask-wearing requirements for staff at schools.[1]

As confounders, we consider a set of county fixed effects as well as interaction terms between state and week fixed effects to control for unobserved time-invariant county-level factors as well as unobserved time-varying state-level factors. County fixed effects control permanent differences across counties in unobserved personal risk-aversion and attitude toward mask-wearing, hand washings, and social distancing. Interaction terms between state dummy variables and week dummy variables capture any change over time in people's behaviors and non-pharmaceutical policy interventions (NPIs) that are common within a state; they also control for changes in weather, temperature, and humidity within a state. We also include county-level NPIs (mask mandates, ban gathering of more than 50 persons, stay-at-home orders) lagged by 2 weeks to control for the effect of people's behavioral

[1]MCH Strategic Data provides the school district level data on whether each school district adopts the following mitigation strategies: (i) mask requirements for staff, (ii) mask requirements for students, (iii) prohibiting sports activities, and (iv) online instruction increases, among other measures. We decided to use mask requirements for staff as the main variable for school mitigation strategy because it has a relatively smaller number of missing values. For regression analysis with the mask requirement variable, we drop counties from the sample when more than 50 percent of students in a county attend school districts of which mask requirements for staff is unknown or pending. Similarly, for specification with different teaching methods, we drop counties from the sample when more than 50 percent of students in a county attend school districts of which teaching methods are unknown or pending.

changes driven by policies on case growths beyond the effect of state-level policies.[2] Furthermore, the logarithm of past weekly cases with 2, 3, and 4 weeks lag lengths are included to capture people's voluntarily behavioral response to new information of transmission risks. The growth rate of the number of tests recorded at the daily frequency for each state is also added as a control for case growth regression.

Because the fixed effects estimator with a set of county dummies for dynamic panel regression could be severely biased when the time dimension is short (Nickell, 1981), we employ the debiased estimator by implementing bias correction (e.g., Chen, Chernozhukov, and Fernández-Val, 2019). Our empirical analysis uses 7-day moving averages of daily variables to deal with periodic fluctuations within a week. Our data set contains 3144 counties for regression analysis using foot traffic data but some county observations are dropped out of samples due to missing values for school opening teaching methods and staff mask requirements in some regression specifications.[3] Our sample period is from April 1, 2020, to December 2, 2020. The analysis was conducted using R software (version 4.0.3).

Results

Table 1 reports the debiased estimates of panel data regression. Clustered standard errors at the state level are reported in the bracket to provide valid inference under possible dependency over time and across counties within each state. The results suggest that an increase in the visits to K-12 schools and colleges/universities as well as opening K-12 schools with in-person learning mode is associated with an increase in the growth rates of cases with 2 weeks lag when schools implement no mask mandate for staff.

In column (1), the estimated coefficient of per-device visits to colleges is 0.14 (SE = 0.07) while that of per-device visits to K-12 schools is 0.47 (SE = 0.07). The change in top 5 percentile values of per-device visits to colleges/universities and K-12 schools between June and September among counties are around 0.1 and 0.15, respectively, in SI Appendix, Fig. S4(d)(e). Taking these values as a benchmark for full openings, fully opening colleges/universities may be associated with (0.14×0.1=) 1.4 percentage points increase in the growth rates of cases while fully opening K-12 schools may have contributed to (0.47×0.15=) 7 percentage points increase in case growth rates. Column (3) indicates that openings of K-12 schools with the in-person mode are associated with 5 (SE = 2) percentage point increases in weekly case growth rates. It also provides evidence that openings of K-12 schools with remote learning mode are associated with a decrease in case growth, perhaps because remote school opening induces more precautionary behavior to reduce transmission risk.

In column (2), the estimated coefficient of the interaction between K-12 school visits and no mask-wearing requirements for staff is 0.24 (SE=0.07), providing some evidence that mask-wearing requirements for staff may have reduced the transmission of SARS-CoV-2

[2]The decision to reopen schools in some states such as California and Oregon depended on trends in local case counts or hospitalizations (Goldhaber-Fiebert, Studdert, and Mello, 2020).

[3]Our regression analysis uses 2788 counties for specification with K-12 school opening with different teaching modes while the sample contains 2204 counties for specification with mask requirements for staff.

Covid Economics 70, 25 February 2021: 70-108

at schools. Similarly, in column (4), the coefficients on the interaction of in-person and hybrid school openings with no mask mandates are positively estimated as 0.04 (SE=0.02) and 0.05 (SE=0.02), respectively. These estimates likely reflect not only the effect of mask-wearing requirements for staff but also that of other mitigation measures. For example, school districts with staff mask-wearing requirements frequently require students to wear masks.

Other studies on COVID-19 spread in schools have also pointed to the importance of mitigation measures. In contact tracing studies of cases in schools, Gillespie et al. (2021) found that 6 out of 7 traceable case clusters were related to clear noncompliance with mitigation protocols, and Zimmerman et al. (2021) found that most secondary transmissions were related to absent face coverings. Hobbs et al. (2020) find that children who tested positive for COVID-19 are considerably less likely to have had reported consistent mask use by students and staff inside their school.

Consistent with evidence from U.S. state-level panel data analysis in Chernozhukov, Kasahara, and Schrimpf (2021), the estimated coefficients of county-wide mask mandate policy are negative and significant in columns (1)-(4), suggesting that mandating masks reduces case growth. The estimated coefficients of ban gatherings and stay-at-home orders are also negative. The negatively estimated coefficients of the log of past weekly cases are consistent with a hypothesis that the information on higher transmission risk induces people to take precautionary actions voluntarily to reduce case growth. The table also highlights the importance of controlling for the test growth rates as a confounder.

Evidence on the role of schools in the spread of COVID-19 from other studies is mixed. Papers that focus on contract tracing of cases among students find limited spread from student infections Zimmerman et al. (2021), Brandal et al. (2021), Ismail et al. (2020), Gillespie et al. (2021), Falk et al. (2021), Willeit et al. (2021). There is also some evidence that school openings are associated with increased cases in the surrounding community. Bignami et al. (2021) provides suggestive evidence that school openings are associated with increased cases in Montreal neighborhoods. Auger et al. (2020) use US state-level data to argue that school closures at the start of the pandemic substantially reduced.

Two closely related papers also examine the relationship between schools and county-level COVID-19 outcomes in the US. Goldhaber et al. (2021) examine the relationship between schooling and cases in counties in Washington and Michigan. They find that in-person schooling is only associated with increased cases in areas with high pre-existing COVID-19 cases. Similarly, Harris, Ziedan, and Hassig (2021) analyze US county-level data on COVID-19 hospitalizations and find that in-person schooling is not associated with increased hospitalizations in counties with low pre-existing COVID-19 hospitalization rates. As discussed in SI Appendix, our regression specification is motivated by a SIRD model, and the dependent variable in our analysis is case growth rates instead of new cases or hospitalizations. Consistent with Goldhaber et al. (2021) and Harris, Ziedan, and Hassig (2021), our finding of a constant increase in growth rates implies a greater increase in cases in counties with more pre-existing cases.

Covid Economics 70, 25 February 2021: 70-108

CEPR PRESS

Covid Economics 70, 25 February 2021: 70-108

TABLE 1. The Association of School/College Openings and NPIs with Case Growth in the United States: Debiased Estimator

	Dependent variable: Case Growth Rates			
	(1)	(2)	(3)	(4)
College Visits, 14d lag	0.139*	0.070	0.132**	0.010
	(0.071)	(0.073)	(0.064)	(0.076)
K-12 Visits, 14d lag	0.467***	0.386***		
	(0.070)	(0.070)		
K-12 Visits × No-Mask		0.297***		
		(0.070)		
K-12 In-person, 14d lag			0.047***	0.023
			(0.017)	(0.021)
K-12 Hybrid, 14d lag			−0.008	−0.037***
			(0.014)	(0.013)
K-12 Remote, 14d lag			−0.082***	−0.102***
			(0.016)	(0.015)
K-12 In-person × No-Mask				0.041**
				(0.019)
K-12 Hybrid × No-Mask				0.049***
				(0.017)
Mandatory mask, 14d lag	−0.113***	−0.123***	−0.128***	−0.128***
	(0.018)	(0.017)	(0.020)	(0.019)
Ban gatherings, 14d lag	−0.124***	−0.136***	−0.135***	−0.137***
	(0.033)	(0.044)	(0.033)	(0.042)
Stay at home, 14d lag	−0.264***	−0.260***	−0.261***	−0.268***
	(0.031)	(0.039)	(0.034)	(0.040)
log(Cases), 14d lag	−0.101***	−0.101***	−0.098***	−0.099***
	(0.009)	(0.010)	(0.010)	(0.010)
log(Cases), 21d lag	−0.061***	−0.060***	−0.060***	−0.059***
	(0.005)	(0.005)	(0.005)	(0.005)
log(Cases), 28d lag	−0.030***	−0.033***	−0.031***	−0.034***
	(0.003)	(0.003)	(0.004)	(0.004)
Test Growth Rates	0.009**	0.008*	0.009**	0.009**
	(0.004)	(0.004)	(0.004)	(0.004)
County Dummies	Yes	Yes	Yes	Yes
State× Week Dummies	Yes	Yes	Yes	Yes
Observations	690,297	545,131	612,963	528,941
R^2	0.092	0.093	0.092	0.094

Notes: Dependent variable is the log difference in weekly positive cases across 2 weeks. Regressors are 7-days moving averages of corresponding daily variables and lagged by 2 weeks to reflect the time between infection and case reporting except that we don't take any lag for the log difference in test growth rates. All regression specifications include county fixed effects and state-week fixed effects to control for any unobserved county-level factors and time-varying state-level factors such as various state-level policies. The debiased fixed effects estimator is applied. The results from the estimator without bias correction is presented in SI Appendix, Table S1. Asymptotic clustered standard errors at the state level are reported in bracket. *p<0.1; **p<0.05; ***p<0.01

Covid Economics 70, 25 February 2021: 70-108

We next provide sensitivity analysis with respect to changes to our regression specification and assumption about delays between infection and reporting cases as follows:

(1) Baseline specifications in columns (1) and (2) of Table 1.
(2),(3) Alternative time lags of 10 and 18 days for visits to colleges and K-12 schools as well as NPIs.
(4) Setting the log of weekly cases to 0 when we observe zero weekly cases to compute the log-difference in weekly cases for outcome variable.
(5) Add the log of weekly cases lagged by 5 weeks and per-capital *cumulative* number of cases lagged by 2 weeks as controls.
(6) Add per-device visits to restaurants, bars, recreational places, and churches lagged by 2 and 4 weeks as controls.
(7) Add per-device visits to full-time and part-time workplaces and a proportion of devices staying at home lagged by 2 weeks as controls.
(8) All of (5)-(7).

Because the actual time lag between infection and reporting cases may be shorter or longer than 14 days, we consider the alternative time lags in (2) and (3). Specification (4) checks the sensitivity of handling zero weekly cases to construct the outcome variable of the log difference in weekly cases.

A major concern for interpreting our estimate in Table 1 as the causal effect is that a choice of opening timing, teaching methods, and mask requirements may be endogenous. Our baseline specification mitigates this concern by controlling for county-fixed effects, state-week fixed effects and the log of past cases but a choice of school openings may be still correlated with time-varying unobserved factors at the county-level. Therefore, we estimate a specification with additional time-varying county-level controls in (5)-(8).

Fig. 3(a) takes column (1) of Table 1 as a baseline specification and plots the estimated coefficients for visits to colleges and K12 schools with the 90 percent confidence intervals across different specifications using the debiased estimator; the estimates using the standard estimator *without* bias correction are qualitatively *similar* and reported in SI Appendix, Fig. S3. The estimated coefficients of K-12 school visits and college visits are all positive across different specifications, suggesting that an increase in visits to K-12 schools and colleges is robustly associated with an increase in case growth. On the other hand, the estimated coefficients often become smaller when we add more controls. In particular, relative to the baseline, adding full-time/part-time workplace visits and staying home devices leads to somewhat smaller estimated coefficients for both K-12 school and college visits, suggesting that opening schools and colleges is associated with people returning to work and/or going outside more frequently.

In Fig. 3(b), the estimated interaction term of K-12 school visits and no mask-wearing requirements for staff in column (2) of Table 1 are all positive and significant, robustly indicating a possibility that mask-wearing requirement for staff may have helped to reduce the transmission of SARS-CoV-2 at schools when K-12 schools opened with the in-person teaching method.

Covid Economics 70, 25 February 2021: 70-108

Association between School Openings and Mobility. As highlighted by a modeling study for the United Kingdom (Panovska-Griffiths et al., 2020), there are at least two reasons why opening K-12 schools in-person may increase the spread of COVID-19. First, opening K-12 schools increases the number of contacts within schools, which may increase the risk of transmission among children, parents, education workers, and communities at large. Second, reopening K-12 schools allow parents to return to work and increase their mobility in general, which may contribute to the transmission of COVID-19 at schools and workplaces.

To give insight on the role of reopening K-12 schools for parents to return to work and to increase their mobility, we conduct panel data regression analysis by taking visits to full-time workplaces and a measure of staying home devices as outcome variables and use a similar set of regressors as in Table 1 but without taking 2 weeks time lags.

Table 2(a) shows how the proportion of devices at full-time workplaces and that of staying home devices are associated with visits to K-12 schools as well as their in-person openings. In columns (1) and (2), the estimated coefficients of per-device K-12 school visits and opening K-12 schools for full-time work outcome variables are positive and especially large for in-person K-12 school opening. Similarly, the estimates in columns (3) and (4) suggest the negative association of per-device K-12 school visits and opening K-12 schools with the proportion of devices that do not leave their home. This is consistent with a hypothesis that opening K-12 school allows parents to return to work and spend more time outside. This result may also reflect education workers returning to work.

Table 3 presents regression analysis similar to that in Table 1 but including the proportion of devices at full-time/part-time workplaces and those at home as additional regressors, which corresponds to specification (7) in Fig. 3. The estimates indicate that the proportion of staying home devices is negatively associated with the subsequent case growth while the proportion of devices at full-time workplaces is positively associated with the case growth. Combined with the estimates in Table 2(a), these results suggest that school openings may have increased the transmission of SARS-CoV-2 by encouraging parents to return to work and to spend more time outside. This mechanism can partially explain the discrepency between our findings and various studies that focus on cases among students. Contract tracing of cases in schools, such as Falk et al. (2021), Zimmerman et al. (2021), Willeit et al. (2021), Brandal et al. (2021), and Ismail et al. (2020), often finds limited direct spread among students. On the other hand, Vlachos, Hertegård, and B. Svaleryd (2021) finds that parents and teachers of students in open schools experience increases in infection rates.

In columns (1)-(2) of Table 3, the estimated coefficients on K-12 school visits remain positive and large in magnitude even after controlling for the mobility measures of returning to work and being outside home which are mediator variables to capture the indirect effect of school openings on case growth through its effect on mobility. The coefficient on K-12 school visits are approximately 75% as large in Table 3 as in Table 1. This suggests that within-school transmission may be the primary channel through which school openings affect the spread of COVID-19.

One likely reason why college openings may increase cases is that students go out for bars (KA et al., 2020; Chang et al., 2021), where properly wearing masks and practicing social distancing are difficult. Table 2(b) presents how visits to restaurants and bars are associated with colleges/universities from panel regressions using per-device visits to restaurants and bars as outcome variables. These results indicate that bar visits are positively associated with college visits, consistent with a hypothesis that the transmission of SARS-CoV-2 may be partly driven by an increase in visits to bars by students.

Death Growth Regression. Many county-day observations report zero weekly deaths in our data set (SI Appendix, Table S4 and Fig. S4(4)). We approximate the weekly death growth rate by the log difference in weekly deaths, where the log of weekly deaths is replaced with -1 when we observe zero weekly deaths. We also consider an alternative measure of death growth rates by replacing the log of weekly deaths by 0 for zero weekly deaths. For death growth regression, we use the sub-sample of larger counties by dropping 10 percent of the smallest counties in terms of their population size for which zero weekly death happens more frequently.

Fig. 4 illustrates the estimated coefficients of visits to colleges and K-12 schools across different specifications for death growth regressions. SI Appendix, Table S3 presents the estimates of death growth regression under baseline specification with a time lag of 21 days.[4] Fig. 4(a) shows that the coefficient of visits to colleges and K-12 schools are positively estimated for (1) baseline, (3) an alternative time lag of 35 days, (4) an alternative measure of death growth, and adding more controls in (5)-(8), providing evidence that an increase in visits to colleges and K-12 schools is positively associated with the subsequent increase in weekly death growth rates. The magnitude of the estimated coefficient of K-12 school visits becomes smaller when the time lag is set to 28 days in (2). Fig. 4(b) shows that the association of K-12 school visits with death growth is stronger when no mask mandate for staff is in place.

Limitations. Our study has the following limitations. First, our study is observational and therefore should be interpreted with great caution. It only has a causal interpretation in a structural model under exogeneity assumptions that might not hold in reality (see the Model and Method in SI Appendix). While we present sensitivity analysis with a variety of controls including county dummies and interactions of state dummies and week dummies, the decisions to open K-12 schools and colleges/universities may be endogenous and correlated with other unobserved time-varying county-level factors that affect the spread of COVID-19. For example, people's attitudes toward social distancing, hand-washing, and mask-wearing may change over time (which we are not able to observe in the data) and their

[4]The time lag of 21 days is taken as a baseline to take into account the time lag of infection and death reporting but we also report the estimates for the time lag of 28 and 35 days in specifications (2) and (3). These choices of time lags are motivated by the numbers reported in Table 2 of `https://www.cdc.gov/coronavirus/2019-ncov/hcp/planning-scenarios.html`. For the age group above 65, the days from exposure to onset range up to 6 days; the interquartile range of days from symptom onset to death is given by 8 and 21 days; the interquartile range of days from death to reporting is 5 and 44 days.

Covid Economics 70, 25 February 2021: 70-108

changes may be correlated with school opening decisions beyond the controls we added to our regression specifications.

Our analysis is also limited by the quality and the availability of the data as follows. The reported number of cases is likely to understate true COVID-19 incidence, especially among children and adolescents because they are less likely to be tested than adults given that children exhibit milder or no symptoms.[5] County-level testing data is not used because of a lack of data although state-week fixed effects control for the weekly difference across counties within the same state and we also control daily state-level test growth rates.

Because foot traffic data is constructed from mobile phone location data, the data on K-12 school visits likely reflects the movements of parents and older children who are allowed to carry mobile phones to schools and excludes those of younger children who do not own mobile phones.[6]

Because COVID-infected children and adolescents are known to be less likely to be hospitalized or die from COVID, the consequence of transmission among children and adolescents driven by school openings crucially depends on whether the transmission of SARS-CoV-2 from infected children and adolescents to the older population can be prevented.[7] Our analysis does not provide any empirical analysis on how school opening is associated with the transmission across different age groups due to data limitations.[8] Vlachos, Hertegård, and B. Svaleryd (2021) show that teachers in open schools experience higher COVID-19 infection rates compared to teachers in closed schools. They also show that this increase in infection rate also occurs in partners of teachers and parents of students in open schools, albeit to a lesser degree.

The impact of school openings on the spread of COVID-19 on case growth may be different across counties and over time because it may depend not only on in-school mitigation measures but also on contact tracing, testing strategies, and the prevalence of community transmissions (Goldhaber-Fiebert, Studdert, and Mello, 2020; Ziauddeen et al., 2020). We do not investigate how the association between school openings and case growths depends on contact tracing and testing strategies at the county-level.

[5]This is consistent with CDC data which shows the lower testing volume and the higher rate of positive test among children and adolescents than adults (Leidman et al., 2021).

[6]We also focus on limited Points-Of-Interest: K-12 schools, colleges and universities, restaurants, drinking places, other recreational places including gyms, and churches. We check the robustness by including visits to assisted living facilities for the elderly as well as nursing care facilities as additional controls but the results are not sensitive to their inclusion.

[7]In the meta-analysis of 54 studies on the household transmission of SARS-CoV-2 Madewell et al. (2020), estimated household secondary attack rate *to* child contacts was 16.8%. Miyahara et al. (2021) reports that household secondary attack rate *from* children and adolescence to other family members was 23.8% and higher than other age groups in Japan.

[8]CDC collects the data on the number of reported cases by age groups from each state whenever such data is available. However, for many counties, the reported cases by age groups are missing or there exists a substantial gap between the sum of cases across different age groups reported by CDC and the total number of cases reported in NYT case data (see, for example, the case of Ingham, MI, in SI Appendix, Fig. S2).

Covid Economics 70, 25 February 2021: 70-108

The result on the association between school opening and death growth in Fig. 4 is suggestive but must be viewed with caution because the magnitude of the estimated coefficient of K-12 school visits is sensitive to the assumption on the time lag from infection to death reporting. The time lag between infection and death is stochastic and spreads over time, making it difficult to uncover the relationship between the timing of school openings and subsequent deaths. Furthermore, while we provide sensitivity analysis for how to handle zero weekly deaths to approximate death growth, our construction of the death growth outcome variable remains somewhat arbitrary.

Finally, our result does not necessarily imply that K-12 schools should be closed. Closing schools have negative impacts on children's learning and may cause declining mental healths among children. The decision to open or close K-12 schools requires careful assessments of the cost and the benefit.

Covid Economics 70, 25 February 2021: 70-108

Covid Economics 70, 25 February 2021: 70-108

FIGURE 3. Sensitivity analysis for the estimated coefficients of K-12 visits and college visits of case growth regressions: Debiased Estimator

(a) Case Growth Estimates

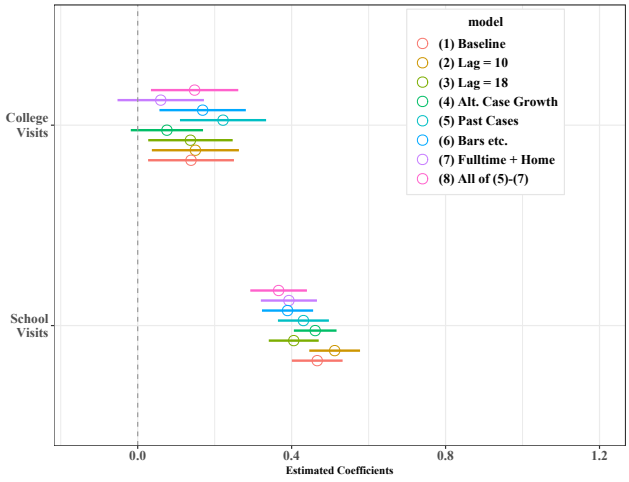

(b) Case Growth Estimates with School Visits × No Mask

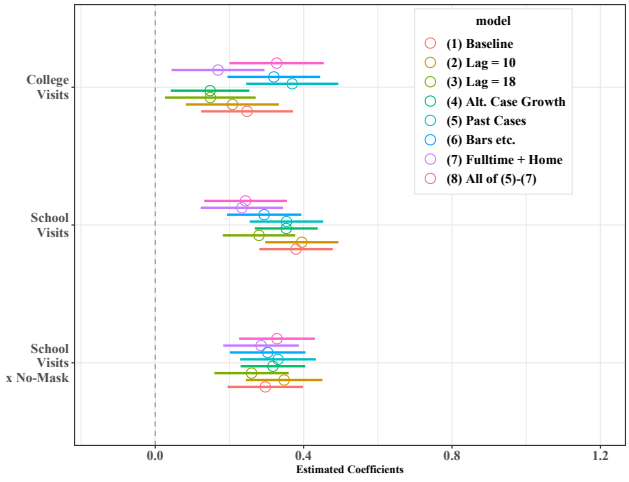

Notes: (a) presents the estimated of college visits and K-12 school visits with the 90 percent confidence intervals across different specifications taking the column (1) of Table 1 as baseline. (b) presents the estimates of college visits , K-12 school visits, and the interaction between K-12 school visits and no mask wearing requirement for staff taking column (2) of Table 1 as baseline. The results are based on the debiased estimator. SI Appendix, Fig. S3 presents the results based on the estimator without bias correction.

Covid Economics 70, 25 February 2021: 70-108

FIGURE 4. Sensitivity analysis for the estimated coefficients of K-12 visits and college visits of death growth regressions: Debiased Estimator

(a) Death Growth Estimates

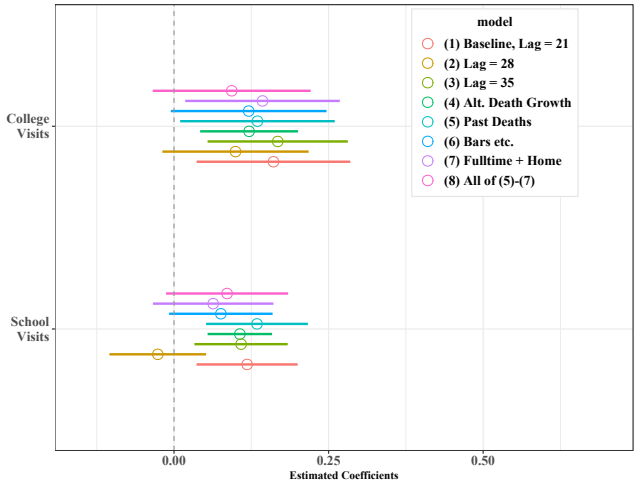

(b) Death Growth Estimates with School Visits × No Mask

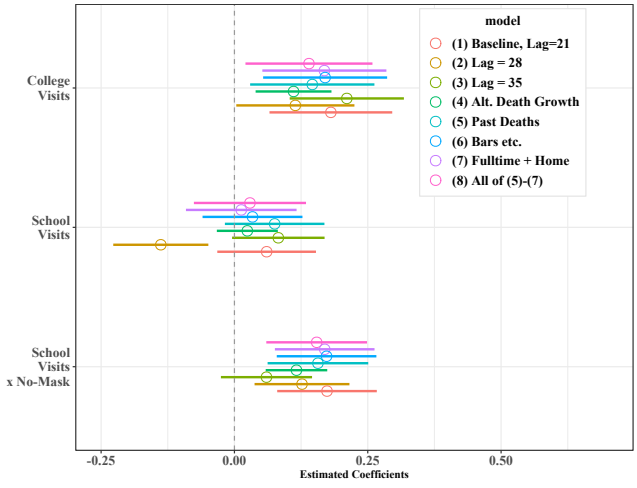

Notes: (a) presents the estimated of college visits and K-12 school visits with the 90 percent confidence intervals across different specifications taking the column (1) of SI Appendix, Table S3 as baseline. (b) presents the estimates of college visits , K-12 school visits, and the interaction between K-12 school visits and no mask wearing requirement for staff taking column (2) of SI Appendix, Table S3 as baseline.

Covid Economics 70, 25 February 2021: 70-108

Materials and Methods

Data. Cases and the deaths for each county are obtained from the New York Times. SafeGraph provides foot traffic data based on a panel of GPS pings from anonymous mobile devices. Per-device visits to K-12 schools, colleges/universities, restaurants, bars, recreational places, and churches are constructed from the ratio of daily device visits to these point-of-interest locations to the number of devices residing in each county. Full-time and part-time workplace visits are the ratio of the number of devices that spent more than 6 hours and between 3 to 6 hours, respectively, at one location other than one's home location to the total number of device counts. Staying home device variable is the ratio of the number of devices that do not leave home locations to the total number of device counts.

MCH Strategy Data provides information on the date of school openings with different teaching methods (in-person, hybrid, and remote) as well as mitigation strategies at 14703 school districts. We link school district-level MCH data to county-level data from NYT and SafeGraph using the file for School Districts and Associated Counties at US Census Bureau. School district data is aggregated up to county using the enrollment of students at the district level. Specifically, we construct the proportion of students with different teaching methods for each county-day observation using the district level information on school opening dates and teaching methods. We also construct a county-level dummy variable of "No mask requirement for staff" which takes a value of 1 if there exists at least one school district without any mask requirement for staff and 0, otherwise. Our regressors are 7 days moving averages of these variables. A substantial fraction of school districts report "unknown" or "pending" for teaching methods and mask requirements. We drop county observations for which more than 50 percent of students attend school districts that report unknown or pending for teaching methods or mask requirements when these variables are included in regressors.

NPIs data on stay-at-home orders and gathering bans is from Jie Ying Wu Killeen et al. (2020) while the data on mask policies is from Wright et al. (2020). These NPI data contain information up to the end of July; in our regression analysis, we set the value of these policy variables after August to be the same as the value of the last day of observations. Cases by age groups for Fig. 2 is from CDC. SI Appendix, Tables S5-S6 present summary statistics and correlation matrix. Fig. S4. presents the evolution of percentiles of these variables over time.

Methods. Our research design closely follows Chernozhukov, Kasahara, and Schrimpf (2021). Fig. 5 is a causal path diagram for our model that describes how policies, behavior, and information interact together:

- The *forward* health outcome, $Y_{i,t+\ell}$, is determined last after all other variables have been determined;
- The policies, P_{it}, affect health outcome $Y_{i,t+\ell}$ either directly, or indirectly by altering human behavior B_{it}, which may be only partially observed;

CEPR PRESS

FIGURE 5. The causal path diagram for our model

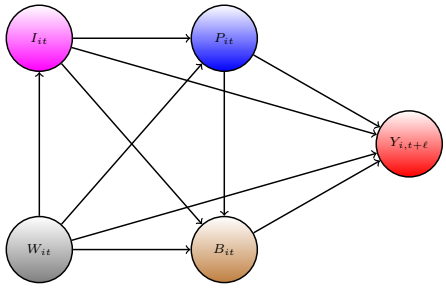

- Information variables, I_{it}, such as lagged values of outcomes can affect human behavior and policies, as well as outcomes;
- The confounders W_{it}, which vary across counties and time, affect all other variables; these include unobserved but estimable county, time, state, state-week effects.

The index i denotes the county i, and t and $t+\ell$ denotes the time, where ℓ represents the time lag between infection and case confirmation or death. Our health outcomes are the growth rates in Covid-19 cases and deaths and policy variables include school reopening in various modes, mask mandates, ban gathering, and stay-at-home orders, and the information variables include lagged values of outcome (as well as other variables described in the sensitivity analysis).

The causal structure allows for the effect of the policy to be either direct or indirect. For example, school openings not only directly affect case growth through the within-school transmission but also indirectly affect case growth by increasing parents' mobility. The structure also allows for changes in behavior to be brought by the change in policies and information. The information variables, such as the number of past cases, can cause people to spend more time at home, regardless of adopted policies; these changes in behavior, in turn, affect the transmission of SARS-CoV-2.

Our measurement equation will take the form:

$$\Delta \log(\Delta C_{it}) = X'_{i,t-14}\theta + \delta_T \Delta \log(T_{it}) + \epsilon_{it},$$

where i is county, t is day, ΔC_{it} is weekly confirmed cases over 7 days, T_{it} is the number of tests over 7 days, Δ is a 7-day differencing operator, ϵ_{it} is an unobserved error term. $X_{i,t-14}$ collects other behavioral, policy, and confounding variables, where the lag of 14 days captures the time lag between infection and confirmed case (see MIDAS (2020)). In SI Appendix, we relate this specification to the SIRD model.

The main regressors of interest are the [1] visits to K-12 schools and colleges/universities as well as the K-12 school opening variables with different teaching methods together with

Covid Economics 70, 25 February 2021: 70-108

Covid Economics 70, 25 February 2021: 70-108

their interactions with mask requirements for staff. As confounders, $X_{i,t-14}$ includes a set of county dummies and a set of all interaction terms between state dummies and week dummies. We also consider 2, 3, and 4 weeks lagged log values of weekly cases as well as three NPI policy variables. The growth rate of tests, $\Delta \log(T_{it})$, is captured by the observed growth rate of tests at state-level as well as interaction terms between state dummy variables and week dummy variables. The standard errors are computed by clustering at the state-level, where its rationale is that the county-level stochastic shocks may be correlated across counties especially within the state.

Our specification effectively contains the lagged dependent variables in a set of regressors because the log of past weekly cases with different lag lengths can be transformed into the log-differences of past weekly cases. Our model is a dynamic panel regression model in which the fixed effects estimator with a set of county dummies may result in the Nickell bias (Nickell, 1981). To eliminate the bias, we construct an estimator with bias correction as follows.

Given our panel data with sample size (N, T), denote a set of counties by $\mathcal{N} = \{1, 2, ..., N\}$. We randomly and repeatedly partition $\mathcal{N}$ into two sets as $\mathcal{N}_1^j$ and $\mathcal{N}_2^j = \mathcal{N} \setminus \mathcal{N}_1^j$ for $j = 1, 2, ..., J$, where $\mathcal{N}_1^j$ and $\mathcal{N}_2^j$ (approximately) contain the same number of counties. For each of $j = 1, ..., J$, consider two sub-panels (where i stands for county and t stands for the day) defined by $\mathbf{S}_1^j = \mathbf{S}_{11}^j \cup \mathbf{S}_{22}^j$ and $\mathbf{S}_2^j = \mathbf{S}_{12}^j \cup \mathbf{S}_{21}^j$ with $\mathbf{S}_{1k}^j = \{(i,t) : i \in \mathcal{N}_k, t \leq \lceil T/2 \rceil\}$ and $\mathbf{S}_{2k}^j = \{(i,t) : i \in \mathcal{N}_k, t \geq \lfloor T/2 + 1 \rfloor\}$ for $k = 1, 2$, where $\lceil . \rceil$ and $\lfloor . \rfloor$ are the ceiling and floor functions. We form the estimator with bias correction as

$$\widehat{\beta}_{\text{BC}} := \widehat{\beta} - \underbrace{(\widehat{\beta} - \widetilde{\beta})}_{\text{bias estimator}} = 2\widehat{\beta} - \widetilde{\beta} \quad \text{with} \quad \widetilde{\beta} := \frac{1}{J} \sum_{j=1}^{J} \widetilde{\beta}_{\mathbf{S}_1^j \cup \mathbf{S}_2^j},$$

where $\widehat{\beta}$ is the standard estimator with a set of N county dummies while $\widetilde{\beta}_{\mathbf{S}_1^j \cup \mathbf{S}_2^j}$ denotes the estimator using the data set $\mathbf{S}_1^j \cup \mathbf{S}_2^j$ but treats the counties in $\mathbf{S}_1^j$ differently from those in $\mathbf{S}_2^j$ to form the estimator— namely, we include approximately $2N$ county dummies to compute $\widetilde{\beta}_{\mathbf{S}_1^j \cup \mathbf{S}_2^j}$. We choose $J = 2$ in our empirical analysis.[9] We report asymptotic standard errors with state-level clustering, justified by the standard asymptotic theory of bias-corrected estimators.

[9]For some specifications, we also experimented with $J = 5$ and obtained the results similar to those with $J = 2$.

CEPR PRESS

Covid Economics 70, 25 February 2021: 70-108

TABLE 2. The Association of School/College Openings with Mobility in the United States: Debiased Estimator

(a) Full-time Workplace Visits and Staying Home Devices

	Dependent variable			
	Full Time	Full Time	Stay Home	Stay Home
	(1)	(2)	(3)	(4)
College Visits	−0.080***	−0.098***	−0.207***	−0.207***
	(0.004)	(0.006)	(0.024)	(0.026)
K-12 School Visits	0.078***		−0.061**	
	(0.006)		(0.026)	
Open K-12 In-person		0.999***		−2.271***
		(0.125)		(0.382)
Open K-12 Hybrid		0.509***		0.094
		(0.051)		(0.186)
Open K-12 Remote		0.211***		0.159
		(0.048)		(0.307)
Observations	670,909	595,886	670,909	595,886
R^2	0.870	0.853	0.889	0.888
Note:				*p<0.1; **p<0.05; ***p<0.01

(b) Visits to Restaurants and Bars

	Dependent variable			
	Restaurants	Restaurants	Bars	Bars
	(1)	(2)	(3)	(4)
College Visits	0.064	0.034	0.016***	0.012**
	(0.053)	(0.051)	(0.006)	(0.005)
K-12 School Visits	0.006		0.008	
	(0.046)		(0.006)	
Open K-12 In-person		−1.367***		−0.177***
		(0.404)		(0.041)
Open K-12 Hybrid		−1.162***		−0.097***
		(0.272)		(0.038)
Open K-12 Remote		−0.512*		0.031
		(0.295)		(0.056)
Observations	670,909	595,886	670,909	595,886
R^2	0.881	0.883	0.807	0.807

Notes: All regression specifications include county fixed effects, state-week fixed effects, three NPIs variables, and the log of cases without lag, lagged by 1 and 2 weeks. See SI Appendix, Table S1 for the estimated coefficients for NPIs and the log of current and past cases. The debiased estimator is used. Clustered standard errors at the state level are reported in the bracket. SI Appendix, Table S2 reports the estimates for NPIs and past cases. *p<0.1; **p<0.05; ***p<0.01

CEPR PRESS

Covid Economics 70, 25 February 2021: 70-108

TABLE 3. The Association of School/College Openings, Full-time/Part-time Work, and Staying Home with Case Growth in the United States: Debiased Estimator

	Dependent variable: ***Case Growth Rates***			
	(1)	(2)	(3)	(4)
College Visits, 14d lag	0.060	0.012	0.114*	0.010
	(0.071)	(0.072)	(0.065)	(0.075)
K-12 Visits, 14d lag	0.393***	0.283***		
	(0.075)	(0.087)		
K-12 Visits × No-Mask		0.287***		
		(0.071)		
K-12 In-person, 14d lag			0.015	−0.007
			(0.016)	(0.020)
K-12 Hybrid, 14d lag			−0.028**	−0.055***
			(0.013)	(0.013)
K-12 Remote, 14d lag			−0.094***	−0.115***
			(0.015)	(0.014)
K-12 In-person × No-Mask				0.034*
				(0.020)
K-12 Hybrid × No-Mask				0.043***
				(0.017)
Full-time Work Device, 14d lag	−0.117	0.186	0.956**	0.967**
	(0.417)	(0.490)	(0.384)	(0.436)
Part-time Work Device, 14d lag	0.262	0.466	0.820***	0.915***
	(0.259)	(0.305)	(0.276)	(0.309)
Staying Home Device, 14d lag	−0.290***	−0.283***	−0.352***	−0.332***
	(0.057)	(0.069)	(0.061)	(0.067)
Observations	690,297	545,131	612,963	528,941
R^2	0.092	0.093	0.092	0.094

Notes: Dependent variable is the log difference in weekly positive cases across 2 weeks. All regression specifications include county fixed effects and state-week fixed effects, three NPIs, and 2, 3, and 4 weeks lagged log of cases. See SI Appendix, Table S3 for the estimated coefficients for NPIs and the log of current and past cases. The debiased fixed effects estimator is applied. Asymptotic clustered standard errors at the state level are reported in the bracket.
*p<0.1; **p<0.05; ***p<0.01

REFERENCES

Auger, Katherine A., Samir S. Shah, Troy Richardson, David Hartley, Matthew Hall, Amanda Warniment, Kristen Timmons, Dianna Bosse, Sarah A. Ferris, Patrick W. Brady, Amanda C. Schondelmeyer, and Joanna E. Thomson. 2020. "Association Between Statewide School Closure and COVID-19 Incidence and Mortality in the US." *JAMA* 324 (9):859–870. URL `https://doi.org/10.1001/jama.2020.14348`.

Bignami, Simona, Yacine Boujija, John Sandberg, and Olivier Drouin. 2021. "Enfants, écoles et COVID-19 : le cas montréalais."

Brandal, Lin T, Trine S Ofitserova, Hinta Meijerink, Rikard Rykkvin, Hilde M Lund, Olav Hungnes, Margrethe Greve-Isdahl, Karoline Bragstad, Karin Nygård, and Winje Brita A. 2021. "Minimal transmission of SARS-CoV-2 from paediatric COVID-19 cases in primary schools, Norway, August to November 2020." *Euro Surveill* URL `https://doi.org/10.2807/1560-7917.ES.2020.26.1.2002011`.

Chang, Serina, Emma Pierson, Pang Wei Koh, Jaline Gerardin, Beth Redbird, David Grusky, and Jure Leskovec. 2021. "Mobility network models of COVID-19 explain inequities and inform reopening." *Nature* 589 (7840):82–87. URL `https://doi.org/10.1038/s41586-020-2923-3`.

Chen, Shuowen, Victor Chernozhukov, and Iván Fernández-Val. 2019. "Mastering panel metrics: causal impact of democracy on growth." In *AEA Papers and Proceedings*, vol. 109. 77–82.

Chen, Shuowen, Victor Chernozhukov, Ivan Fernandez-Val, Hiroyuki Kasahara, and Paul Schrimpf. 2020. "Cross-Over Jackknife Bias Correction for Non-Stationary Nonlinear Panel Data."

Chernozhukov, Victor, Hiroyuki Kasahara, and Paul Schrimpf. 2021. "Causal impact of masks, policies, behavior on early covid-19 pandemic in the U.S." *Journal of Econometrics* 220 (1):23–62.

Falk, A, A Benda, P Falk, S Steffen, Z Wallace, and TB Høeg. 2021. "COVID-19 Cases and Transmission in 17 K–12 Schools — Wood County, Wisconsin, August 31–November 29, 2020." *Morbidity and Mortality Weekly Report* 70:136–140. URL http://dx.doi.org/10.15585/mmwr.mm7004e3.

Gillespie, Darria Long, Lauren Ancel Meyers, Michael Lachmann, Stephen C Redd, and Jonathan M Zenilman. 2021. "The Experience of Two Independent Schools with In-Person Learning During the COVID-19 Pandemic." *medRxiv* URL https://www.medrxiv.org/content/early/2021/01/29/2021.01.26.21250065.

Goldhaber, Dan, Scott A Imberman, Katharine O Strunk, Bryant Hopkins, Nate Brown, Erica Harbatkin, and Tara Kilbride. 2021. "To What Extent Does In-Person Schooling Contribute to the Spread of COVID-19? Evidence from Michigan and Washington." Working Paper 28455, National Bureau of Economic Research. URL http://www.nber.org/papers/w28455.

Goldhaber-Fiebert, Jeremy D., David M. Studdert, and Michelle M. Mello. 2020. "School Reopenings and the Community During the COVID-19 Pandemic." *JAMA Health Forum* 1 (10):e201294–e201294. URL https://doi.org/10.1001/jamahealthforum.2020.1294.

Hahn, Jinyong and Whitney Newey. 2004. "Jackknife and Analytical Bias Reduction for Nonlinear Panel Models." *Econometrica* 72 (4):1295–1319. URL https://EconPapers.repec.org/RePEc:ecm:emetrp:v:72:y:2004:i:4:p:1295-1319.

Harris, Douglas N., Engy Ziedan, and Susan Hassig. 2021. "The Effects of School Reopenings on COVID-19 Hospitalizations." Tech. rep. URL https://www.reachcentered.org/publications/the-effects-of-school-reopenings-on-covid-19-hospitalizations.

Hobbs, Charlotte V., Lora M. Martin, Sara S. Kim, Brian M. Kirmse, Lisa Haynie, Sarah McGraw, Paul Byers, Kathryn G. Taylor, Manish M. Patel, Brendan Flannery, and CDC COVID-19 Response Team. 2020. "Factors Associated with Positive SARS-CoV-2 Test Results in Outpatient Health Facilities and Emergency Departments Among Children and Adolescents Aged ¡18 Years - Mississippi, September-November 2020." *MMWR. Morbidity and Mortality Weekly Report* 69 (50):1925–1929. URL https://pubmed.ncbi.nlm.nih.gov/33332298.

Ismail, Sharif A., Vanessa Saliba, Jamie Lopez Bernal, Mary E. Ramsay, and Shamez N. Ladhani. 2020. "SARS-CoV-2 infection and transmission in educational settings: a prospective, cross-sectional analysis of infection clusters and outbreaks in England." *The Lancet Infectious Diseases* URL https://doi.org/10.1016/S1473-3099(20)30882-3.

KA, Fisher, Tenforde MW, Feldstein LR, Christopher J. Lindsell, Nathan I. Shapiro, D. Clark Files, Kevin W. Gibbs, Heidi L. Erickson, Matthew E. Prekker, Jay S. Steingrub, Matthew C. Exline, Daniel J. Henning, Jennifer G. Wilson, Samuel M. Brown, Ithan D. Peltan, Todd W. Rice, David N. Hager, Adit A. Ginde, H. Keipp Talbot, Jonathan D. Casey, Carlos G. Grijalva, Brendan Flannery, Manish M. Patel, and Wesley H. Self. 2020. "Community and Close Contact Exposures Associated with COVID-19 Among Symptomatic Adults $\geq$ 18 Years in 11 Outpatient Health Care Facilities — United States, July 2020." *MMWR Morb Mortal Wkly Rep* 69:1258–1264. URL http://dx.doi.org/10.15585/mmwr.mm6936a5.

Killeen, Benjamin D., Jie Ying Wu, Kinjal Shah, Anna Zapaishchykova, Philipp Nikutta, Aniruddha Tamhane, Shreya Chakraborty, Jinchi Wei, Tiger Gao, Mareike Thies, and Mathias Unberath. 2020. "A County-Level Dataset for Informing the United States' Response to COVID-19."

Leidman, Eva, Lindsey M. Duca, John D. Omura, Krista Proia, James W. Stephens, and Erin K. Sauber-Schatz. 2021. "COVID-19 Trends Among Persons Aged 0–24 Years — United States, March 1–December 12, 2020." *MMWR Morb Mortal Wkly Rep* 70. URL http://dx.doi.org/10.15585/mmwr.mm7003e1.

Madewell, Zachary J., Yang Yang, Jr Longini, Ira M., M. Elizabeth Halloran, and Natalie E. Dean. 2020. "Household Transmission of SARS-CoV-2: A Systematic Review and Meta-analysis." *JAMA Network Open* 3 (12):e2031756–e2031756. URL https://doi.org/10.1001/jamanetworkopen.2020.31756.

MIDAS. 2020. "MIDAS 2019 Novel Coronavirus Repository: Parameter Estimates." URL https://github.com/midas-network/COVID-19/tree/master/parameter_estimates/2019_novel_coronavirus.

Covid Economics 70, 25 February 2021: 70-108

Miyahara, Reiko, Naho Tsuchiya, Ikkoh Yasuda, Yura Ko, Yuki Furuse, Eiichiro Sando, Shohei Nagata, Tadatsugu Imamura, Mayuko Saito, Konosuke Morimoto, Takeaki Imamura, Yugo Shobugawa, Hiroshi Nishiura, Motoi Suzuki, and Hitoshi Oshitani. 2021. "Familial Clusters of Coronavirus Disease in 10 Prefectures, Japan, February-May 2020." *Emerging Infectious Diseases* 27 (3). URL https://wwwnc.cdc.gov/eid/article/27/3/20-3882_article.

Nickell, Stephen. 1981. "Biases in Dynamic Models with Fixed Effects." *Econometrica* 49 (6):1417–26. URL https://EconPapers.repec.org/RePEc:ecm:emetrp:v:49:y:1981:i:6:p:1417-26.

Panovska-Griffiths, Jasmina, Cliff C Kerr, Robyn M Stuart, Dina Mistry, Daniel J Klein, Russell M Viner, and Chris Bonell. 2020. "Determining the optimal strategy for reopening schools, the impact of test and trace interventions, and the risk of occurrence of a second COVID-19 epidemic wave in the UK: a modelling study." *The Lancet Child & Adolescent Health* 4 (11):817–827.

Parisi, Joe. 2020. "the letter from Dane County Executive to the UW-Madison." https://www.channel3000.com/content/uploads/2020/09/Parisi-letter-to-UW-9-9-20.pdf.

Pearl, Judea. 2009. *Causality*. Cambridge university press.

Vlachos, Jonas, Edvin Hertegård, and Helena B. Svaleryd. 2021. "The effects of school closures on SARS-CoV-2 among parents and teachers." *medRxiv* 118 (9). URL https://www.medrxiv.org/content/early/2021/01/29/2021.01.26.21250065.

White House, The. 2020. "Guidelines for Opening Up America Again." URL https://www.whitehouse.gov/openingamerica/.

Willeit, Peter, Robert Krause, Bernd Lamprecht, Andrea Berghold, Buck Hanson, Evelyn Stelzl, Heribert Stoiber, Johannes Zuber, Robert Heinen, Alwin Köhler, David Bernhard, Wegene Borena, Christian Doppler, Dorothee von Laer, Hannes Schmidt, Johannes Pröll, Ivo Steinmetz, and Michael Wagner. 2021. "Prevalence of RT-PCR-detected SARS-CoV-2 infection at schools: First results from the Austrian School-SARS-CoV-2 Study." *medRxiv* URL https://www.medrxiv.org/content/early/2021/01/06/2021.01.05.20248952.

Wright, Austin L., Konstantin Sonin, Jesse Driscoll, and Jarnickae Wilson. 2020. "Poverty and Economic Dislocation Reduce Compliance with COVID-19 Shelter-in-Place Protocols." *SSRN Electronic Journal* .

Ziauddeen, Nida, Kathryn Woods-Townsend, Sonia Saxena, Ruth Gilbert, and Nisreen A Alwan. 2020. "Schools and COVID-19: Reopening Pandora's box?" *Public Health in Practice* 1:100039–100039. URL https://www.ncbi.nlm.nih.gov/pmc/articles/PMC7486860/. Edition: 2020/12/22 Publisher: The Authors. Published by Elsevier Ltd on behalf of The Royal Society for Public Health.

Zimmerman, Kanecia O., Ibukunoluwa C. Akinboyo, M. Alan Brookhart, Angelique E. Boutzoukas, Kathleen McGann, Michael J. Smith, Gabriela Maradiaga Panayotti, Sarah C. Armstrong, Helen Bristow, Donna Parker, Sabrina Zadrozny, David J. Weber, and Daniel K. Benjamin. 2021. "Incidence and Secondary Transmission of SARS-CoV-2 Infections in Schools." *Pediatrics* URL https://pediatrics.aappublications.org/content/early/2021/01/06/peds.2020-048090.

Covid Economics 70, 25 February 2021: 70-108

2. Supplementary Information Appendix

The Model and Methods.

The Structural Causal Model. Our approach draws on the framework presented in our previous paper Chernozhukov, Kasahara, and Schrimpf (2021). Here we summarize the approach for completeness, highlighting the main difference (here we do not assume that all relevant social distancing behavioral variables are observed).

We begin with a qualitative description of the model via a causal path diagram shown in Figure 6, which describes how policies, behavior, and information interact together:

- The *forward* health outcome, $Y_{i,t+\ell}$, is determined last, after all other variables have been determined;
- The adopted vector of policies, P_{it}, affect health outcome $Y_{i,t+\ell}$ either directly, or indirectly by altering individual distancing and other precautioanry behavior B_{it}, which may be only partially observed;
- Information variables, I_{it}, such as lagged values of outcomes and other lagged observable variables (see robustness checks) can affect human behavior and policies, as well as outcomes;
- The confounding factors W_{it}, which vary across counties and time, affect all other variables; these include unobserved though estimable county, time, state, state-week effects.

The index i denotes observational unit, the county, and t and $t+\ell$ denotes the time, where ℓ represents the typical time lag between infection and case confirmation or death.

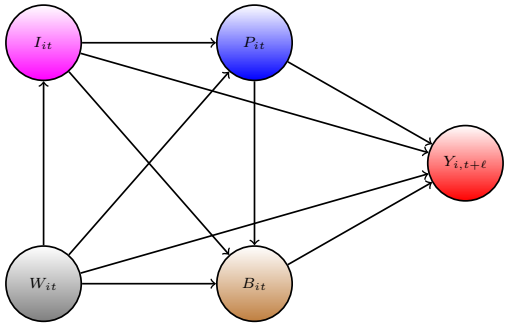

Figure 6. The causal path diagram for our model.

Our main outcomes of interest are the growth rates in Covid-19 cases and deaths and policy variables include school reopening in various modes, mask mandates, ban gathering,

and stay-at-home orders, and the information variables include lagged values of outcome (as well as other variables described in the sensitivity checks).

The role of behavioral variables in the model is two-fold. First, the presence of these variables in the model requires us to control for the information variables – even when information variables affect outcomes only through policies or behavior. In this case conditioning on the information blocks the backdoor path (see, Pearl (2009)) creating confounding

$$Y_{i,t+\ell} \longleftarrow B_{it} \longleftarrow I_{it} \longrightarrow P_{it}.$$

Therefore conditioning on the information is important even when there is no direct effect $I_{it} \longrightarrow Y_{i,t+\ell}$. This observation motivates our main dynamic specification below, where information variables include lagged growth rates and new cases or new deaths per capita. Second, while not all behavioral variables may be observable, we can still study as the matter of supporting analysis, the effects of policies on observed behavioral variables (the portion of time in workplace, restaurants, and bars) and of behavioral variables on outcomes, thereby gaining insight as to whether policies have changed private behavior and to what extent this private behavior changed the outcomes (for the analysis, of early pandemic data in this vein, see our previous paper).

The causal structure allows for the effect of the policy to be either direct or indirect. The structure also allows for changes in behavior to be brought by the change in policies and information. These are all realistic properties that we expect from the context of the problem. Policies such as closures and reopenings of schools, closures or reopening of non-essential business, and restaurants, affect the behavior in strong ways. In contrast, policies such as mandating employees to wear masks can potentially affect the Covid-19 transmission directly. The information variables, such as recent growth in the number of cases, can cause people to spend more time at home, regardless of adopted policies; these changes in behavior, in turn, affect the transmission of Covid-19.

The causal ordering induced by this directed acyclical graph is determined by the following timing sequence:

(1) information and confounders get determined at t,
(2) policies are set in place, given information and confounders at t;
(3) behavior is realized, given policies, information, and confounders at t;
(4) outcomes get realized at $t+\ell$ given policies, behavior, information, and confounders.

The model also allows for direct dynamic effects of information variables on the outcome through autoregressive structures that capture persistence in growth patterns. We do not highlight these dynamic effects and only study the short-term effects (longer-run effects get typically amplified; see our previous paper Chernozhukov, Kasahara, and Schrimpf (2021) for more details.)

Covid Economics 70, 25 February 2021: 70-108

Covid Economics 70, 25 February 2021: 70-108

Our quantitative model for causal structure in Figure 6 is given by the following econometric structural equation model:

$$\begin{aligned} Y_{i,t+\ell}(b,p,\iota) &:= \alpha' b + \pi' p + \mu' \iota + \delta_Y' W_{it} + \varepsilon_{it}^y, \\ B_{it}(p,\iota) &:= \beta' p + \gamma' \iota + \delta_B' W_{it} + \varepsilon_{it}^b, \\ P_{it}(\iota) &:= p(\eta' \iota, W_{it}, \varepsilon_{it}^p), \end{aligned} \tag{SEM}$$

which is a collection of structural potential response functions (potential outcomes), where the stochastic schocks are decomposed into an observable part $\delta' W$ and unobservable part ε. Lower case letters ι, b and p denote the potential values of information, behavior, and policy variables. The restrictions on shocks are described below.

The observed outcomes, policy, and behavior variables are generated by setting $\iota = I_{it}$ and propagating the system from the last equation to the first:

$$\begin{aligned} Y_{i,t+\ell} &:= Y_{i,t+\ell}(B_{it}, P_{it}, I_{it}), \\ B_{it} &:= B_{it}(P_{it}, I_{it}), \\ P_{it} &:= P_{it}(I_{it}). \end{aligned}$$

The orthogonality restrictions on the stochastic components are as follows: The stochastic shocks ε_{it}^y and ε_{it}^p are centered and furthermore,

$$\begin{aligned} \varepsilon_{it}^y &\perp (\varepsilon_{it}^b, P_{it}, W_{it}, I_{it}), \\ \varepsilon_{it}^b &\perp (P_{it}, W_{it}, I_{it}), \\ \varepsilon_{it}^p &\perp\!\!\!\perp (W_{it}, I_{it}), \end{aligned} \tag{O}$$

where we say that $V \perp U$ if $\mathrm{E}VU = 0$. This is a standard way of representing restrictions on errors in structural equation modeling. The last equation states that variation in policies is exogenous conditionally on confounders and information variables.

The system above together with orthogonality restrictions (O) implies the following collection of stochastic equations for realized variables:

$$Y_{i,t+\ell} = \alpha' B_{it} + \pi' P_{it} + \mu' I_{it} + \delta_Y' W_{it} + \varepsilon_{it}^y, \qquad \varepsilon_{it}^y \perp B_{it}, P_{it}, I_{it}, W_{it} \tag{BPI→Y}$$

$$B_{it} = \beta' P_{it} + \gamma' I_{it} + \delta_B' W_{it} + \varepsilon_{it}^b, \qquad \varepsilon_{it}^b \perp P_{it}, I_{it}, W_{it} \tag{PI→B}$$

As discussed below, the information variable includes case growth. Therefore, the orthogonality restriction $\varepsilon_{it}^y \perp P_{it}$ holds if the government does not have knowledge on future case growth beyond what is predicted by the information set and the confounders; even when the government has some knowledge on ε_{it}^y, the orthogonality restriction may hold if there is a time lag for the government to implement its policies based on ε_{it}^y.

We stress that our main analysis does not require all components of B_{it} to be observable.

Main Implication. The model stated above implies the following projection equation:

$$Y_{i,t+\ell} = a' P_{it} + b' I_{it} + c' W_{it} + \bar{\varepsilon}_{it}, \quad \bar{\varepsilon}_{it} \perp P_{it}, I_{it}, W_{it}, \qquad \text{(PI→Y)}$$

where

$$a' := (\alpha'\beta' + \pi'), \quad b' := (\alpha'\gamma' + \mu'), \quad c' := (\alpha'\delta_B' + \delta_Y')$$

This follows immediately from plugging equation (PI → B) to equation (BPI → Y) and verifying that the composite stochastic shock $\bar{\varepsilon}_{it}$ obeys the orthogonality condition stated in (PI→Y).

The main parameter of interest is the structural causal effect of the policy:

$$a' = (\alpha'\beta' + \pi').$$

It comprises direct policy effect π' as well as the indirect effect $\alpha'\beta'$, realized by the policy changing observed and unobserved behavior variables B_{it}. This coefficient a and b can estimated directly using the dynamic panel data methods described in more detail below.

As additional analysis, we can estimate the determinants for the observed behavioral mobility measures– the observed part of B_{it}.

Identification and Parameter Estimation. The orthogonality equations imply that the main equation is the projection equation, and parameters a and b are identified if P_{it} and I_{it} have sufficient variation left after partialling out the effect of controls:

$$\tilde{Y}_{i,t+\ell} = a' \tilde{P}_{it} + c' \tilde{I}_{it} + \bar{\varepsilon}_{it}, \quad \bar{\varepsilon}_{it} \perp \tilde{P}_{it}, \tilde{I}_{it}, \qquad (1)$$

where $\tilde{V}_{it} = V_{it} - W_{it}' \mathrm{E}[W_{it} W_{it}']^{-} \mathrm{E}[W_{it} V_{it}]$ denotes the residual after removing the orthogonal projection of V_{it} on W_{it}. The residualization is a linear operator, implying that (1) follows immediately from the above. The parameters of (1) are identified as projection coefficients in these equations, provided that residualized vectors have non-singular variance matrix:

$$\mathrm{Var}(\tilde{P}_{it}', \tilde{I}_{it}') > 0. \qquad (2)$$

Our main estimation method is the fixed effects estimator, where the county, state, state-week effects are treated as unobserved components of W_{it} and estimated directly from the panel data, so they are rendered (approximately) observable once the history is sufficiently long. The stochastic shocks $\{\varepsilon_{it}\}_{t=1}^{T}$ are treated as independent across states and can be arbitrarily dependent across time t within a state. In other words, the standard errors will be clustered at the state level. When histories are not long, substantial biases emerge from working with the estimated version $\widehat{W}_{it}$ of W_{it} (known as the Nickel bias (Nickell, 1981)) and they need to be removed using debiasing methods. In our context, debiasing changes the magnitudes of the original biased fixed effect estimator but does not change the qualitative conclusions reached without any debiasing.

Covid Economics 70, 25 February 2021: 70-108

Formulating Outcome and Key Confounders via SIR model. Letting C_{it} denote the cumulative number of confirmed cases in county i at time t, our outcome

$$Y_{it} = \Delta \log(\Delta C_{it}) := \log(\Delta C_{it}) - \log(\Delta C_{i,t-7}) \tag{3}$$

approximates the weekly growth rate in new cases from $t-7$ to t.[10] Here Δ denotes the differencing operator over 7 days from t to $t-7$, so that $\Delta C_{it} := C_{it} - C_{i,t-7}$ is the number of new confirmed cases in the past 7 days.

We chose this metric as this is the key metric for policymakers deciding when to relax Covid mitigation policies. The U.S. government's guidelines for state reopening recommend that states display a "downward trajectory of documented cases within a 14-day period" (White House, 2020). A negative value of Y_{it} is an indication of meeting these criteria for reopening. By focusing on weekly cases rather than daily cases, we smooth idiosyncratic daily fluctuations as well as periodic fluctuations associated with the days of the week.

Our measurement equation for estimating equations (BPI→Y) and (PI→Y) will take the form:

$$\Delta \log(\Delta C_{it}) = X'_{i,t-14}\theta + \delta_T \Delta \log(T_{it}) + \epsilon_{it}, \tag{M-C}$$

where i is county, t is day, C_{it} is cumulative confirmed cases, T_{it} is the number of tests over 7 days, Δ is a 7-days differencing operator, ϵ_{it} is an unobserved error term. $X_{i,t-14}$ collects other behavioral, policy, and confounding variables, depending on whether we estimate (BPI→Y) or (PI→Y), where the lag of 14 days captures the time lag between infection and confirmed case (see MIDAS (2020)). Here

$$\Delta \log(T_{it}) := \log(T_{it}) - \log(T_{i,t-7})$$

is the key confounding variable, derived from considering the SIR model below. We describe other confounders in the empirical analysis section.

Our main estimating equation (M-C) is motivated by a variant of SIR model, where we add confirmed cases and infection detection via testing. Let S, $\mathcal{I}$, R, and D denote the number of susceptible, infected, recovered, and dead individuals in a given state. Each of these variables are a function of time. We model them as evolving as

$$\dot{S}(t) = -\frac{S(t)}{N}\beta(t)\mathcal{I}(t) \tag{4}$$

$$\dot{\mathcal{I}}(t) = \frac{S(t)}{N}\beta(t)\mathcal{I}(t) - \gamma\mathcal{I}(t) \tag{5}$$

$$\dot{R}(t) = (1-\kappa)\gamma\mathcal{I}(t) \tag{6}$$

$$\dot{D}(t) = \kappa\gamma\mathcal{I}(t) \tag{7}$$

where N is the population, $\beta(t)$ is the rate of infection spread, γ is the rate of recovery or death, and κ is the probability of death conditional on infection.

[10] We may show that $\log(\Delta C_{it}) - \log(\Delta C_{i,t-7})$ approximates the average growth rate of cases from $t-7$ to t.

Covid Economics 70, 25 February 2021: 70-108

Covid Economics 70, 25 February 2021: 70-108

Confirmed cases, $C(t)$, evolve as

$$\dot{C}(t) = \tau(t)\mathcal{I}(t), \tag{8}$$

where $\tau(t)$ is the rate that infections are detected.

Our goal is to examine how the rate of infection $\beta(t)$ varies with observed policies and measures of social distancing behavior. A key challenge is that we only observed $C(t)$ and $D(t)$, but not $\mathcal{I}(t)$. The unobserved $\mathcal{I}(t)$ can be eliminated by differentiating (8) and using (5) as

$$\frac{\ddot{C}(t)}{\dot{C}(t)} = \frac{S(t)}{N}\beta(t) - \gamma + \frac{\dot{\tau}(t)}{\tau(t)}. \tag{9}$$

We consider a discrete-time analogue of equation (9) to motivate our empirical specification by relating the detection rate $\tau(t)$ to the number of tests T_{it} while specifying $\frac{S(t)}{N}\beta(t)$ as a linear function of variables $X_{i,t-14}$. This results in

$$\underbrace{\Delta \log(\Delta C_{it})}_{\frac{\ddot{C}(t)}{\dot{C}(t)}} = \underbrace{X'_{i,t-14}\theta + \epsilon_{it}}_{\frac{S(t)}{N}\beta(t)-\gamma} + \underbrace{\delta_T \Delta \log(T)_{it}}_{\frac{\dot{\tau}(t)}{\tau(t)}}$$

which is equation (M-C), where $X_{i,t-14}$ captures a vector of variables related to $\beta(t)$.

> Structural Interpretation. The component $X'_{i,t-14}\theta$ is the projection of $\beta_i(t)S_i(t)/N_i(t) - \gamma$ on $X_{i,t-14}$ (including testing variable).

Growth Rate in Deaths as Outcome. By differentiating (7) and (8) with respect to t and using (9), we obtain

$$\frac{\ddot{D}(t)}{\dot{D}(t)} = \frac{\ddot{C}(t)}{\dot{C}(t)} - \frac{\dot{\tau}(t)}{\tau(t)} = \frac{S(t)}{N}\beta(t) - \gamma. \tag{10}$$

Our measurement equation for the growth rate of deaths is based on equation (10) but account for a 21 day lag between infection and death as

$$\Delta \log(\Delta D_{it}) = X'_{i,t-21}\theta + \epsilon_{it}, \tag{M-D}$$

where

$$\Delta \log(\Delta D_{it}) := \log(\Delta D_{it}) - \log(\Delta D_{i,t-7}) \tag{11}$$

approximates the weekly growth rate in deaths from $t-7$ to t in state i. Sensitivity analysis also provides results for the case of 28 and 35 lag.

Debiased Fixed Effects Dynamic Panel Data Estimator. We apply Jackknife bias corrections; see Chen et al. (2020) and Hahn and Newey (2004) for more details. Here, we briefly describe the debiased fixed effects estimator we use.

Given our panel data with sample size (N, T), denote a set of counties by $\mathcal{N} = \{1, 2, ..., N\}$. We randomly and repeatedly partition $\mathcal{N}$ into two sets as $\mathcal{N}_1^j$ and $\mathcal{N}_2^j = \mathcal{N} \setminus \mathcal{N}_1^j$ for $j = 1, 2, ..., J$, where $\mathcal{N}_1^j$ and $\mathcal{N}_2^j$ (approximately) contain the same number of counties. For

each of $j = 1, ..., J$, consider two sub-panels (where i stands for county and t stands for the day) defined by

$$\mathbf{S}_1^j = \mathbf{S}_{11}^j \cup \mathbf{S}_{22}^j \quad \text{and} \quad \mathbf{S}_2^j = \mathbf{S}_{12}^j \cup \mathbf{S}_{21}^j$$

with $\mathbf{S}_{1k}^j = \{(i,t) : i \in \mathcal{N}_k, t \leq \lceil T/2 \rceil\}$ and $\mathbf{S}_{2k}^j = \{(i,t) : i \in \mathcal{N}_k, t \geq \lfloor T/2+1 \rfloor\}$ for $k = 1, 2$, where $\lceil . \rceil$ and $\lfloor . \rfloor$ are the ceiling and floor functions. Each of these two subpanels, $\mathbf{S}_1^j$ and $\mathbf{S}_2^j$, includes observations for all cross-sectional units and time periods.

We form the estimator with bias-correction as

$$\widehat{\beta}_{\text{BC}} := 2\widehat{\beta} - \widetilde{\beta} \quad \text{with} \quad \widetilde{\beta} := \frac{1}{J}\sum_{j=1}^{J} \widetilde{\beta}_{\mathbf{S}_1^j \cup \mathbf{S}_2^j},$$

where $\widehat{\beta}$ is the standard estimator with a set of N county dummies while $\widetilde{\beta}_{\mathbf{S}_1^j \cup \mathbf{S}_2^j}$ denotes the estimator using the data set $\mathbf{S}_1^j \cup \mathbf{S}_2^j$ but treats the counties in $\mathbf{S}_1^j$ differently from those in $\mathbf{S}_2^j$ to form the estimator— namely, we include approximately $2N$ county dummies to compute $\widetilde{\beta}_{\mathbf{S}_1^j \cup \mathbf{S}_2^j}$. Thus, $(\widehat{\beta} - \widetilde{\beta})$ is the approximation to the bias of $\widehat{\beta}$, subtracting which from $\widehat{\beta}$ gives the formula given above. We set $J = 2$ in our empirical analysis. When we choose $J = 5$ for some specifications, we obtained similar results.

An alternative jacknife bias-corrected estimator is $\widehat{\beta}_{\text{CBC}} = 2\widehat{\beta} - \frac{1}{J}\sum_{j=1}^{J}(\widetilde{\beta}_{\mathbf{S}_1^j} + \widetilde{\beta}_{\mathbf{S}_2^j})/2$, where $\widetilde{\beta}_{\mathbf{S}_k^j}$ denotes the fixed effect estimator using the subpanel $\mathbf{S}_k^j$ for $k = 1, 2$. In our empirical analysis, these two cross-over jackknife bias corrected estimators give similar result; in simulation experiments, the first form performed somewhat better, so we settled out choice on it.

We report asymptotic standard errors with state-level clustering, justified by the standard asymptotic theory of bias corrected estimators. The rationale for state-level clustering is that the stochastic shocks in the model can be correlated across counties, especially within the state. A simple way to model this is to allow for the arbitrary within-state correlation and adjust the standard errors to account for this (state-level clustering).

Covid Economics 70, 25 February 2021: 70-108

Covid Economics 70, 25 February 2021: 70-108

TABLE S1. The Association of School/College Openings and NPI Policies with Case Growth in the United States: Standard Fixed Effects Estimator without Bias Correction

	Dependent variable: ***Case Growth Rates***			
	(1)	(2)	(3)	(4)
College Visits, 14d lag	0.359***	0.412***	0.326***	0.371***
	(0.071)	(0.073)	(0.064)	(0.076)
K-12 Visits, 14d lag	0.393***	0.429***		
	(0.070)	(0.070)		
K-12 Visits × No-Mask		0.100		
		(0.070)		
K-12 In-person, 14d lag			0.062***	0.062***
			(0.017)	(0.021)
K-12 Hybrid, 14d lag			0.040***	0.033**
			(0.014)	(0.013)
K-12 Remote, 14d lag			0.030*	0.027*
			(0.016)	(0.015)
K-12 In-person × No-Mask				0.009
				(0.019)
K-12 Hybrid × No-Mask				0.032*
				(0.017)
Mandatory mask 14d lag	−0.006	−0.006	−0.015	−0.017
	(0.018)	(0.017)	(0.020)	(0.019)
Ban gatherings 14d lag	−0.066*	−0.068	−0.068**	−0.067
	(0.033)	(0.044)	(0.033)	(0.042)
Stay at home 14d lag	−0.203***	−0.198***	−0.200***	−0.200***
	(0.031)	(0.039)	(0.034)	(0.040)
log(Cases), 14d lag	−0.088***	−0.092***	−0.088***	−0.092***
	(0.009)	(0.010)	(0.010)	(0.010)
log(Cases), 21d lag	−0.042***	−0.043***	−0.043***	−0.043***
	(0.005)	(0.005)	(0.005)	(0.005)
log(Cases), 28d lag	−0.017***	−0.020***	−0.018***	−0.021***
	(0.003)	(0.003)	(0.004)	(0.004)
Test Growth Rates	0.009**	0.008*	0.009**	0.009*
	(0.004)	(0.004)	(0.004)	(0.004)
County Dummies	Yes	Yes	Yes	Yes
State× Week Dummies	Yes	Yes	Yes	Yes
Observations	690,297	545,131	612,963	528,941
R^2	0.092	0.093	0.092	0.094

Notes: Dependent variable is the log difference in weekly positive cases across 2 weeks. Regressors are 7-day moving averages of corresponding daily variables and lagged by 2 weeks to reflect the time between infection and case reporting except that we don't take any lag for the log difference in test growth rates. All regression specifications include county fixed effects and state-week fixed effects to control for any unobserved county-level factors and time-varying state-level factors such as various state-level policies as well as 2, 3, and 4 weeks lagged log of cases. The standard fixed effects estimator without bias-correction is applied. Asymptotic clustered standard errors at the state level are reported in the bracket. *p<0.1; **p<0.05; ***p<0.01

Covid Economics 70, 25 February 2021: 70-108

FIGURE S1. Average weekly cases and deaths are associated with different modes of opening K-12 schools, visits to K-12 schools, and visits to colleges/universities

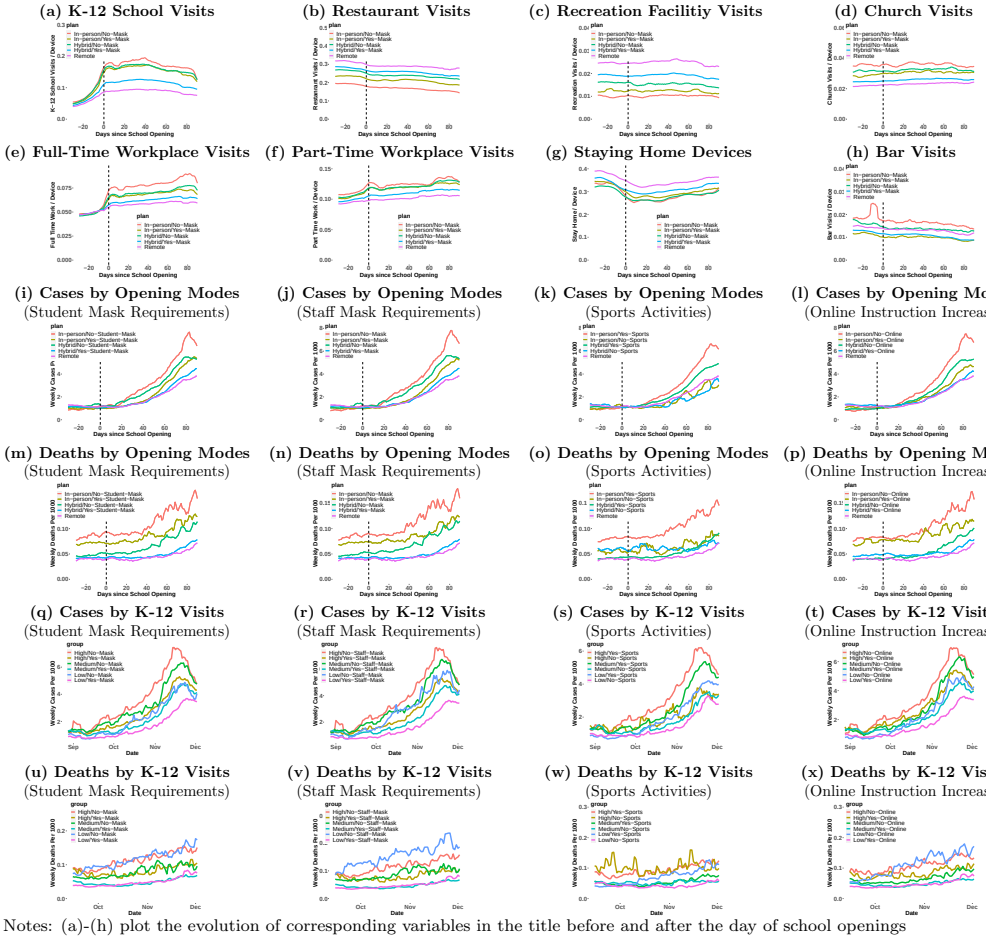

Notes: (a)-(h) plot the evolution of corresponding variables in the title before and after the day of school openings and corresponding to figures reported in Fig. 1(c)(d) in the main text. (i)-(p) corresponds to Fig.(a)(b) and plot the evolution of weekly cases or deaths per 1000 persons averaged across counties within each group of counties classified by K-12 school teaching methods and different mitigation strategies (mask requirements for students, mask requirements for staffs, allowing for sports activities, and increase in online instructions) against the days since K-12 school opening. In (i) and (m), counties that implement in-person teaching are classified into "In-person/Yes-Mask" and "In-person/No-Mask" based on whether at least one school district requires students to wear masks or not. In (k) and (o), counties that implement in-person teaching are classified into "In-person/Yes-Sports" and "In-person/No-Sports" based on whether at least one school district requires students to allow sports activities or not. In (l) and (p), counties that implement in-person teaching are classified into "In-person/No-Online" and "In-person/Yes-Online" based on whether at least one school district answer that no increase in online instruction. (q)-(x) are similar to (i)-(p) but classify counties by the volume of per-device K-12 school visits and take the calendar dates instead of the days since opening schools as x-axis, where "Low," "Middle," and "High" are county-day observations of which 14 days lagged per-device K-12 school visits less than the first quartile, between the first and the third quartiles, and larger than the third quartile, respectively. In (q) and (u), "Low/No-Mask," "Middle/No-Mask," and "High/No-Mask" are a subset of low, middle, and high visits groups of counties for which at least one school district does not require students to wear masks.

Covid Economics 70, 25 February 2021: 70-108

FIGURE S2. The number of cases by age groups and the number of visits to colleges/universities, bars, restaurants, recreation facilities, K-12 schools, and a comparison of reported cases between CDC and NYT data

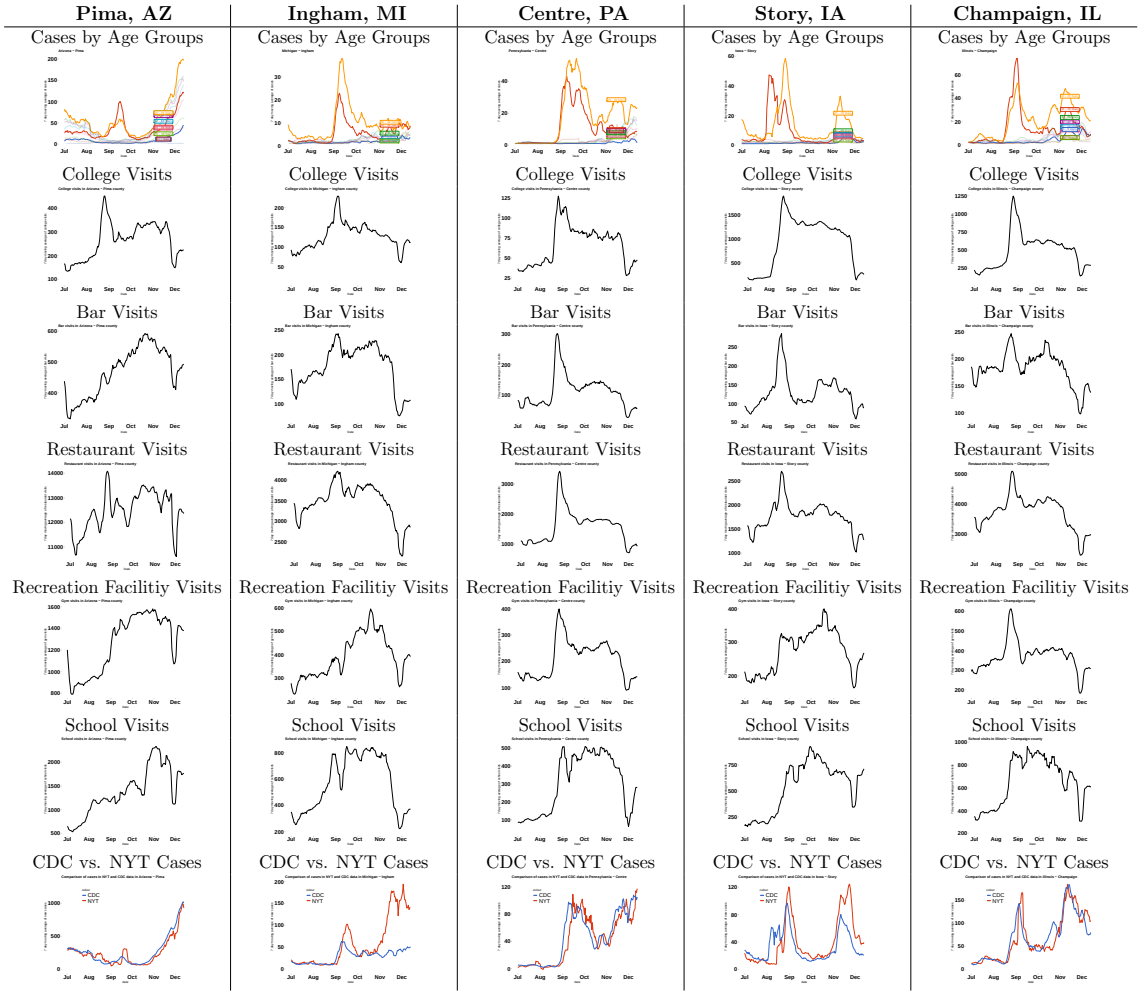

Notes: Figure corresponds to Fig. 2 in the main text but for Pima, AZ, Ingham, MI, Centre, PA, Story, IA, and Champaign, IL. Across various counties, we also report the evolution of visits to recreation facilities and K-12 school visits. The last panel at the bottom compares the sum of weekly cases across all age groups reported in CDC dataset with the weekly reported case in NYT dataset.

Covid Economics 70, 25 February 2021: 70-108

FIGURE S3. Sensitivity analysis for the estimated coefficients of K-12 visits and college visits of case growth regressions: Estimator without Bias Correction

(a) Case Growth Estimates

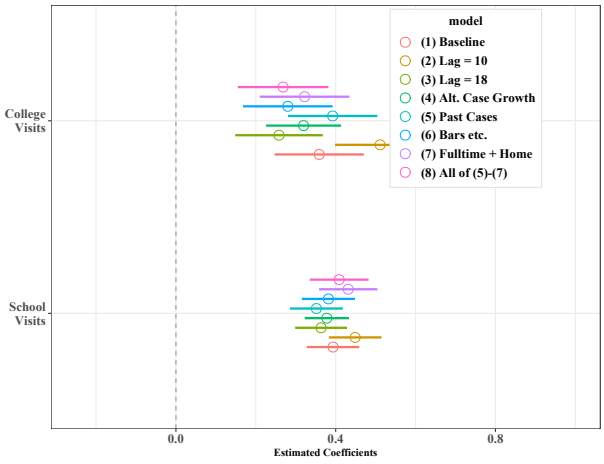

(b) Case Growth Estimates with School Visits × No Mask

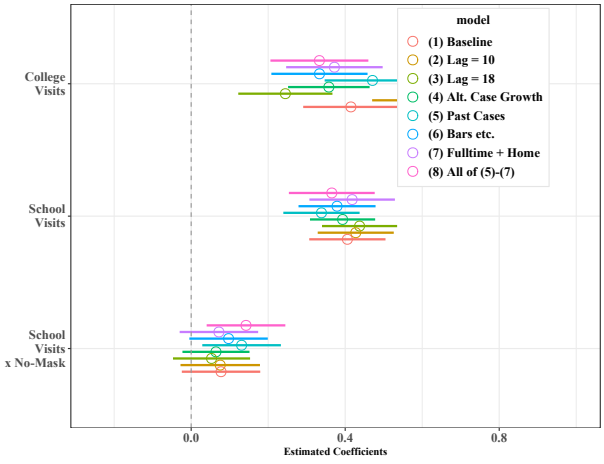

Notes: These figures corresponds to Fig. 3 of the main text but report the result of the (standard) fixed effects estimator without bias correction.

Covid Economics 70, 25 February 2021: 70-108

FIGURE S4. Evolution of Cases/Deaths per 1000 Persons, Case/Death Growth, Visits to K-12 Schools, Colleges, Restaurants, Bars, Gyms, Churches, K-12 School Opening Modes, and NPIs across U.S. counties

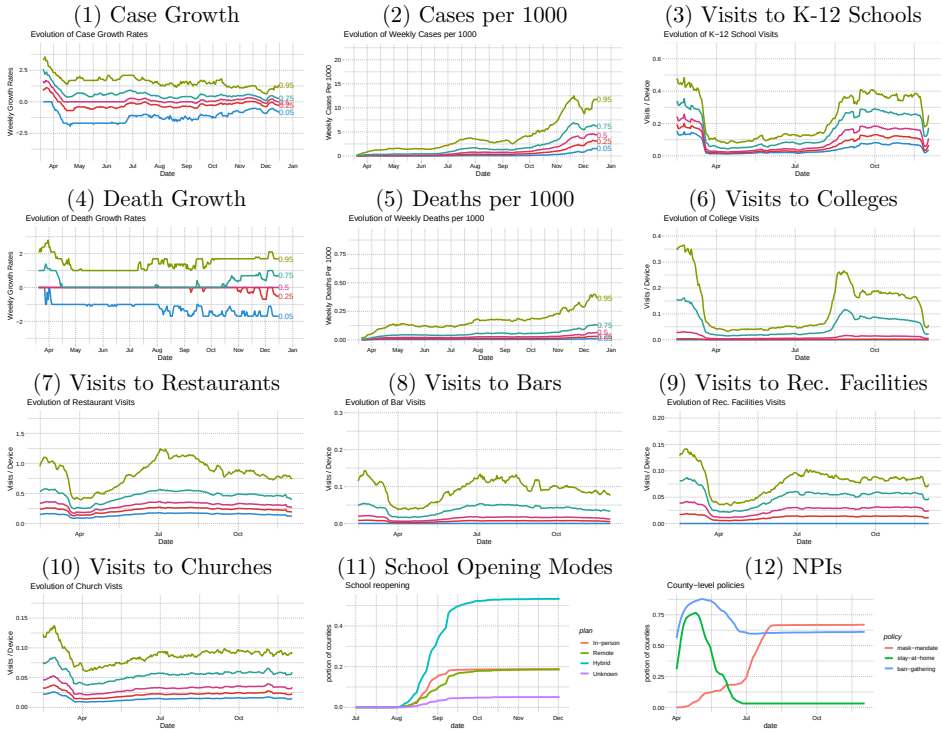

Notes: (1)-(10) report the evolution of various percentiles of corresponding variables in the title over time. (10) reports the proportion of counties that open K-12 schools with different teaching methods including "Unknown" over time while (11) reports the proportion of counties that implement three NPIs over time.

Covid Economics 70, 25 February 2021: 70-108

TABLE S2. The Association of School/College Openings with Mobility in the United States: All Estimates

(a) Full-time Workplace Visits and Staying Home Devices

	Dependent variable			
	Full Time	Full Time	Stay Home	Stay Home
	(1)	(2)	(3)	(4)
College Visits	−0.080***	−0.098***	−0.207***	−0.207***
	(0.004)	(0.006)	(0.024)	(0.026)
K-12 School Visits	0.078***		−0.061**	
	(0.006)		(0.026)	
Open K-12 In-person		0.999***		−2.271***
		(0.125)		(0.382)
Open K-12 Hybrid		0.509***		0.094
		(0.051)		(0.186)
Open K-12 Remote		0.211***		0.159
		(0.048)		(0.307)
Mandatory mask	−0.152***	−0.306***	0.204	0.222
	(0.042)	(0.053)	(0.260)	(0.250)
Ban gatherings	0.067	0.097*	0.870	0.754
	(0.047)	(0.051)	(0.561)	(0.521)
Stay at home	−0.039	−0.028	2.881***	2.895***
	(0.031)	(0.033)	(0.330)	(0.340)
log(Cases), 14d lag	0.004	0.007	0.273***	0.273***
	(0.004)	(0.005)	(0.028)	(0.028)
log(Cases), 21d lag	0.002	−0.001	0.283***	0.281***
	(0.002)	(0.003)	(0.019)	(0.017)
log(Cases), 28d lag	0.006***	0.005*	0.221***	0.215***
	(0.002)	(0.002)	(0.023)	(0.024)
County Dummies	Yes	Yes	Yes	Yes
State× Week Dummies	Yes	Yes	Yes	Yes
Observations	670,909	595,886	670,909	595,886
R^2	0.870	0.853	0.889	0.888

(b) Visits to Restaurants and Bars

	Dependent variable			
	Restaurants	Restaurants	Bars	Bars
	(1)	(2)	(3)	(4)
College Visits	0.064	0.034	0.016***	0.012**
	(0.053)	(0.051)	(0.006)	(0.005)
K-12 School Visits	0.006		0.008	
	(0.046)		(0.006)	
Open K-12 In-person		−1.367***		−0.177***
		(0.404)		(0.041)
Open K-12 Hybrid		−1.162***		−0.097***
		(0.272)		(0.038)
Open K-12 Remote		−0.512*		0.031
		(0.295)		(0.056)
Mandatory mask	0.542	0.037	0.191***	0.113
	(0.371)	(0.403)	(0.067)	(0.069)
Ban gatherings	0.067	0.135	−0.066	−0.070
	(0.920)	(0.897)	(0.117)	(0.118)
Stay at home	−2.232***	−2.170***	−0.228***	−0.204***
	(0.203)	(0.241)	(0.025)	(0.025)
log(Cases), 14d lag	−0.096**	−0.072	−0.010*	−0.004
	(0.047)	(0.050)	(0.006)	(0.007)
log(Cases), 21d lag	−0.084***	−0.087***	−0.011**	−0.009*
	(0.032)	(0.032)	(0.005)	(0.005)
log(Cases), 28d lag	−0.150***	−0.161***	−0.014**	−0.015***
	(0.043)	(0.042)	(0.005)	(0.005)
County Dummies	Yes	Yes	Yes	Yes
State× Week Dummies	Yes	Yes	Yes	Yes
Observations	670,909	595,886	670,909	595,886
R^2	0.881	0.883	0.807	0.807

Notes: These tables report the omitted estimates of Table 2 in the main text. All regression specifications include county fixed effects and state-week fixed effects. The debiased estimator is used. Clustered standard errors at the state level are reported in the bracket. *p<0.1; **p<0.05; ***p<0.01

Covid Economics 70, 25 February 2021: 70-108

TABLE S3. The Association of School/College Openings, NPI Policies, Full-time/Part-time Work, and Staying Home Devices with Case Growth in the United States: Debiased Fixed Effects Estimator

	Dependent variable: ***Case Growth Rates***			
	(1)	(2)	(3)	(4)
College Visits, 14d lag	0.060	0.012	0.114*	0.010
	(0.071)	(0.072)	(0.065)	(0.075)
K-12 Visits, 14d lag	0.393***	0.283***		
	(0.075)	(0.087)		
K-12 Visits × No-Mask		0.287***		
		(0.071)		
K-12 In-person, 14d lag			0.015	−0.007
			(0.016)	(0.020)
K-12 Hybrid, 14d lag			−0.028**	−0.055***
			(0.013)	(0.013)
K-12 Remote, 14d lag			−0.094***	−0.115***
			(0.015)	(0.014)
K-12 In-person × No-Mask				0.034*
				(0.020)
K-12 Hybrid × No-Mask				0.043***
				(0.017)
Full-time Work Device, 14d lag	−0.117	0.186	0.956**	0.967**
	(0.417)	(0.490)	(0.384)	(0.436)
Part-time Work Device, 14d lag	0.262	0.466	0.820***	0.915***
	(0.259)	(0.305)	(0.276)	(0.309)
Staying Home Device, 14d lag	−0.290***	−0.283***	−0.352***	−0.332***
	(0.057)	(0.069)	(0.061)	(0.067)
Mandatory mask 14d lag	−0.114***	−0.124***	−0.128***	−0.128***
	(0.018)	(0.017)	(0.019)	(0.019)
Ban gatherings 14d lag	−0.120***	−0.127***	−0.125***	−0.126***
	(0.034)	(0.044)	(0.034)	(0.043)
Stay at home 14d lag	−0.246***	−0.241***	−0.232***	−0.239***
	(0.033)	(0.040)	(0.034)	(0.040)
log(Cases), 14d lag	−0.100***	−0.101***	−0.096***	−0.098***
	(0.009)	(0.010)	(0.010)	(0.010)
log(Cases), 21d lag	−0.060***	−0.059***	−0.059***	−0.058***
	(0.004)	(0.005)	(0.005)	(0.005)
log(Cases), 28d lag	−0.030***	−0.033***	−0.030***	−0.033***
	(0.003)	(0.003)	(0.004)	(0.003)
Test Growth Rates	0.009**	0.008*	0.009**	0.009**
	(0.004)	(0.004)	(0.004)	(0.004)
County Dummies	Yes	Yes	Yes	Yes
State× Week Dummies	Yes	Yes	Yes	Yes
Observations	690,297	545,131	612,963	528,941
R^2	0.092	0.093	0.092	0.094

Notes: Dependent variable is the log difference in weekly positive cases across 2 weeks. All regression specifications include county fixed effects and state-week fixed effects to control for any unobserved county-level factors and time-varying state-level factors such as various state-level policies. The debiased fixed effects estimator is applied. Asymptotic clustered standard errors at the state level are reported in the bracket. *p<0.1; **p<0.05; ***p<0.01

TABLE S4. The Association of School/College Openings and NPI Policies with Death Growth in the United States: Debiased Fixed Effects Estimator

	Dependent variable: ***Death Growth Rates***			
	(1)	(2)	(3)	(4)
College Visits, 21d lag	0.142***	0.181***	0.189***	0.170***
	(0.047)	(0.057)	(0.058)	(0.055)
K-12 Visits, 21d lag	0.160***	0.060		
	(0.048)	(0.066)		
K-12 Visits × No-Mask		0.174**		
		(0.073)		
K-12 In-person, 21d lag			−0.002	−0.012
			(0.019)	(0.019)
K-12 Hybrid, 21d lag			0.013	0.014
			(0.014)	(0.014)
K-12 Remote, 21d lag			0.018	0.015
			(0.015)	(0.017)
K-12 In-person × No-Mask				0.050***
				(0.016)
K-12 Hybrid × No-Mask				0.017
				(0.015)
Mandatory mask, 21d lag	−0.019**	−0.018**	−0.028***	−0.023**
	(0.009)	(0.009)	(0.009)	(0.009)
Ban gatherings, 21d lag	−0.044	−0.056**	−0.053**	−0.055**
	(0.027)	(0.025)	(0.027)	(0.025)
Stay at home, 21d lag	−0.087***	−0.076**	−0.078***	−0.067**
	(0.032)	(0.030)	(0.030)	(0.029)
log(Deaths), 21d lag	−0.053***	−0.049***	−0.052***	−0.047***
	(0.004)	(0.005)	(0.004)	(0.006)
log(Deaths), 28d lag	−0.036***	−0.041***	−0.037***	−0.042***
	(0.004)	(0.005)	(0.005)	(0.005)
log(Deaths), 35d lag	−0.031***	−0.032***	−0.032***	−0.033***
	(0.004)	(0.005)	(0.004)	(0.005)
County Dummies	Yes	Yes	Yes	Yes
State× Week Dummies	Yes	Yes	Yes	Yes
Observations	628,061	490,568	557,219	476,794
R^2	0.049	0.050	0.050	0.051

Notes: Dependent variable is the log difference in weekly reported deaths across 2 weeks. Regressors are 7-day moving averages of corresponding daily variables and lagged by 3 weeks to reflect the time between infection and case reporting. All regression specifications include county fixed effects and state-week fixed effects to control for any unobserved county-level factors and time-varying state-level factors such as various state-level policies. The debiased fixed effects estimator is applied. Asymptotic clustered standard errors at the state level are reported in the bracket. Estimates are based on the sample of counties after dropping the smallest 10 percent in population sizes because the number of reported deaths is zero for many observations in small counties. *p<0.1; **p<0.05; ***p<0.01

Covid Economics 70, 25 February 2021: 70-108

TABLE S5. Summary Statistics

Statistic	N	Mean	St. Dev.	Min	Pctl(25)	Pctl(75)	Max
Case Growth Rate	698,278	0.099	0.901	−8.107	−0.288	0.495	8.002
Death Growth Rate	698,278	0.023	0.790	−6.170	0.000	0.000	6.170
log(Cases)	703,702	2.829	2.140	−1.000	1.386	4.331	10.488
log(Deaths)	703,702	−0.269	1.147	−1.000	−1.000	0.000	6.479
College Visits	728,228	0.010	0.031	0.000	0.000	0.008	1.827
K-12 School Visits	728,228	0.074	0.072	0.000	0.024	0.103	1.167
K-12 opening, in-person	646,816	0.079	0.207	0.000	0.000	0.000	1.000
K-12 opening, Hybrid	646,816	0.224	0.357	0.000	0.000	0.424	1.000
K-12 opening, Remote	646,816	0.078	0.227	0.000	0.000	0.000	1.000
No-Mask for Staffs	577,680	0.293	0.455	0.000	0.000	1.000	1.000
Mandatory Mask	728,944	0.461	0.495	0	0	1	1
Ban Gathering	728,944	0.658	0.472	0	0	1	1
Stay at Home	728,944	0.143	0.345	0	0	0	1
Full Time Workplace Visits	728,206	0.054	0.018	0.010	0.042	0.061	0.484
Part Time Workplace Visits	728,206	0.101	0.025	0.023	0.084	0.113	0.567
Staying Home Devices	728,206	0.342	0.116	0.021	0.267	0.393	3.657
Recreational Place Visits	728,228	0.017	0.022	0.000	0.000	0.026	0.786
Church Visits	728,228	0.025	0.018	0.000	0.014	0.032	0.583
Drinking Place Visits	728,228	0.012	0.024	0.000	0.0001	0.015	1.461
Restaurant Visits	728,228	0.250	0.175	0.000	0.150	0.315	4.261
Test Growth Rates	698,278	0.067	1.099	−13.616	−0.051	0.178	13.111
Population in 2018 (millions)	706,966	0.104	0.331	0.0002	0.012	0.071	10.106

Notes: Based on observations from April 15, 2020 to December 2, 2020 for the maximum of 3142 counties.

Covid Economics 70, 25 February 2021: 70-108

CEPR PRESS

TABLE S6. Correlation across variables

	College Visits	K-12 School Visits	Open K-12 In-person	Open K-12 Hybrid	Open K-12 Remote	No-Mask for Staffs	Mandatory mask	Ban gatherings	Stay at home	Full-time Workplace Visits	Part-time Workplace Visits	Staying Home Devices	Bar Visits	Restaurant Visits	Rec. Facilities Visits	Church Vists
College Visits	1.00															
K-12 School Visits	0.09	1.00														
Open K-12 In-person	0.05	0.43	1.00													
Open K-12 Hybrid	0.11	0.44	0.04	1.00												
Open K-12 Remote	0.05	0.09	-0.06	-0.06	1.00											
No-Mask for Staffs	0.01	0.16	0.15	-0.02	-0.10	1.00										
Mandatory mask	0.09	0.10	0.03	0.24	0.23	-0.31	1.00									
Ban gatherings	-0.03	-0.14	-0.09	-0.06	0.00	-0.03	-0.09	1.00								
Stay at home	-0.06	-0.24	-0.14	-0.21	-0.13	-0.08	-0.19	0.20	1.00							
Full-time Workplace Visits	0.04	0.56	0.37	0.36	0.10	0.12	0.05	-0.17	-0.21	1.00						
Part-time Workplace Visits	0.06	0.60	0.32	0.34	0.04	0.20	-0.01	-0.12	-0.31	0.71	1.00					
Staying Home Devices	-0.04	-0.27	-0.18	-0.23	-0.02	-0.10	0.01	-0.00	0.27	0.06	-0.19	1.00				
Bar Visits	0.05	0.08	0.02	-0.02	0.01	0.08	0.01	-0.06	-0.08	0.12	0.11	0.15	1.00			
Restaurant Visits	0.17	0.02	-0.10	0.00	0.06	-0.10	0.14	0.10	-0.08	-0.07	0.07	0.04	0.34	1.00		
Rec. Facilities Visits	0.15	-0.00	-0.07	0.03	0.11	-0.08	0.18	0.03	-0.08	-0.05	-0.03	0.09	0.26	0.52	1.00	
Church Vists	0.06	0.32	0.13	0.08	-0.03	0.17	-0.06	-0.07	-0.16	0.15	0.37	-0.18	0.11	0.18	0.03	1.00

Notes: Based on observations from April 15, 2020 to December 2, 2020 for the maximum of 3142 counties.

Covid Economics 70, 25 February 2021: 70-108

The macroeconomics of Covid-19 exit strategy: The case of Japan[1]

So Kubota[2]

Date submitted: 21 February 2021; Date accepted: 23 February 2021

In this paper, I study a simple SIR-Macro model to examine Japan's second soft lockdown, starting on January 2021. The model's parameters are calibrated to capture both infection and economic fluctuations in 2020. I find that the government should extend this lockdown long enough to avoid another future lockdown, given the country's medical capacity. In addition, I consider the ICU targeting policy that keeps the number of severe patients at a constant level, mimicking the monetary policy's inflation targeting. These macro-level containment policies can help develop age-dependent strategies using the timing differences of vaccinations between the young and the old.

Covid Economics 70, 25 February 2021: 109-133

1 This paper was originally written as a policy report submitted to the Japanese government's new coronavirus advisory subcommittee. I appreciate the cooperation of the Japan-SIR-Econ project members: Asako Chiba, Daisuke Fujii, Keiichiro Kobayashi, Taisuke Nakata, and Fumio Ohtake. I also thank Hiroshi Fujiki, Masashige Hamano, Yasushi Iwamoto, Munechika Katayama, Haruko Noguchi, and Satoshi Tanaka for their helpful comments. In addition, Fei Gao did excellent research assistance. All errors are my own.

2 Associate Professor, School of Political Science and Economics, Waseda University.

Covid Economics 70, 25 February 2021: 109-133

1 Introduction

Reacting to the first wave of the COVID-19 pandemic, numerous countries imposed containment policies, such as curfews, school closures, and quarantines in the spring of 2020. The infection rate stayed at low levels in the summer, but most countries experienced their second or third waves in the autumn or winter. As of January 2021, many countries have returned to lockdowns to a greater or lesser extent, mainly due to their medical capacities. The spread of infection in some countries has been suppressed enough to lift such containment measures. However, these countries are also concerned about the necessity of deploying a recurrent lockdown in a future pandemic wave. Although the COVID-19 crisis may be in its final stage given the arrival of vaccines, containment policies remain adrift.

This paper aims to provide policy implications of Japan's 2021 lockdown policy regarding the economy and infection. The COVID-19 pandemic in Japan has been milder than in European and American countries; however, its economic impacts have been comparable to those of these countries. In April and May 2020, the Japanese government declared a state of emergency to stop the growing first wave of infections. This policy is called a *soft lockdown* or *voluntary lockdown* (Watanabe and Yabu, 2020) since the restrictions were much weaker than those of the severe lockdowns in most countries[1]. However, this soft lockdown significantly slowed the exponential increase of infections. Since the fall of 2020, Japan has been under the third wave of the pandemic. In January 2021, the Japanese government declared a second state of emergency to limit social activities and reduce the spread of the new coronavirus.

In this paper, to study Japan's 2021 lockdown, I construct a simple SIR-Macro model following Eichenbaum et al. (2020a). This model includes agents' optimizations of economic behaviors, which are in line with empirical findings of voluntary behavioral changes in people (Goolsbee and Syverson (2020); Watanabe and Yabu (2020); Sheridan et al. (2020)) and market equilibrium. I incorporate two factors into the SIR-Macro model. The first one is a decreasing trend of people's subjective perceptions about COVID-19 infection, which is crucial to capturing Japan's initial economic downturn in the spring of 2020 and sustaining recovery in the fall. The second is two divided sectors, where one is associated with infection such as service, and the other one is independent of virus transmission, such as online shopping. This model does a reasonable job of capturing both infection trends and economic dynamics during the first soft lockdown in April and May 2020 and

[1]The Japanese government enacted new legislation to levy fines against those breaking lockdown rules in February 2021.

the long-run trends throughout 2020.

On top of that, my model conducts policy exercises about the second soft lockdown, starting from January 2021. It measures the policy efficiency as the dominance relationship on the pandemic possibility frontiers, which describe the tradeoffs between economic welfare costs and mortality rate, following Kaplan et al. (2020). It is a conservative policy evaluation method independent of normative judgment about the values of life.

The first policy I consider involves extensions of the second soft lockdown, which began in January 2021. If the government lifts this lockdown too early, the number of severely ill patients treated in the ICU will spike. Thus, the government needs to impose one more lockdown, given the medical capacity constraint. These recurrent lockdowns have been observed in many countries since 2020. In this study, the first quantitative policy implication is that the government should extend the soft lockdown to sufficiently reduce the infections so that Japan can avoid another lockdown until vaccine distribution occurs. In SIR models, after lifting lockdowns, infections again begin to increase. Accelerating and breaking the infection repeatedly by the recurrent lockdowns has almost no impact on the overall process of the pandemic (Moll, 2020). Therefore, lockdown should be a one-time event, keeping society safe until a vaccine is available for all.

I also considered one other policy, called ICU targeting, that keeps the number of severe patients treated in the ICU at a constant level. It is similar to inflation targeting in monetary policy, in which the policy instrument is the nominal interest rate, and the goal is to control the inflation rate. Under this ICU targeting policy, the policy tool becomes the method of containment, and the goal is to keep the number of ICU patients. It is a variant of Miclo et al. (2020)'s filling-the-box strategy, designed to maintain ICU constraints until herd immunity is achieved. This ICU targeting policy can lead to less economic damage than the extensions of the soft lockdowns can attain under the capacity constraint. This is accomplished by keeping the ICU target close to the limit. However, I also show that the ICU targeting policy is less efficient than a one-time lockdown of sufficient length. It is because ICU targeting tends to sustain behavioral restrictions for too long.

Although these two rules are conducted at the macro level, they also impose different levels of restrictions on the young and the old. The degree of behavioral restriction is relatively stringent at first. Next, the initial phase of delivering vaccinations to the elderly reduces the fear of hitting ICU capacity constraints. After enough older people are immunized, the containment policy can be completely lifted. After that, the economy rapidly recovers to the pre-pandemic level, and the new coronavirus drastically spreads among the young. However, the number of deaths is limited,

Covid Economics 70, 25 February 2021: 109-133

given this population's low mortality rate. Eventually, the pandemic ceases after the young also get vaccinated. Several pieces of research demonstrate the efficiency of individual-level, age-dependent policies (for example, Acemoglu et al. (2020), Favero et al. (2020)). In my simulation, both the extension of soft lockdowns and ICU targeting can impose different degrees of social distancing by age given vaccination time differences. Therefore, the economic costs of these policies are limited in the COVID-19 exit period.

This research contributes to the rapidly growing literature of incorporating epidemiological SIR models into economics analysis. The closest paper to my research is Fujii and Nakata (2021)[2]. They also study Japan's soft lockdown using a reduced-form epidemiological model and consider future recurrent lockdowns. My model complements their analyses by a SIR model with economic agents' rational behaviors and equilibrium[3] with the age-dependence of the COVID-19 exit strategies according to the timing of vaccinations. In addition, the ICU capacity constraint and its implications on lockdowns are studied by Miclo et al. (2020) and Moll (2020). My model's basic structure follows the work of Eichenbaum et al. (2020a). The formulation of the substitution between the two sectors is borrowed from Krueger et al. (2020). The subjective perception of the infection is also introduced in the work of Aum et al. (2020), von Carnap et al. (2020), and Hamano et al. (2020). In addition, there are many SIR-macro models focusing on time-varying optimal containment policies, age-dependent lockdowns, and testing and case-dependent quarantines[4]. Furthermore, this paper is related to pure epidemiological models with economic costs studying lockdown policies, such as the model developed by Alvarez et al. (2020).

This model is introduced in Section 2. Section 3 provides calibration, computation methods, and the model's quantitative fits in 2020 data. The policies are discussed in Section 4, and the conclusion appears in Section 5.

2 Model

I extend the SIR-macro model presented in Eichenbaum et al. (2020a) to include two sectors, following the work of Krueger et al. (2020), and subjective perception about the infection, following

[2]The authors provide real-time updates of the COVID-19 infection and output loss. https://covid19outputjapan.github.io

[3]To bolster the Japanese policy discussion, I summarize both qualitative and quantitative differences between my model and that of Fujii and Nakata (2021) in Appendix.

[4]Bethune and Korinek (2020), Farboodi et al. (2020), Makris and Toxvaerd (2020), and Toxvaerd (2020) study abstract models, Brotherhood et al. (2020), Eichenbaum et al. (2020b,c), Giagheddu and Papetti (2020), Glover et al. (2020), Hsu et al. (2020), and Kaplan et al. (2020) construct general equilibrium models. In addition, Kapicka and Rupert (2020) and Kang and Wang (2021) consider search markets.

Covid Economics 70, 25 February 2021: 109-133

studies by Aum et al. (2020), von Carnap et al. (2020), and Hamano et al. (2020).

2.1 Economic Environment

I consider a weekly model of discrete periods, $t = 0, 1, 2, \ldots$. There is a unit mass of agents, and each maximizes the following discounted sum of utilities:

$$\sum_{t=0}^{\infty} \beta^t \left[\ln c_t - \theta \frac{n_t^2}{2} \right], \tag{1}$$

where c_t is aggregated consumption and n_t is hours of work. There are two types of goods: Good 1, which affects the infection such as service good, and Good 2, including activities such as online shopping. The aggregated consumption c_t is a bundle of two goods defined by the CES function with the elasticity of substitution η:

$$c_t = \left[\frac{1}{2}(c_{1,t})^{1-1/\eta} + \frac{1}{2}(c_{2,t})^{1-1/\eta} \right]^{\frac{\eta}{\eta-1}}. \tag{2}$$

For simplicity, I assume the share of each good to be 1/2. As Krueger et al. (2020) emphasize, this two-sector assumption helps to capture the low infection rate in Japan, resulting from the substitution of Good 1 for Good 2. Moreover, this helps to explain the large drop observed in consumption under the first soft lockdown in April and May 2020.

The production of each good is linear in labor with the same productivity, A. Furthermore, the labor inputs are perfect substitutes between the two sectors; thus, the the wage becomes constant. I normalize the wage as 1. The good markets are also perfectly competitive, and the prices of both goods are equal to the marginal productivity A.

2.2 Infection

The infection follows the basic SIR epidemiology model. People are divided into four groups within each period t. The first one is susceptible at a mass of S_t, who are not yet infected but could potentially get sick in the future. The next one is infected at a mass of I_t, who are currently sick. After I_t, people enter the recovered group at a mass of R_t, or dead, a population of D_t.

Covid Economics 70, 25 February 2021: 109-133

Given the mass of new infections, T_t, each population evolves as

$$S_{t+1} = S_t - T_t - \delta_t S_t, \tag{3}$$

$$I_{t+1} = I_t + T_t - (\pi_r + \pi_d)\, I_t, \tag{4}$$

$$R_{t+1} = R_t + \pi_r I_t + \delta_t S(t), \tag{5}$$

$$D_{t+1} = D_t + \pi_d I_t, \tag{6}$$

where π_r and π_d are the recovery rate and death rate, respectively, and the fraction of vaccinated people among those susceptible is δ_t. I assume the time-dependent rate to consider a realistic vaccination schedule in 2021.

I use superscripts j for each type: $j = s$ is for susceptible, $j = i$ for infected, and $j = r$ for the recovered. The allocation of each type j is a bundle of consumption and labor of Good 1 and Good 2, $\big((c^j_{1,t}, c^j_{2,t}), (n^j_{1,t}, n^j_{2,t})\big)$. In this model, I assume that the mass of new infections depend only on the aggregate consumption of susceptible and infected population. Specifically,

$$T_t = \pi_c\big(S_t c^s_{1,t}\big)\big(I_t c^i_{1,t}\big), \tag{7}$$

where π_c is the degree of infection through the economic interaction. This assumption is made for both simplicity and catching Japanese data. Eliminating infection through labor simplifies the equations of the dynamic system, whereas this assumption does not significantly alter the quantitative results. Regarding data fit, the elimination of autonomous infection outside economic activities is used for magnifying the reduction of infection during Japan's state of emergency in April and May 2020. One interpretation is that all social activities inevitably involve some level of spending.

The infection probability of each susceptible person consuming $c^s_{1,t}$ amount of Good 1 is represented by the function τ_t that

$$\tau_t(c^s_{1,t}) = \pi_c\big(I_t c^i_{1,t}\big) c^s_{1,t}, \tag{8}$$

given the macro-level variables I_t and $c^i_{1,t}$. The effective reproduction number in this model is defined as follows:

$$\mathcal{R}^0_t = \frac{T_t}{(\pi_r + \pi_d)(S_t + I_t + R_t) I_t}. \tag{9}$$

Covid Economics 70, 25 February 2021: 109-133

Covid Economics 70, 25 February 2021: 109-133

2.3 Decision Problems

Susceptible To match Japan's data, I introduce the susceptibles' subjective perception about the total infected population, I_t. This subjective perception is represented as an exogenous variable ψ_t, which shows how much higher people believe the number of new infections is compared with the actual or reported number. That is, a susceptible person's perception rate $\tau_t(c^s_{1,t})$ is replaced by $\psi_t\tau_t(c^s_{1,t})$ in her or his optimization problem. In the simulation, ψ_t is initially assumed to be large because of people's anxiety about the new coronavirus. As time goes by, however, people acquire better information, and then ψ_t gradually decreases. This process follows a logistic function:

$$\psi_{t+1} = \psi_t - \hat{\psi}\frac{(1-\psi_t)\psi_t^2}{\bar{\psi}}, \tag{10}$$

where $\bar{\psi}$ is the initial value equivalent to ψ_0, and $\hat{\psi}$ controls the speed of reduction. This perception factor ψ_t is necessary to capture Japan's large economic downturn under the backdrop of the small number of infections in March and April 2020. Moreover, the decreasing ψ_t also traces out the recovery of consumption in the fall of 2020. A similar variable, called the fear factor, is also introduced by Aum et al. (2020) to capture the economic drop before in the United Kingdom and South Korea in the spring of 2020. von Carnap et al. (2020) assumes $\psi(t)$ to be a time-invariant parameter to explain the voluntary reduction of Uganda's economic activities, and Hamano et al. (2020) discuss its implications for welfare-maximizing policies.

The following Bellman equation describes the optimization problem of each susceptible person:

$$\begin{aligned} U^s_t = \frac{\eta}{\eta-1}\ln\left[\frac{1}{2}(c^s_{1,t})^{1-1/\eta} + \frac{1}{2}(c^s_{2,t})^{1-1/\eta}\right] - \theta\frac{(n^s_t)^2}{2} \\ + \beta\left\{\psi_t\tau_t(c^s_{1,t})U^i_{t+1} + \delta_t U^r_t + \left[1-\psi_t\tau_t(c^s_{1,t})-\delta_t\right]U^s_{t+1}\right\}, \end{aligned} \tag{11}$$

where U^s_t is the discounted sum of utilities of a susceptible person, and U^i_t is that of an infected person. A susceptible person believes that he or she gets infected with probability $\psi_t\tau_t(c^s_{1,t})$ instead of $\tau_t(c^s_{1,t})$. If vaccines are distributed, she directly acquires immunization and joins R_t with probability δ_t. Each susceptible person maximizes her lifetime utility in Equation (11) under the budget constraint:

$$(1+\mu_t)\,c^s_{1,t} + c^s_{2,t} = An^s_t. \tag{12}$$

Covid Economics 70, 25 February 2021: 109-133

The consumption tax rate of Good 1, μ_t, represents Japan's soft lockdown in this model. The lockdown burdens the costs of infection-related economic activities[5]. In this paper, I focus on economiy-wide policies, where μ_t is independent of type $j = s, i, r$. The interpretation assuming this one sector shock to be lockdown may be debatable. In Western countries, strict lockdowns shut down almost all sectors, but the Japanese policy is a voluntary lockdown. The government asks for a reduction of operations in restaurants and bars, but many people still go outside to purchase necessities.

The optimality conditions for a susceptible person's decision are obtained as follows:

$$\frac{(c^s_{1,t})^{-1/\eta}}{(c^s_{1,t})^{1-1/\eta} + (c^s_{2,t})^{1-1/\eta}} = (1+\mu_t)\left(\frac{\theta}{A}\right) n^s_t + \beta\pi_c\psi_t\left[(U^s_{t+1} - U^i_{t+1})I_t c^i_{1,t}\right], \tag{13}$$

$$\frac{(c^s_{2,t})^{-1/\eta}}{(c^s_{1,t})^{1-1/\eta} + (c^s_{2,t})^{1-1/\eta}} = \left(\frac{\theta}{A}\right) n^s_t. \tag{14}$$

Infected The problem of an infected person is much simpler because this person will not become reinfected. Each infected person solves the following equation:

$$U^i_t = \frac{\eta}{\eta-1}\ln\left[\frac{1}{2}(c^i_{1,t})^{1-1/\eta} + \frac{1}{2}(c^i_{2,t})^{1-1/\eta}\right] - \theta\frac{(n^i_t)^2}{2} + \beta\left[\pi_r U^r_{t+1} + \pi_d \times 0 + (1-\pi_r-\pi_d)\,U^i_{t+1}\right] \tag{15}$$

$$\text{s.t.} \quad (1+\mu_t)\,c^i_{1,t} + c^i_{2,t} = An^i_t. \tag{16}$$

An infected person will be recovered at probability π_r and obtain the discounted sum of utility U^r_{t+1}. The value of death is normalized as 0, following Eichenbaum et al. (2020a). With probability $1-\pi_r-\pi_d$, such as a person remains as infected. For simplicity, I do not assume a labor productivity decline due to infection, which makes the dynamic system drastically simple, as shown by Krueger et al. (2020). The first-order conditions are

$$\frac{(c^i_{1,t})^{-1/\eta}}{(c^i_{1,t})^{1-1/\eta} + (c^i 2,t)^{1-1/\eta}} = (1+\mu_t)\left(\frac{\theta}{A}\right) n^i_t, \tag{17}$$

$$\frac{(c^i 2,t)^{-1/\eta}}{(c^i 1,t)^{1-1/\eta} + (c^i 2,t)^{1-1/\eta}} = \left(\frac{\theta}{A}\right) n^i_t. \tag{18}$$

[5]This burden is purely an economic loss. Since there is no tax revenue from the lockdown, I excludes the government budget constraint.

Contrary to the susceptible person's problem, the choice of $c^i_{1,t}$ does not affect future values. Given the two first-order conditions and the budget constraint, the infected person chooses the allocation $(c^i_{1,t}, c^i_{2,t}, n^i_t)$.

Recovered Finally, the decision problem of each recovered person is similarly defined as

$$U^r_t = \frac{\eta}{\eta-1}\ln\left[\frac{1}{2}(c^r_{1,t})^{1-1/\eta} + \frac{1}{2}(c^r_{2,t})^{1-1/\eta}\right] - \theta\frac{(n^r_t)^2}{2} + \beta U^r_{t+1} \tag{19}$$

$$\text{s.t.} \quad (1+\mu_t)\, c^r_{1,t} + c^r_{2,t} = An^r_t. \tag{20}$$

A recovered person retains this recovered status. As the infected person's problem, Good 1 consumption of recovered person, $c^r_{1,t}$, is also independent of future values. Next, as in Krueger et al. (2020), the allocation of a recovered person becomes the same as that of an infected patient[6]: $(c^i_{1,t}, c^i_{2,t}, n^i_t) = (c^r_{1,t}, c^r_{2,t}, n^r_t)$. Therefore, this model's dynamic system includes only $(c^i_{1,t}, c^i_{2,t}, n^i_t)$.

2.4 Equilibrium

Given the perfect substitution of labor inputs between Sector 1 and 2 and the equal linear labor productivity, the equilibrium conditions of both goods are integrated into

$$(1+\mu_t)S_t(c^s_{1,t} + c^s_{2,t}) + (1+\mu_t)(I_t + R_t)(c^i_{1,t} + c^i_{2,t}) = AS_t n^s_t + A(I_t + R_t)n^i_t. \tag{21}$$

It is redundant[7] given the budget constraints of the three types: Equation (12), (16), and (20).

Finally, the dynamic system of the equilibrium equations is summarized by

$$\begin{cases} \text{15 variables:} & c^s_{1,t}, c^s_{2,t}, n^s_t, c^i_{1,t}, c^i_{2,t}, n^i_t, \tau_t, T_t, S_t, I_t, R_t, D_t, U^s_t, U^i_t, U^r_t \\ \text{15 equations:} & (3), (4), (5), (6), (7), (8), (11), (12), (13), (14), (15), (16), (17), (18), (19). \end{cases}$$

given the exogenous path of ψ_t following Equation (10), and exogenous shocks of μ_t and δ_t.

[6] This property is violated if the infection status declines the labor productivity. However, given the large number of patients who exhibit no symptoms, this assumption may be plausible.

[7] By Walras law, the labor market clearing condition can be ignored. Moreover, the prices of the two goods are already determined as A.

Covid Economics 70, 25 February 2021: 109-133

3 Calibration and Model's Evaluation

3.1 Calibration

I use Our World in Data COVID-19 database maintained by Max Roser and Hasell (2020) for infection. The daily data are summed up on a weekly basis, and the consumption statistics are taken from the Survey of Household Economy. I use a seasonally adjusted monthly series, normalize the level as 1 in January 2020, and covert to weekly data through linear interpolation. The estimated effective reproduction number is taken from Toyo-Keizai Online[8]. Following Eichenbaum et al. (2020a), the discount factor β is $(0.96)^{1/52}$. I assume 18 weeks for average infection periods. At the end of 2020, the number of total deaths in Japan is 3292 out of 235811 total cases. By $0.014 = 3292/235811$, I set[9] $\pi_d = (7/18) \times 0.014$, and $\pi_r = (7/18) \times [1 - 0.014]$. The elasticity of substitution is assumed to be $\eta = 3$ from the lower case number of Krueger et al. (2020)[10]. Next, A and θ are calculated from the equations in the pre-pandemic steady state, when all people are susceptible and $c^1_{s,0} = c^2_{s,0} = 1/c_{s,0}$. In the Survey on Time Use and Leisure Activities in 2016, the average hours of paid work are 241 minutes among the entire population over age 10. Following this, weekly hours of work in the pre-pandemic steady state are $n_{s,0} = 241 \times 7/60$. From the World Bank data, the Japanese GDP per capita in 2016 is $52 \times c_{s,0} = 39289$ to the US dollar. Then, $A = c_{s,0}/n_{s,0} = 26.8729$. The labor disutility weight θ is obtained from the pre-pandemic steady-state condition $\theta = 1/(n^s_0)^2 = 0.001264$, which is derived from Equation (12), (13), and (14).

The exogenous path of the perception rate, $\bar{\psi}$ is calibrated to roughly capture the observed reduction of consumption before the soft lockdown in April and May 2020. Moving forward, $\hat{\psi}$ is decided so that ψ_t becomes about 1 at the end of 2021. It is reasonable that people perceive the infection rate almost correctly around the end of the pandemic. I choose[11] $\bar{\psi} = 15$ and $\hat{\psi} = 0.015$. Finally, I set $\pi_c = 0.00000416$ to roughly match the total number of deaths at the end of 2020[12]. To explain the consumption drop during the first soft lockdown, from the second week of April

[8] https://toyokeizai.net/sp/visual/tko/covid19/en.html

[9] This assumption does not perfectly fit the simulation results of the cumulative number of total cases and death to data possibly because of the reporting lag, infection periods until death, and the rapid increase in the number of new infection cases from November 2020.

[10] Krueger et al. (2020)'s baseline case is $\eta = 10$. In my model, this makes the total consumption response to the soft lockdown too small to catch data.

[11] Given the low reported number of cases due to the limited capacity of PCR tests in Japan, $\bar{\psi} = 15$ may still carry a lower expectation than the potential number of infections.

[12] I use only the time-series data in 2020 as the calibration target; otherwise, the parameter settings are also affected by the second soft lockdown, starting in January 2021.

Covid Economics 70, 25 February 2021: 109-133

Figure 1: Infection and Economy in 2020

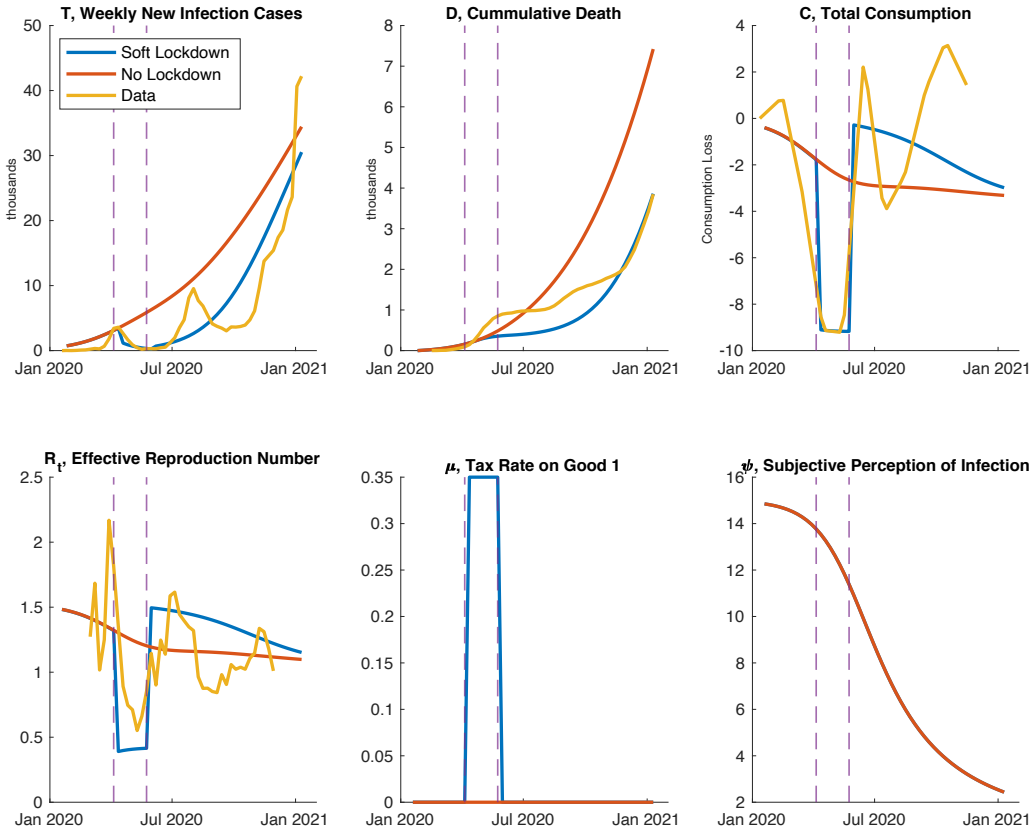

until the third week of May 2020, I set $\mu_t = 0.35$.

This simulation begins from the exogenous initial infection shock $I_1 = 0.00001$ in the second week of January[13]. This economy follows the perfect foresight path until it converges to the new steady state in 150 weeks[14].

3.2 Japan's COVID-19 Infection and Economy in 2020

Figure 1 shows the simulation results both with and without the soft lockdown and data in 2020. Given the only two exogenous variables μ_t and ψ_t, the simulation with the soft lockdown captures

[13]It may be a bit higher number given the low infection rate in Japan. However, if I assume a lower number, numerical simulation fails due to a floating-point precision error. In the same week, I also introduce a 1% reduction of ψ_1, otherwise ψ_t stays at the constant number $\overline{\psi}$.

[14]I use Dynare for the computation, following Krueger et al. (2020) and Eichenbaum et al. (2020b).

both the infection and economic paths of Japan from January to December 2020. In addition, this model explains the impacts of the soft lockdown in April and May on new infections, consumption, and the effective reproduction number. Beyond this, the model shows the number of the cumulative deaths at the end of 2020. However, it fails to describe the second wave of infection and the short-term fluctuation of consumption in the summer and fall of 2020. This may be caused by the cash-transfer policy called the Special Fixed Benefits or the subsidy for travel called the "GoTo Travel" program. I do not include these factors in the model to concentrate on analyzing the soft lockdown and avoid risks due to the uncertain quantitative impacts of these policies[15]. Additionaly, this simulation implies that, if there had been no soft lockdown, the cumulative death total would have been nearly twiced as high in 2020.

3.3 Medical Environment for Policy Analysis in 2021.

Beyond the calibrations using 2020 data, I introduce the ICU capacity constraint and vaccine plans. They are redundant in 2020 but crucial for the policy exercise in 2021[16].

The ICU Capacity Constraint The total number of severely ill patients must be below the maximum level that the available medical facilities can accommodate. In January 2021, during the second soft lockdown, the actual number of ICU patients was about 1000. Although Japan's official total ICU capacity is 3600, hospitals in urban areas had difficulty accepting severe patients needing immediate treatment. Given these conditions, I set Japan's ICU capacity constraint at 1200.

Because the model does not explicitly include the stage of severe illness, I calculate the number of ICU patients in simulation from the observed relationship between the number of patients and the number of deaths in data. Using the nonlinear least square regression for a quadratic equation using the data between the fourth week of October and the second week of January, I obtain

$$ICU_t = 0.66506 * (D_t - D_{t-1}) + 636620 * (D_t - D_{t-1})^2, \tag{22}$$

where ICU_t is the number of ICU patients in Week t and $D_t - D_{t-1}$ is the number of new deaths given the normalized population 1. The constant term is omitted because $ICU_t = D_t = D_{t-1} = 0$

[15] Kubota et al. (2020) estimate the marginal propensity to consume using a large bank's individual-level de-identified large bank's account data. They capture the transfer of money after the cash payment well, but the final effects on consumption remain unclear.

[16] Since the model is solved under agents' perfect-foresight expectations, the scenarios in 2021 affect the equilibrium path in 2020 as well. However, since the model excludes the intertemporal saving decision, the 2021 plans are quantitatively negligible in the infection and economic paths in 2020.

Covid Economics 70, 25 February 2021: 109-133

in the pre-pandemic steady state.

Two Vaccine Scenarios The new coronavirus infection eventually disappears due to the introduction of a vaccine in 2021. Thus, I conduct policy exercises under the following opportunistic and pessimistic scenarios.

- **Vaccine 1**: This is an opportunistic scenario, following the government's ideal vaccine distribution plan as of January 2021. In the first week of April, the vaccine administration to the elderly and people with underlying conditions begins. Given that each vaccine requires two shots with a three-week interval, they begin to get immunized in the third week of April. The government finishes their second shots at the end of June, and then immunization begin for other people. Because the total elderly population is about 36 million, I assume 4 million people obtain immunization per week. Moreover, the vaccination rate continues to increase; that is, 4 million people get vaccinated after July as well. As a result of the vaccination of the elderly, the death rate declines from 0.014 to 0.0035 between the first week of April and the end of June[17].

- **Vaccine 2**: This is a relatively pessimistic but realistic scenario roughly following Fujii and Nakata (2021). It is based on the evidence of countries showing when vaccination begins in Japan and the observed delays from their original plans. As in the opportunistic scenario, people begin getting immunized during the third week of April. The weekly number of people obtaining immunization linearly and gradually increases from 0.1 million in the third week of April to 1.6 million at the end of June. After that, the weekly number stays constant at 1.6 million. The elderly becomes immunized beginning in the third week of April, and it takes 23 weeks (until the last week of September) for 80% of them to acquire immunity. In these 23 weeks, the death rate linearly declines from 0.014 to 0.0035, as in the opportunistic case.

4 Policy Exercise in 2021

In this section, I consider two policies following the second soft lockdown originally planned to be lifted in the first week of February. The first one is extending the soft lockdown with the same degree of stringency. Under this policy, if the government stops the behavioral restrictions too

[17]The death rate of patients under 65 is about 0.001. I choose a higher value by taking into account the elderly who refuse vaccine into account, following the estimation of Fujii and Nakata (2021).

Covid Economics 70, 25 February 2021: 109-133

early, it will need to declare one more lockdown due to the ICU capacity constraint. The second case is beginning a new policy during the second week of February that keeps the number of ICU patients at a constant level, below the ICU capacity.

4.1 Extending Soft Lockdown

The first policy I consider is a prolonged soft lockdown, starting in January. By matching the model and the observed number of new infections at the end of January, I calculate the second lockdown's tax rate as half of the first one, $\mu_t = 0.175$. The government maintains the same stringency in the extended periods as well. If the government lifts the second lockdown quickly, another one will be required to maintain the ICU capacity constraint. I assume that the government imposes a four-week lockdown with $\mu_t = 0.175$ if the patients fill more than 70% of the ICU capacity. In the simulation, this simple rule keeps the medical capacity at a favorable margin.

Two Examples of Equilibrium Paths Figure 2 shows two examples of the equilibrium paths in 2021 with Vaccine 1 for illustration. One is a short soft lockdown lifted in the first week of February, as the original government policy plan, and the other is a long lockdown with and eight-week extension. In the first case, the number of ICU patients increases after the release and reaches the 1200 ICU capacity constraint in April. Next, the government imposes one more lockdown for four weeks. The consumption almost fully recovers in the summer of 2020 because the risk of infection declines due to the lockdowns and vaccines. In the second case, the soft lockdown in January stays the infection low enough to avoid filling all the ICU beds. The consumption also recovers quickly. A key feature of this plan is that the number of new infections increases drastically in the summer, while the number of ICU patients drops down due to vaccination among the older population. By allowing the virus to flourish among the young, the economy quickly recovers but limits the number of deaths. These combinations of a lockdown before the vaccine and no restriction after could be effective. They implicitly implement age-dependent policies, which significantly reduce the economic costs while keeping the high-risk elderly safe (Acemoglu et al., 2020; Favero et al., 2020).

Pandemic Possibility Frontiers These policies are evaluated using the dominance relationship in terms of both the health and economic damages on the pandemic possibility frontiers, following Kaplan et al. (2020). Specifically, I illustrate a tradeoff between the number of total deaths at the

Covid Economics 70, 25 February 2021: 109-133

Covid Economics 70, 25 February 2021: 109-133

Figure 2: Extending the soft lockdown under Vaccine 1

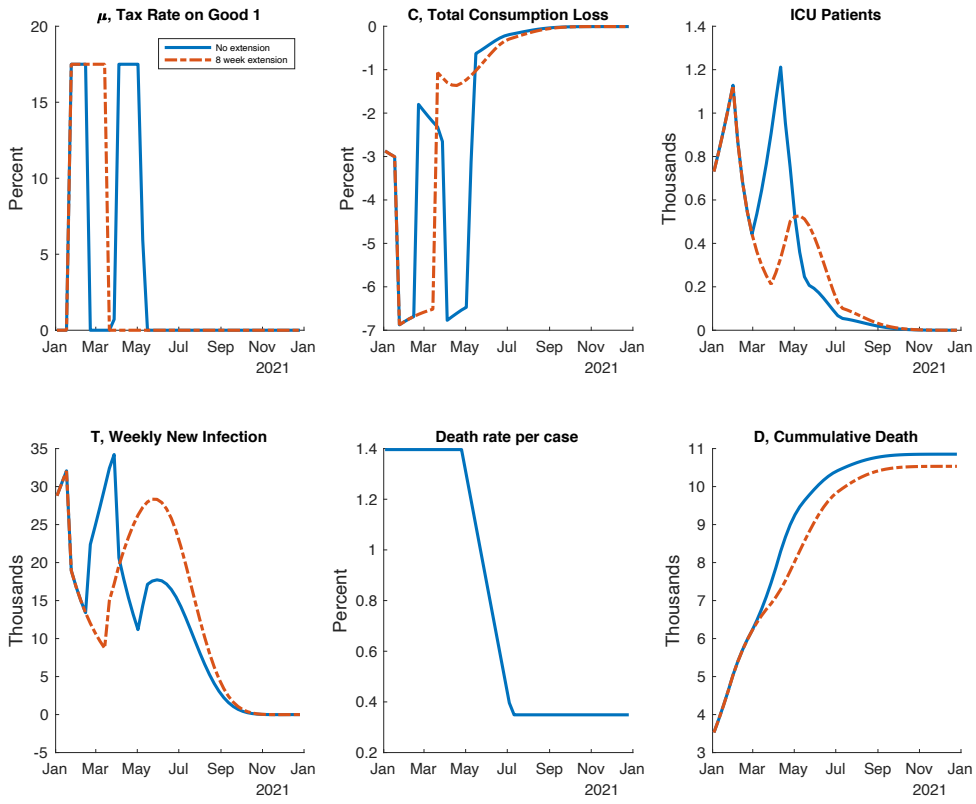

end of 2021 and the economic welfare costs of living people in 2021[18]. I measure the latter as the consumption equivalence, which is defined as the solution x to the following equation:

$$\left[\sum_{\tau=0}^{52}\beta^{\tau}\right]\left[\ln\left(c_0(1-x)\right)-\theta\frac{(n_0)^2}{2}\right] = \sum_{\tau=0}^{52}\beta^{\tau}\left\{\frac{S_\tau\left[\ln\left(c_\tau^s\right)-\theta\frac{(n_\tau^s)^2}{2}\right]+\left(I_\tau+R_\tau\right)\left[\ln\left(c_\tau^i\right)-\theta\frac{(n_\tau^i)^2}{2}\right]}{S_\tau+I_\tau+R_\tau}\right\}, \tag{23}$$

[18] In the model, each agent evaluates the value of death as sudden termination of his or her utility flow. In this sense, the individual-level costs of death are already included in the model. However, this could be different from society-level costs; for example, this excludes a family's sadness over a member's death. Because the normative costs vary, this paper takes a conservative approach, providing only pandemic possibility frontiers.

Covid Economics 70, 25 February 2021: 109-133

Figure 3: Pandemic possibility frontier under the extension of soft lockdown

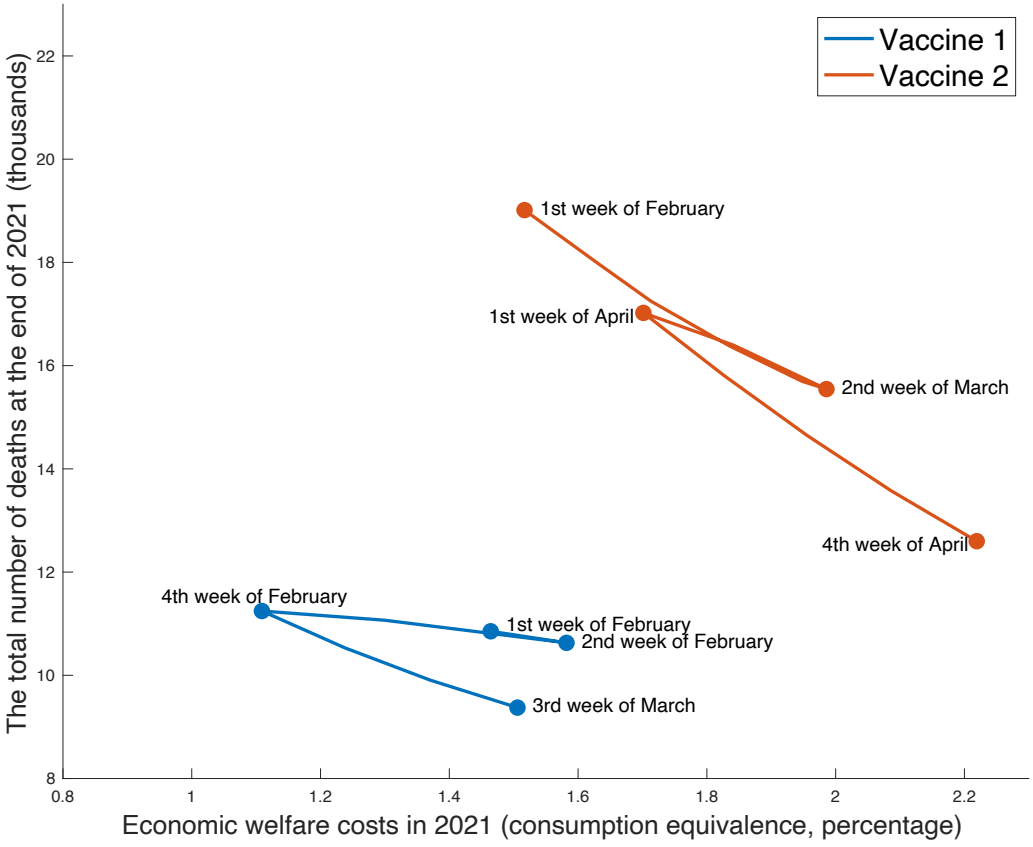

where c_0 and n_0 are the pre-pandemic steady state total consumption and labor, respectively, and the period τ is normalized as the first week of January 2021.

Figure 3 shows the frontiers of the soft lockdown extensions with Vaccine 1 and Vaccine 2. These two are quantitatively different due to differing speeds of vaccine distribution, but their qualitative implications are similar. In particular, both show the inefficiency of the recurrent lockdowns. If the soft lockdown lifts before the fourth week of February under Vaccine 1 or the first week of April under Vaccine 2, the government will need to impose one more lockdown given the ICU capacity constraint. Next, sufficiently long lockdowns achieve both lower economic losses and fewer deaths than the recurrent cases in certain regions on the diagram. In general, lockdowns are similar to time machines; that is, they push the state of infection back to the level before the policy. In

Covid Economics 70, 25 February 2021: 109-133

Figure 4: ICU targeting under Vaccine 1

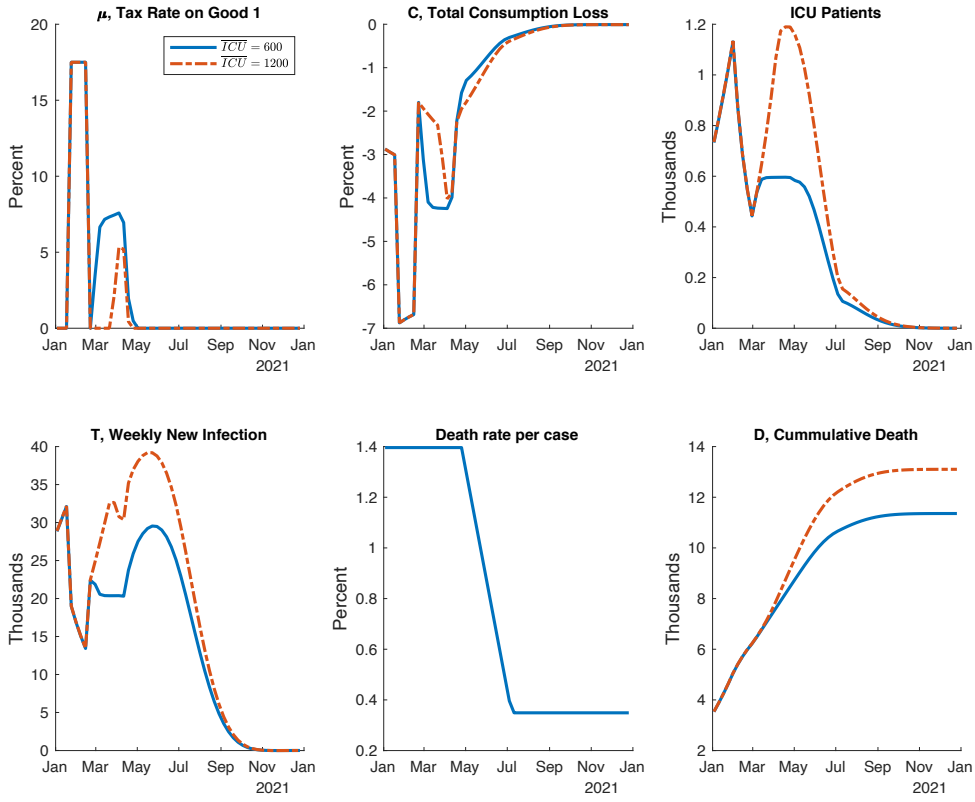

other words, the infection rate similarly grows again after lifting lockdowns. The primary role of lockdowns is not eliminating the entire pandemic but postponing the exponential increase of infections to allow for the arrival of vaccine. Thus, if there is a repeating expansion and contraction of infections caused by recurrent lockdowns, the time machine just goes to the past and comes back. It has almost no impact on the spread of the new coronavirus or on the economy. Therefore, the lockdowns should be one-time events to keep the number of ICU patients below the capacity until the arrival of vaccine.

4.2 ICU Targeting

Next, ICU targeting is another policy rule that keeps the number of patients in the ICU at a constant level $\overline{ICU}$ below the 1200 capacity. To keep this target, the government flexibly adjusts the tax

rate μ_t. This idea is similar to the inflation targeting in monetary policy. In many countries, central banks adjust the nominal interest rates to achieve the target rate of inflation. In ICU targeting, the policy goal is changed to the number of severe patients, and the policy tool becomes the degree of the restrictions.

In my scenario, the government lifts the soft lockdown in the first week of February according to the original plan and changes the policy rule to ICU targeting, beginning from the second week of February. To keep the number of ICU patients ICU_t around the target $\overline{ICU}$, the government adjusts the tax rate following the equation below:

$$\mu_t = \min\left\{0.1,\ \frac{40}{(\overline{ICU})^2}\left[\max\{0,\ ICU_t - 0.95\cdot\overline{ICU}\}\right]^2\right\}. \tag{24}$$

This equation means that the tax rate μ_t increases from 0% to 10%, while ICU_t increases from 5% below $\overline{ICU}$ to $\overline{ICU}$. If $ICU_t > \overline{ICU}$, the tax rate μ_t is constant at 10%. Although this policy does not precisely maintain the ICU_t at $\overline{ICU}$ exactly, it reasonably achieves the goal. I do not impose the exact targeting to avoid the critical non-linearity in the computation.

Two ICU Targeting Examples Figure 4 describes two equilibrium paths under ICU targeting policy, where $\overline{ICU} = 600$ and $\overline{ICU} = 1200$. The latter decides the target at the capacity. The tax rate μ_t is flexibly adjusted to keep the number of severe patients at 600 or 1200 in the spring of 2021. Because of the rapid decline of the death rate in the summer, the government ends the behavioral restrictions, allowing ICU_t to decline. As in the case of the extension of the soft lockdown, the rise in the number of new infections in May and June implements an age-dependent policy. In addition, the consumption quickly recovers in the summer while limiting the deaths.

Pandemic Possibility Frontiers Figure 5 shows the pandemic possibility frontiers under the ICU targeting policies in Vaccines 1 and 2, as well as those of soft lockdown extensions, which appear in Figure 3 for comparison. From the upper-left to the bottom-right, I move the target level from the maximum 1200 down to 200 and illustrate the consequences of economic losses and deaths as a locus. Thus, the ICU targeting policy can achieve less economic damage that is not obtained by the soft lockdown. The ICU targeting is necessary to push the economic welfare costs lower than about 1.1% under Vaccine 1 or 1.5% under Vaccine 2. This is achieved if the Japanese government keeps the number of ICU patients close to the limit. This can be justified if the society

Covid Economics 70, 25 February 2021: 109-133

Figure 5: ICU targeting under Vaccine 1

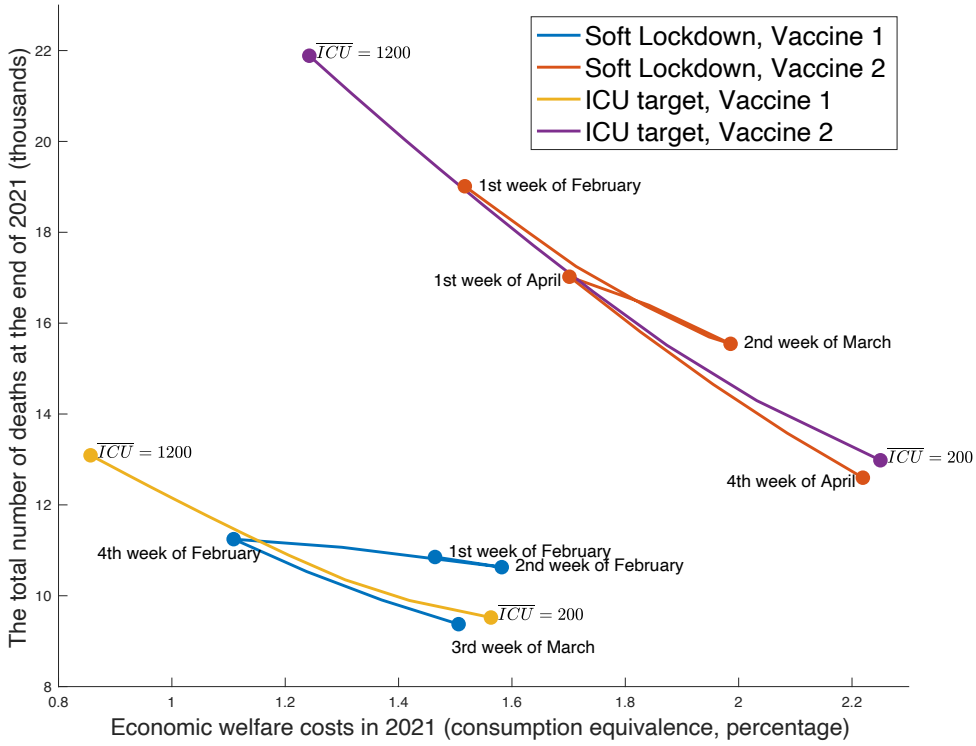

values the life less than a certain level[19]. However, the ICU targeting is inferior to the one-time prolonged lockdown, in which the time of lifting is between the fourth week of February and the third week of March under Vaccine 1 and the first week of April and fourth week of April under Vaccine 2. This is because the ICU targeting tends to continue restrictions for too long after the start of vaccination, which distorts the young's economic activities.

The pandemic possibility frontiers also illustrates substantial economic and health benefits by hastening the vaccine distribution. If the Japanese society chooses the economic damage as 1.5% of the consumption under both vaccine cases, the number of deaths can be reduced from about 19,000 with Vaccine 2 to 9,000 with Vaccine 1. On the other hand, if the number of deaths is

[19]Given Japan's significantly lower number of deaths than that of other countries, the corner solutions with the lowest economic damage may be realistic. On these pandemic possibility frontiers, the corner solutions are selected if the value of a statistical life (VSL) is less than about 240 years of annual GDP per capita under Vaccine 1 and 120 years under Vaccine 2. For a comparison, Hall et al. (2020) derive a realistic VSL of approximately 50 years, and Alvarez et al. (2020) assume this figure to be 40 years.

Covid Economics 70, 25 February 2021: 109-133

fixed at 13,000, the economic damage can be reduced from about 2.2% to less than 0.9% in the consumption. For comparison, Japan's total budget of both the central and local governments for the vaccine distribution is about only 0.25% of the GDP[20]. By accelerating only the vaccine supply, the economic damage can be improved by 1.3% of the consumption. Acharya et al. (2020) estimate a greater economic value by studying stock price reactions to the development progress indicator and yielding an even higher value.

5 Conclusion

I use a tractable SIR Macro model to quantitatively examine Japan's second soft lockdown, starting in January 2021. The results are summarized by the pandemic possibility frontiers between the economic welfare loss and the total number of deaths. Thus, the Japanese government should continue the soft lockdown for long enough to avoid recurrent lockdowns. To achieve lower economic damage, the government can adopt another strategy, accepting more ICU patients.

[20]The central government's plan is about 500 billion yen. Among local municipalities, Yokohama city, which has about 3.7 million population out of 125 million total population in Japan, plans 25 billion yen for vaccine. Thus, the total budget of all municipalities is estimated to be 850 billion yen. The total of the central and local, 1350 billion yen, is about 0.25% of Japan's GDP, which is approximately 550 trillion yen.

Covid Economics 70, 25 February 2021: 109-133

References

Acemoglu, Daron, Victor Chernozhukov, Iván Werning, and Michael D Whinston (2020), "Optimal targeted lockdowns in a multi-group sir model." *NBER Working Paper*.

Acharya, Viral V, Timothy Johnson, Suresh Sundaresan, and Steven Zheng (2020), "The value of a cure: An asset pricing perspective." *Covid Economics: Vetted and Real-Time Papers*, 61, 1–72.

Alvarez, Fernando E, David Argente, and Francesco Lippi (2020), "A simple planning problem for covid-19 lockdown." *Covid Economics: Vetted and Real-Time Papers*, 14, 1–32.

Aum, Sangmin, Sang Yoon Tim Lee, and Yongseok Shin (2020), "Inequality of fear and self-quarantine: Is there a trade-off between gdp and public health?" *Covid Economics, Vetted and Real Time Papers*, 14, 143–174.

Bethune, Zachary and Anton Korinek (2020), "Covid 19 infection externalities: Pursuing herd immunity or containment." *Covid Economics, Vetted and Real Time Papers*, 11, 1.

Brotherhood, Luiz, Philipp Kircher, Cezar Santos, and Michèle Tertilt (2020), "An economic model of the covid-19 epidemic: The importance of testing and age-specific policies." *CESifo Working Paper*.

Eichenbaum, Martin S, Sergio Rebelo, and Mathias Trabandt (2020a), "The macroeconomics of epidemics." *NBER Working Paper*.

Eichenbaum, Martin S, Sergio Rebelo, and Mathias Trabandt (2020b), "The macroeconomics of testing and quarantining." Technical Report w27104, National Bureau of Economic Research.

Farboodi, Maryam, Gregor Jarosch, and Robert Shimer (2020), "Internal and external effects of social distancing in a pandemic." *Covid Economics: Vetted and Real-Time Papers*, 9, 25–61.

Favero, Carlo A, Andrea Ichino, and Aldo Rustichini (2020), "Restarting the economy while saving lives under covid-19." *CEPR Discussion Paper Series*.

Fujii, Daisuke and Taisuke Nakata (2021), "Covid-19 and output in japan." *CARF Working Paper*.

Giagheddu, Marta and Andrea Papetti (2020), "The macroeconomics of age-varying epidemics." *Covid Economics: Vetted and Real-Time Papers*, 58, 22–56.

Covid Economics 70, 25 February 2021: 109-133

Glover, Andrew, Jonathan Heathcote, Dirk Krueger, and José-Víctor Ríos-Rull (2020), "Health versus wealth: On the distributional effects of controlling a pandemic." *Covid Economics: Vetted and Real-Time Papers*, 6, 22–64.

Goolsbee, Austan and Chad Syverson (2020), "Fear, lockdown, and diversion: Comparing drivers of pandemic economic decline 2020." *Journal of Public Economics*, 193, 104,311.

Hall, Robert E, Charles I Jones, and Peter J Klenow (2020), "Trading off consumption and covid-19 deaths." *Quarterly Review*, 42, 1–14.

Hamano, Masashige., Munechika Katayama, and So Kubota (2020), "Covid-19 misperception and macroeconomy." *WINPEC Working Paper Series*.

Hsu, Wen-Tai, Hsuan-Chih Luke Lin, and YANG Han (2020), "Between lives and economy: Optimal covid-19 containment policy in open economies." *SMU Economics and Statistics Working Paper Series*, 20-2020.

Kang, Kee-Youn and Xi Wang (2021), "Search, infection, and government policy." *SSRN*.

Kapicka, Marek and Peter Rupert (2020), "Labor markets during pandemics." *Manuscript, UC Santa Barbara*.

Kaplan, Greg, Benjamin Moll, and Giovanni L Violante (2020), "The great lockdown and the big stimulus: Tracing the pandemic possibility frontier for the us." *NBER Working Paper Series*.

Krueger, Dirk, Harald Uhlig, and Taojun Xie (2020), "Macroeconomic dynamics and reallocation in an epidemic." *Covid Economics: Vetted and Real-Time Papers*, 5, 22–64.

Kubota, So, Koichiro Onishi, and Yuta Toyama (2020), "Consumption responses to covid-19 payments: Evidence from a natural experiment and bank account data." *Covid Economics: Vetted and Real-Time Papers*, 62, 90–123.

Makris, Miltiadis and Flavio Toxvaerd (2020), "Great expectations: Social distancing in anticipation of pharmaceutical innovations." *Covid Economics, Vetted and Real Time Papers*, 56, 1–19.

Max Roser, Esteban Ortiz-Ospina, Hannah Ritchie and Joe Hasell (2020), "Coronavirus pandemic (covid-19)." *Our World in Data*. Https://ourworldindata.org/coronavirus.

Covid Economics 70, 25 February 2021: 109-133

Miclo, Laurent, Daniel Spiro, and Jörgen Weibull (2020), "Optimal epidemic suppression under an icu constraint." *arXiv preprint*.

Moll, Ben (2020), "Lockdowns in sir models." *Lecture Notes*, URL https://benjaminmoll.com/wp-content/uploads/2020/05/SIR_notes.pdf.

Sheridan, Adam, Asger Lau Andersen, Emil Toft Hansen, and Niels Johannesen (2020), "Social distancing laws cause only small losses of economic activity during the covid-19 pandemic in scandinavia." *Proceedings of the National Academy of Sciences*, 117, 20468–20473.

Toxvaerd, Flavio (2020), "Equilibrium social distancing1." *Covid Economics, Vetted and Real Time Papers*, 15, 110–133.

von Carnap, Tillmann, Ingvild Almås, Tessa Bold, Selene Ghisolfi, and Justin Sandefur (2020), "The macroeconomics of pandemics in developing countries: An application to uganda." *Covid Economics, Vetted and Real Time Papers*, 27, 104.

Watanabe, Tsutomu and Tomoyoshi Yabu (2020), "Japan's voluntary lockdown." *Covid Economics: Vetted and Real-Time Papers*, 46, 1–31.

Covid Economics 70, 25 February 2021: 109-133

Covid Economics 70, 25 February 2021: 109-133

Appendix

A note on the difference between structural and reduced-form SIR models

This note compares structural SIR models, including optimization and economy, as in my model, and reduced-form SIR models, such as those shown by Fujii and Nakata (2021). Both models analyze Japan's COVID-19 infection rate, output, and policies. I discuss both the similarities and differences between these factors for policy discussion. In this appendix, I follow almost all of the same notation as Fujii and Nakata (2021). Suppose that the true state is described as this present paper's model with no perception bias ($\forall t, \psi_t = 1$). Let the percentage decline of output be $\tilde{Y}_t = 1 - Y_t/\overline{Y}_t$. I first simulate a toy economy with the soft lockdown between Periods 20 and 30 and between Periods 50 and 60. It derives the the true equilibrium path of $(N_t, S_t, I_t, \tilde{Y}_t)_{t=1}^{100}$. Next, following Fujii and Nakata (2021), I estimate their output-infection relation parameter h from the true model's results between Periods 10 and 49. My goal is to evaluate the reduced-form model's prediction using an estimation including past data and one experience of the soft lockdown.

The modified infection rate becomes

$$\tilde{\beta}_t = \beta_t(1 - h\tilde{Y}_t)$$

Given a unit population, the new infection is

$$N_t = \tilde{\beta}_t I_t S_t = \beta_t(1 - h\tilde{Y}_t) I_t S_t.$$

I estimate h using the nonlienar OLS, given the following equation:

$$\ln\left(\frac{N_t}{I_t S_t}\right) = \beta_0 + \ln\left(1 - h\tilde{Y}_t\right) + \varepsilon_t,$$

where $\ln \beta_t$ is divided into the constant term and error term: $\ln \beta_t = \beta_0 + \varepsilon_t$. I assume that $\beta_t = \exp(\beta_0)$ for all t and the true path of $\left(\tilde{Y}_t\right)_{t=50}^{100}$. Next, given the estimated h, I back out $\left(N_t, I_t, S_t\right)_{t=50}^{100}$ using SIR equations.

The results are shown in Figure A.1. Overall, there is only a small difference. In general, reduced-form models capture only the correlation between infection and economy, which could include two-way causalities. However, the causality is almost solely one-way when considering lockdowns. The soft lockdowns first change economic activities and then affect infections. Thus,

the estimated reduced-form correlation mainly capturing the causality from economy to infection is sufficient.

On the other hand, the estimated model predicts a slightly larger decline in the new infections. The true model includes a smoothing in the event of a large shock, given the causality from infection to economy. Under the containment policy, households consume less and mitigate the infection. This effect makes less linearity under a large fluctuation than models estimated in relatively moderate periods. Nevertheless, the magnitudes look negligible.

Structural models may be required by some exercises in which causalities are crucial. For example, distributing masks is associated with a reverse causality that reduces infection first and enhances economic activities second. It improves both infection and economy, which cannot be explained by reduced-form models.

Figure A.1: True and predicted paths of infections given the output path

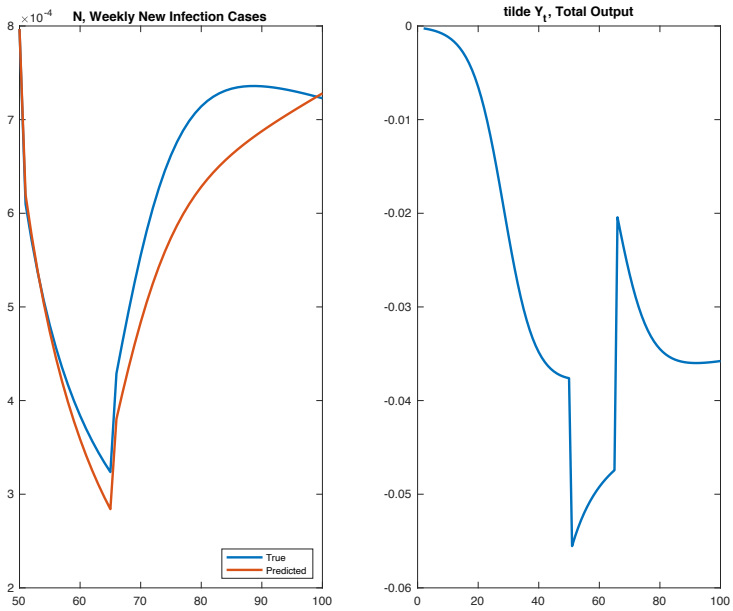

Covid Economics 70, 25 February 2021: 109-133

Covid Economics **Issue 70, 25 February 2021**

Partisan differences in COVID-19 prevalence among politicians suggest important role for protective behaviours[1]

Patrick Carlin,[2] Sumedha Gupta,[3] Daniel W. Sacks[4] and Coady Wing[5]

Date submitted: 16 February 2021; Date accepted: 17 February 2021

How important are risk-avoidance behaviors for preventing the spread of COVID-19? Answering this question is difficult because risk-avoidance behaviors may be correlated with non-behavioral risks (such as occupational risk) and because COVID-19 prevalence is poorly measured due to limited testing. We study the prevalence of COVID-19 infections among state governors and members of the U.S. Congress. These politicians face similar occupational risks and are frequently tested. Yet we find large differences in COVID-19 prevalence along party lines: Republican politicians are three times as likely as Democratic ones to have ever reported a COVID case. The association between COVID-19 and party affiliation is not due to demographic differences, differences in state riskiness, or differential campaign strategies. Given well-documented differences in risk attitudes and preventive behavior along political lines, the differential COVID-19 rate we document is consistent with the view that behavioral risk is a key determinant of COVID-19 infections.

Covid Economics 70, 25 February 2021: 134-147

1 The authors have no competing interests or funding sources to declare. All data and code will be made available, except data on the covariates of members of congress, which requires a data license. The authors are grateful to Daniel Simon for helpful conversations, and to Hessam Bavafa, Anthony Defusco, Denvil Duncan, Anita Mukherjee, and Justin Ross for valuable comments.

2 Indiana University.
3 Indiana University-Purdue University Indianapolis.
4 Indiana University.
5 Indiana University.

1 Introduction

Efforts to contain the COVID-19 pandemic are premised on the theory that infection risks can be reduced through behavioral modifications, including face masks, six-foot distancing, and substitution to online interactions. These behavioral changes have disrupted employment, reduced mobility, and hindered learning (Montenovo et al., 2020; Chetty et al., 2020; Goolsbee and Syverson, 2020; Kaufman et al., 2020; Gupta et al., 2020). Behavioral modifications have been widely but unevenly adopted, and they remain controversial because they are costly and their protective efficacy has not been proven.

Research based on aggregate data suggests that masks may reduce COVID-19 infections (Betsch et al., 2020; Van Dyke, 2020). A small trial conducted during a period of low prevalence in Denmark found small, imprecise effects of providing masks (Bundgaard et al., 2020). Studying the effect of risk avoidance on prevalence is difficult because COVID-19 testing is highly rationed, and risk-avoidance are likely correlated with non-behavioral (workplace, co-morbidity, and family structure) risk factors that might also explain prevalence.

This study examines the connection between risk avoidance and COVID-19 prevalence in the population of Governors, U.S. Senators, and U.S. Representatives. An observational study in this population eases some of the difficulties in studying risk avoidance and COVID prevalence. These politicians plausibly face comparable non-behavioral risks because they all hold the same job, reducing concerns about uncontrolled confounding. Further, prevalence is better measured among politicians because they are tested more regularly than the general population.

Like other studies (Betsch et al., 2020; Van Dyke, 2020), we lack individual measures of risk avoidance. We therefore turn to political party affiliation as a plausible proxy for risk avoidance behaviors. The connection between party affiliation and COVID-19 risk avoidance is supported by previous research. In surveys, Republicans are less likely to report social distancing and less likely to consider COVID-19 a serious health risk (Allcott et al., 2020; Kushner Gadarian et al., 2020). Social distancing and mask wearing are less common in areas with a higher share of Republican voters (Allcott et al., 2020; Gollwitzer et al., 2020). Green et al. (2020) show that the tweets of U.S. Representatives and Senators show a partisan divide, with Republicans less likely to emphasize threats to public health early in the pandemic. Social distancing policies were imposed later in states with Republican governors (Adolph et al., 2020). The Democrat-controlled House of Representatives has stricter COVID-precautions in place than the Republican-controlled Senate; for example, allowing remote voting (DeBonis, 2020; Grisales, 2020). Anecdotal reports indicate that, among na-

Covid Economics 70, 25 February 2021: 134-147

tional politicians, Republicans are less likely than Democrats to consistently wear masks (Everett, 2020).

We find that 10.1% of Republican politicians and 3.3% of Democrat politicians have had a confirmed case of COVID-19. We investigate several alternative explanations for the elevated COVID-19 prevalence among Republican politicians. Adjusting for age, gender, race/ethnicity, education, and population density does not alter the association. If anything, Democrats tend to represent areas with higher population density and greater geographic susceptibility to COVID-19. It is possible that more Democrats were infected earlier in the pandemic, when testing was less common, but we show that in every month since April, Republicans have been more likely than Democrats to have ever had COVID-19. We present evidence that differential campaign style is unlikely to explain Republican's higher COVID-19 prevalence. Taken together, our results are consistent with the view that personal protective behaviors can have a large impact on COVID-19 prevalence. Though others such as Reimann (2020) have observed that Republicans make up a disproportionate share of COVID-19-infected politicians, our primary contribution is to show that this difference is not explained by many plausible factors, including geographic differences or incentives to campaign. We are also the first to systematically measure gubernatorial COVID cases.

Covid Economics 70, 25 February 2021: 134-147

2 Data and Methods

Data: Our sample includes all Governors, House Representatives, and Senators serving as of December 1, 2020.[1] Information on gender, age, race, and education came from CQ Press (2020) for Senators and House Representatives and from Wikipedia for Governors. We defined the political territory as the state for Senators and Governors and as the congressional district for House Representatives, and we computed the corresponding population density using using shape files from US Census Bureau (2020b) and population data from US Census Bureau (2020a). To measure electoral competition, we usedFiveThirtyEight (2020)'s August 1, 2020 predicted probability that each incumbent would be re-elected in 2020. In some analyses, we define an "uncontested" sub-sample of Senators and House Representatives who either lost the primary, were not running for re-election in 2020, or who were engaged in a race where the forecasted win rate was more than 99%. Governors are excluded from these analyses because forecasts are not available. Throughout, we classify two independent Senators as Democrat because they caucus with Democrats, and one libertarian House

[1]The California 50th, Georgia 5th, and Texas 4th districts were vacant at data collection, leaving us with 432 House Representatives.

Representative as Republican because he caucuses with Republicans.

We obtained data on the COVID-19 status of Senators and House Representatives from GovTrack (2020), which maintains a list of which members of Congress have reported a positive test, along with references for the positive test, which we checked. We collected data on COVID-19 status of Governors using Google news searches for Governor's name combined with the term "COVID positive". We coded Governors as COVID-19 positive if we found at least one article reporting that the Governor had a COVID-19 case.[2] The main outcome variable in our analysis is a binary measure of whether the politician had a (publicly disclosed) COVID-19 infection by December 3, 2020.

Methods: We measure unadjusted and adjusted mean differences in COVID-19 prevalence between Republican and Democratic politicians. One concern with unadjusted mean differences is that the gap in COVID-19 prevalence may arise not only from differences in risk avoidance but also from pre-existing differences in the characteristics of the Republican and Democrat politicians (Holtgrave et al., 2020; Cutler and Lleras-Muney, 2006). A separate concern is that Republicans are more likely to represent states and districts with low-population density, and less likely to represent coastal states. Since the early pandemic was severe in high-density and coastal areas, the association between prevalence and political party could be due to geographic factors rather than preventive behaviors (Allcott et al., 2020).

We address these concerns in two ways. First, we compare COVID-19 prevalence politicians from the same state but different political parties. Second, we estimate linear probability models of COVID-19 infection against dummies for political party, political office, demographic controls, population density, and state fixed effects. These models adjust for demographic as well as geographic differences. Standard errors are estimated using a heteroskedasticity-robust variance matrix that allows for dependence at the state level.

Covid Economics 70, 25 February 2021: 134-147

3 Results

Table 1 shows the prevalence of COVID-19 by political party and political office. Overall, COVID-19 prevalence is 10.1% among Republican politicians and 3.3% among Democratic politicians. Among House Representatives, prevalence is 9% for Republicans and 3.4% of Democrats. In the Senate, 15.1% of Republicans and no Democrats had been infected. Among state governors, prevalence is 8% in both parties.

[2]Articles reporting one governor's case often listed other COVID positive governors, providing a cross-check.

Covid Economics 70, 25 February 2021: 134-147

Figure 1: COVID-19 prevalence by state and party, among national politicians

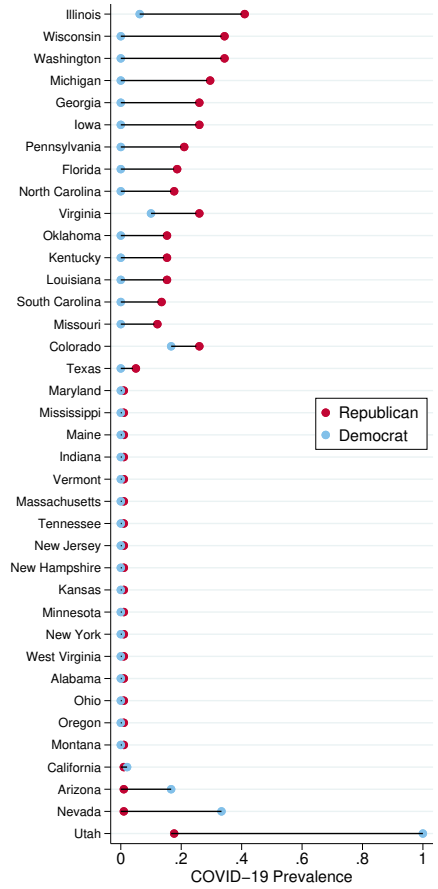

Notes: Figure reports the percentage of governors, representatives, and senators whom we count as ever having had COVID-19, separately by state and party. COVID counts are from GovTrack (2020); gubernatorial data were hand-collected by the authors from news reports. We treat politicians independent politicians who caucus with the Democratic party as Democrats. The figure is limited to the 38 states which have both Democratic and Republican politicians, and states are sorted by the difference between Republican and Democratic rates. In Illinois-Texas (17 states), COVID-19 prevalence is higher among Republicans than Democrats. In Vermont-New Hampshire (17 states) the proportions are equal. In California-Utah (four states), COVID-19 prevalence is higher among Democrats than Republicans.

Table 1: SARS CoV-2 Cases among Representatives, Senators, and Governors, by party

Party	Republican	Democratic	All
Representatives	18 / 199 9.0%	8 / 233 3.4%	26 / 432 6.0%
Senator	8 / 53 15.1%	0 / 47 0.0%	8 / 100 8.0%
Governors	2 / 25 8.0%	2 / 25 8.0%	4 / 50 8.0%
All	28 / 277 10.1%	10 / 305 3.3%	38 / 582 6.5%

Notes: Table reports COVID counts / total number of politicians. COVID counts are from GovTrack (2020); gubernatorial data were hand-collected by the authors from news reports. We treat independent politicians who caucus with the Democratic party as Democrats, and we code 1 Libertarian as a Republican because he caucuses with Republicans.

The unadjusted differences in Table 1 could be misleading if Republicans locate in states with higher COVID-19 caseloads. Figure 1 shows COVID-19 prevalence among Democratic and Republican national politicians within each state for the set of 38 states where there are both Republican and Democratic national politicians. Among these 38 states, prevalence is higher among Republicans in 17 states, equal in 17 states (where prevalence is zero), and higher among Democrats in the remaining four states.

Both unadjusted and within state contrasts could be confounded by differences in the characteristics of Democrats and Republicans. Table 2 reports covariate averages for Democrat and Republican politicians, and shows that the parties have different gender, age, race/ethnicity, and gender composition.

Table 3 presents covariate adjusted estimates of the difference in prevalence between Republicans and Democrats based on linear regressions. The first column shows that prevalence is 6.8% points ($p = 0.002$) higher among Republicans in a model that controls for political office but no additional covariates. The second column shows that, after adding state fixed effects, prevalence is 9.2% points ($p=0.002$) higher among Republicans. Relative to base rate of 3.2% among Democrats, this difference implies that COVID-19 is four times more prevalent among Republicans. The third column adds controls for population density,

Covid Economics 70, 25 February 2021: 134-147

Table 2: Covariates, by political party

	Republicans		Democratics		Difference		
	Mean	(SD)	Mean	(SD)	Mean	[SE])	p-value
House	0.72	(0.45)	0.76	(0.43)	-0.05	[0.04]	0.212
Senate	0.19	(0.39)	0.15	(0.36)	0.04	[0.03]	0.237
Population density	89.00	(157.61)	1066.61	(2578.36)	-977.61	[147.95]	<0.001
Female	0.09	(0.29)	0.36	(0.48)	-0.27	[0.03]	<0.001
Age	58.75	(10.63)	60.18	(12.21)	-1.44	[0.95]	0.130
Bachelor's degree	0.32	(0.47)	0.17	(0.38)	0.15	[0.04]	<0.001
Graduate degree	0.52	(0.50)	0.62	(0.49)	-0.10	[0.04]	0.015
Joint education							<0.001
White (not Hispanic)	0.95	(0.21)	0.65	(0.48)	0.30	[0.03]	<0.001
Hispanic	0.03	(0.18)	0.12	(0.32)	-0.09	[0.02]	<0.001
African American	0.01	(0.08)	0.17	(0.37)	-0.16	[0.02]	<0.001
Joint race/ethnicity							<0.001
Joint significance							<0.001

Notes: Table reports the means and, in parentheses, standard deviations of the indicated variables, by political party, as well the difference in means and its standard error. The final column is the p-value of the hypothesis that the parties have equal means. We also report p-values for tests of joint significance of groups of variables and all variables.

Covid Economics 70, 25 February 2021: 134-147

adjusting for the fact that Republicans tend to represent low-density districts. The fourth column adds demographic controls (age, education, gender, and race). These controls make very little difference.

Beyond observed covariates, Republicans and Democrats may have pursued different campaign strategies in 2020 and these strategies may have led to different occupation related COVID-19 risks. Many Republicans held in-person rallies while Democrats pursued non-traditional campaign events with more social distancing (Reuters Staff, 2020). To guard against confounding from differential campaign strategies, we re-estimate the full model in a sample limited to Senators and Representatives who are not in contested elections, defined as elections where the predicted win probability from FiveThirtyEight (2020) is less than 99 percent. Although the politicians in the limited sample have little incentive to engage in risky campaigning, the estimates in the fifth column shows that the Republican differential remains large at 11.7 % points (p=.026). This finding is robust to alternative definitions of the uncontested sample; see Supplemental Table 4.

Another concern is that Republicans have been infected late in the epidemic when testing was widely available, while Democrats were infected earlier when testing was in short supply. Elevated Republican prevalence might reflect better measurement rather than genuine

Covid Economics 70, 25 February 2021: 134-147

Table 3: Adjusting for demographics and state fixed effects does not alter the Republican-COVID association

	(1)	(2)	(3)	(4)	(5)
Republican-Democrat Differential	0.068	0.092	0.091	0.089	0.117
	(0.021)	(0.028)	(0.028)	(0.029)	(0.051)
Sample size	582	582	582	582	291
Sample	All	All	All	All	Uncontested
Controls for ...					
Position	Yes	Yes	Yes	Yes	Yes
State fixed effects	No	Yes	Yes	Yes	Yes
Population density	No	No	Yes	Yes	Yes
Demographics	No	No	No	Yes	Yes

Notes: Table reports the coefficient on Republican from a linear probability model of ever-COVID-19 on Republican and the indicated controls. Position controls are dummy variables for senator or representative, omitting governor. The demographic controls are age, dummy variables for education categories (bachelors's degree, higher than bachelor's), female, and race categories (African America, Hispanic, White; the omitted category is Asian/Native/not disclosed). "Uncontested" sample is limited to Representatives and Senators and excludes politicians whose predicted probability of reelection is less than 99 percent. We report heteroskedasticity-robust standard errors, clustered on state, in parentheses.

Figure 2: COVID-19 prevalence by date and party, among national politicians

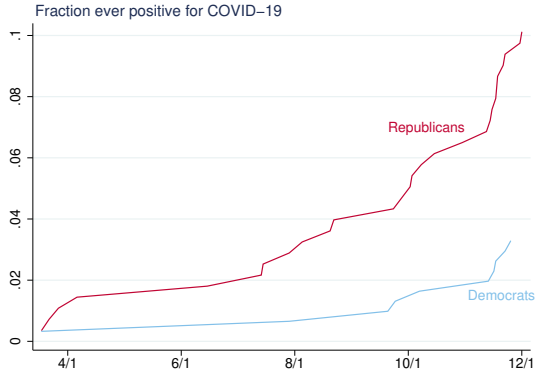

Notes: Figure reports the percentage of governors, representatives, and senators whom we count as ever having had COVID-19, separately by party and day. See text for definitions and sources.

difference in exposure. Figure 2 plots the cumulative fraction of Republicans or Democrats testing positive for COVID-19 by day. Republican prevalence is higher than Democratic prevalence throughout the pandemic, casting doubt on this explanation.

4 Conclusion

Among Governors, Senators, and Representatives, Republicans are three times as likely as Democrats to have reported a COVID-19 case by December, 2020. In principle this higher COVID-19 prevalence could reflect differences in the baseline risks facing Republicans and Democrats, differences in testing or reporting, or differences in preventive behaviors. We have shown that several possible sources of differential risk do not explain the higher COVID-19 rate among Republicans. The gap is not accounted for by Republican-Democratic differences in demographics, district population density, or state-specific unobservables. We also show that the gap is unlikely to be explained by differential testing over time or campaign riskiness.

We conclude that a likely explanation for higher COVID-19 prevalence among Republicans politicians is that Republicans are less likely to engage in precautionary behavior. Under this explanation, the differential prevalence that we document may reflect the combined effect of the politicians' individual behavior as well as the behavior of their extended network, including family, staff, and constituents. This conclusion is subject to two important limitations. First, we do not observe individual politicians' behaviors, and so cannot confirm that politicians engaging in more precautionary behavior are less likely to report a COVID-19 case. Second, our sample of politicians need not be representative of the general public. It is possible that politicians—who travel frequently and interact with diverse constituencies—may face greater risks than the general population. Risk avoidance strategies may have a larger protective effect for politicians than they would for the general population. Furthermore, politicians are not demographically representative of the population: they are much older than the general population, and much more likely to be male and white (Ruggles et al., 2021).

Although our study does not provide evidence about the importance of any particular behavior such as mask wearing or six-foot distancing, it suggests that collectively these behaviors can have a large effect on COVID-19 risks.

Covid Economics 70, 25 February 2021: 134-147

References

Adolph, C., K. Amano, B. Bang-Jensen, N. Fullman, and J. Wilkerson (2020). Pandemic Politics: Timing State-Level Social Distancing Responses to COVID-19. *Journal of Health Politics, Policy and Law*. _eprint: https://read.dukeupress.edu/jhppl/article-pdf/doi/10.1215/03616878-8802162/820900/8802162.pdf.

Allcott, H., L. Boxell, J. Conway, M. Gentzkow, M. Thaler, and D. Y. Yang (2020). Polarization and public health: Partisan differences in social distancing during the coronavirus pandemic. *Journal of Public Economics* (191).

Allcott, H., L. Boxell, J. C. Conway, B. A. Ferguson, M. Gentzkow, B. Goldman, et al. (2020). What explains temporal and geographic variation in the early us coronavirus pandemic? *NBER Working Paper* (27965).

Betsch, C., L. Korn, P. Sprengholz, L. Felgendreff, S. Eitze, P. Schmid, and R. Böhm (2020). Social and behavioral consequences of mask policies during the covid-19 pandemic. *Proceedings of the National Academy of Sciences 117*(36), 21851–21853.

Bundgaard, H., J. S. Bundgaard, D. E. T. Raaschou-Pedersen, C. von Buchwald, T. Todsen, J. B. Norsk, M. M. Pries-Heje, C. R. Vissing, P. B. Nielsen, U. C. Winsløw, et al. (2020). Effectiveness of adding a mask recommendation to other public health measures to prevent sars-cov-2 infection in danish mask wearers: a randomized controlled trial. *Annals of Internal Medicine*.

Chetty, R., J. Friedman, N. Hendren, and M. Stepner (2020). The economic impacts of covid-19: Evidence from a new public database built from private sector data. *Opportunity Insights*.

CQ Press (2020). Cq press congress collection. `https://library.cqpress.com/congress/`, last accessed December 2, 2020.

Cutler, D. M. and A. Lleras-Muney (2006). Education and health: evaluating theories and evidence. Technical report, National bureau of economic research.

DeBonis, M. (2020, May). House changes its rules during pandemic, allowing remote voting for the first time in its 231-year history. *The Washington Post*.

Covid Economics 70, 25 February 2021: 134-147

Everett, B. (2020, November). Senators clash over masks on senate floor. *Politico*. https://www.politico.com/news/2020/11/16/masks-senate-floor-brown-sullivan-436911, last accessed December 4, 2020.

FiveThirtyEight (2020). 2020 election forecast. https://projects.fivethirtyeight.com/2020-election-forecast/, last accessed December 9, 2020.

Gollwitzer, A., C. Martel, W. J. Brady, P. Pärnamets, I. G. Freedman, E. D. Knowles, and J. J. Van Bavel (2020). Partisan differences in physical distancing are linked to health outcomes during the covid-19 pandemic. *Nature Human Behaviour*, 1–12.

Goolsbee, A. and C. Syverson (2020). Fear, lockdown, and diversion: Comparing drivers of pandemic economic decline 2020. *Journal of Public Economics 193*, 104311.

GovTrack (2020). Covid-19 in congress. https://www.govtrack.us/covid-19, last accessed November 23, 2020.

Green, J., J. Edgerton, D. Naftel, K. Shoub, and S. J. Cranmer (2020). Elusive consensus: Polarization in elite communication on the covid-19 pandemic. *Science Advances 6*(28).

Grisales, C. (2020, May). Despite coronavirus risks, the u.s. senate returns for normal business. *NPR*.

Gupta, S., K. I. Simon, and C. Wing (2020). Mandated and voluntary social distancing during the covid-19 epidemic: A review. *NBER Working Paper* (w28139).

Holtgrave, D. R., M. A. Barranco, J. M. Tesoriero, D. S. Blog, and E. S. Rosenberg (2020). Assessing racial and ethnic disparities using a covid-19 outcomes continuum for new york state. *Annals of epidemiology 48*, 9–14.

Kaufman, J. H., M. Diliberti, G. P. Hunter, D. Grant, L. S. Hamilton, H. L. Schwartz, C. M. Setodji, J. Snoke, and C. J. Young (2020). *COVID-19 and the State of K-12 Schools: Results and Technical Documentation from the Fall 2020 American Educator Panels COVID-19 Surveys*. Santa Monica, CA: RAND Corporation.

Kushner Gadarian, S., S. W. Goodman, and T. B. Pepinsky (2020). Partisanship, health behavior, and policy attitudes in the early stages of the covid-19 pandemic. *Health Behavior, and Policy Attitudes in the Early Stages of the COVID-19 Pandemic (March 27, 2020)*.

Montenovo, L., X. Jiang, F. L. Rojas, I. M. Schmutte, K. I. Simon, B. A. Weinberg, and C. Wing (2020). Determinants of disparities in covid-19 job losses. Technical report, National Bureau of Economic Research.

Reimann, N. (2020). Congressional republicans infected with covid 3 times more than democrats. https://www.forbes.com/sites/nicholasreimann/2020/12/18/congressional-republicans-infected-with-covid-3-times-more-than-democrats/, last accessed January 7, 2020.

Reuters Staff (2020, October). Fact check: Crowd size at trump and biden events reflect campaign strategy, not support. *Reuters*. https://www.reuters.com/article/uk-factcheck-crowd-biden-trump-support/fact-check-crowd-size-at-trump-and-biden-events-reflect-campaign-strategy-not-support last accessed December 11, 2020.

Ruggles, S., S. Flood, S. Foster, R. Goeken, J. Pacas, M. Schouweiler, and M. Sobek (2021). Ipums usa: Version 11.0 [dataset]. Technical report, Minneapolis, MN: IPUMS. https://doi.org/10.18128/D010.V11.0.

US Census Bureau (2020a). Census api total population series b01003_001e. https://api.census.gov/data/2017/acs/acs5/variables.html, last accessed December 2, 2020.

US Census Bureau (2020b). Tiger/line shapefile, 2018, nation, u.s. 116th congress. https://catalog.data.gov/dataset/tiger-line-shapefile-2018-nation-u-s-116th-congressional-district-national, last accessed December 2, 2020.

Van Dyke, M. E. (2020). Trends in county-level covid-19 incidence in counties with and without a mask mandate—kansas, june 1–august 23, 2020. *MMWR. Morbidity and Mortality Weekly Report 69*.

Supplemental material

Figure 3: Distribution of incumbent's predicted win probabilities

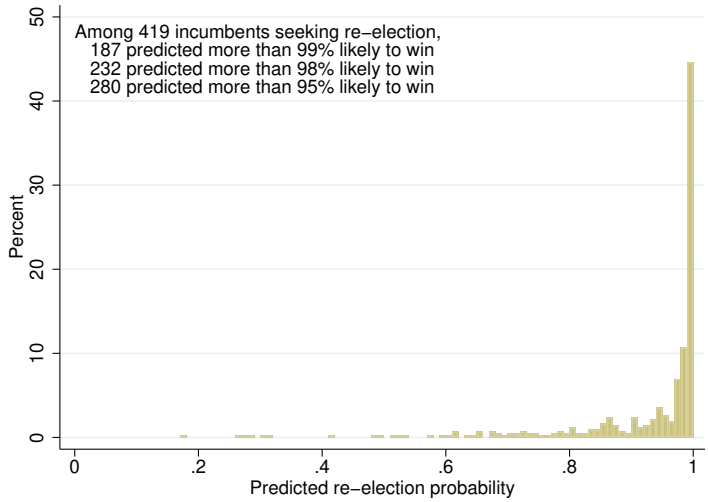

Notes: Sample consists of incumbent representatives and senators seeking re-election. Figure plots the distribution of predicted win probabilities as of August 1, 2020, from FiveThirtyEight (2020).

Covid Economics 70, 25 February 2021: 134-147

Covid Economics 70, 25 February 2021: 134-147

Table 4: Robustness to alternative definitions of uncontested elections

	(1)	(2)	(3)	(4)	(5)
Republican-Democrat Differential	0.089	0.117	0.102	0.113	0.088
	(0.029)	(0.051)	(0.043)	(0.035)	(0.028)
Sample size	582	291	300	384	434
Win cutoff	Any	99%	99 %	95%	95%
Include primary losers	Yes	No	Yes	No	Yes

Notes: Table reports the coefficient on Republican from a linear probability model of ever-COVID-19 on Republican dummy, as well as the following additional controls: dummy for senator (and representative in column 1), age, dummy variables for education categories (bachelor's degree, higher than bachelor's), female, and race categories (African America, Hispanic, White; the omitted category is Asian/Native/not disclosed), and state fixed effects. The sample in column (2)-(5) always excludes governors, includes incumbents who lost their primary as indicated, and is limited to politicians either not seeking reelection or with a predicted win rate above the indicated cutoff, based on reelection probabilities from FiveThirtyEight (2020). We report heteroskedasticity-robust standard errors, clustered on state, in parentheses.